PhD PROCEEDINGS

ANNUAL ISSUES OF THE DOCTORAL SCHOOL

FACULTY OF INFORMATION TECHNOLOGY & BIONICS

2024

PhD PROCEEDINGS

ANNUAL ISSUES OF THE DOCTORAL SCHOOL

FACULTY OF INFORMATION TECHNOLOGY & BIONICS
PÁZMÁNY PÉTER CATHOLIC UNIVERSITY

PhD PROCEEDINGS

ANNUAL ISSUES OF THE DOCTORAL SCHOOL

FACULTY OF INFORMATION TECHNOLOGY & BIONICS

2024

PÁZMÁNY UNIVERSITY *e*PRESS
BUDAPEST, 2024

HU ISSN 2064-7271

Kiadja a Pázmány Egyetem eKiadó
Budapest, 2024

Felelős kiadó
Rev. Mons. Dr. Kuminetz Géza
a Pázmány Péter Katolikus Egyetem rektora

Cover image by Eszter Nagy-Kanta: *NMR and molecular dynamics (MD) analysis of the bivalent DLC2-binding segment of the intrinsically disordered protein GKAP.* ***A*** *The experimental design of the NMR titration measurements illustrated with the initial structure of the molecular dynamics simulations.* ***B*** *$^{1}H^{15}N$-HSQC spectra of the titration points with the stoichiometry of 1:1 (blue), 1:2 (green), 1:4 (yellow) and 1:8 (red). Amide NH peaks chemical shift assignment of the free GKAP is visible on the spectrum.* ***C*** *One example of the molecular dynamics calculations representing the complex structure. The calculations support the hypothesis that both binding sites participate in the binding, and GKAP retains partial flexibility even in bound form. Structural illustrations were created with ChimeraX.*

Contents

Introduction

It is our pleasure to publish this Annual Proceedings again to demonstrate the genuine multidisciplinary research done at the Jedlik Laboratories by young talents working in the Roska Tamás Doctoral School of Sciences and Technology of the Faculty of Information Technology and Bionics at Pázmány Péter Catholic University. The scientific results of our PhD students outline the main recent research directions in which our faculty is engaged. We also appreciate the support of the supervisors and consultants, as well as that of the five collaborating National Research Laboratories of the Hungarian Research Network, Semmelweis University and the University of Pannonia. The collaborative work with the partner universities, especially Katolieke Universiteit Leuven, Politecnico di Torino, Technische Universität München, University of California at Berkeley, University of Notre Dame, Universidad de Sevilla, Università di Catania, Université de Bordeaux and Universidad Autónoma de Madrid is gratefully acknowledged.

We acknowledge the support of numerous institutes, organizations and companies:

- Hungarian Research Network (HUN-REN),
- National Research, Development and Innovation Office (NKFIH),
- Hungarian Academy of Sciences (MTA),
- ÚNKP Programme, Ministry of Culture and Innovation, Hungarian Government,
- KDP Programme, Ministry of Culture and Innovation, Hungarian Government,
- Gedeon Richter Co.,
- Office of Naval Research (ONR) of the US,
- NVIDIA Ltd.,
- Verizon Computer Vision Center of Excellence (CV CoE), Budapest,
- MorphoLogic Ltd., Budapest,
- AnaFocus Ltd., Seville,

and several other companies and individuals.

Needless to say, the resources and support of the Pázmány Péter Catholic University are gratefully acknowledged.

Budapest, June 2024.

GÁBOR PRÓSZÉKY

Chairman of the Board of the Doctoral School

GÁBOR SZEDERKÉNYI

Head of the Doctoral School

PROGRAM 1
BIONICS, BIO-INSPIRED WAVE COMPUTERS, NEUROMORPHIC MODELS

Heads: Tamás FREUND, Zsolt LIPOSITS, Sándor PONGOR

Dependence of BCI performance on preprocessing steps

András ADOLF
(Supervisor: István ULBERT)
Pázmány Péter Catholic University, Faculty of Information Technology and Bionics
50/a Práter street, 1083 Budapest, Hungary
adolf.andras@itk.ppke.hu

***Abstract*—In the development of Brain-computer-interface systems, the accurate classification of EEG signals constitutes a crucial step. During EEG signal measurement, various artifacts can arise, resulting from both biological sources (e.g. muscle movements) and environmental noise. To address this challenge, various artifact rejection methods have been developed, one of which is the FASTER algorithm. In this study, I compare the performance of multiple neural networks with and without the application of the mentioned method. I also examined the effect of Transfer Learning method, as well as the differences caused by applying frequency filters on the data.**

***Keywords*-Artifact Rejection; BCI; FASTER; CNN**

I. Summary

Our evaluation was performed on a diverse set of subjects from the Physionet database [1] and was based on a comparison of the results obtained from five different convolution-based machine learning models. A 2-dimensional Convolutional Neural Network (noted as Conv2D) was devised, wherein the input to the system comprised a 3-dimensional configuration of the electroencephalogram (EEG) signal. This representation encompassed one dimension denoting time, while the remaining two dimensions corresponded to the 2D layout of the electrodes' spatial arrangement. Subsequently, a 3-dimensional neural network was constructed with input dimensions identical to those of the preceding system. Three alternative machine learning architectures, namely EEGNet [2], Multi Branch 3D CNN [3], and Shallow CNN [4], were also evaluated for their efficacy regarding the influence of Artifact Rejection.

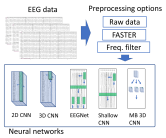

Fig. 1. The examined preprocessing methods and neural networks

The study underscores the impact of Artifact Rejection, which is contingent on both the specific classification system employed and the characteristics of the individual subjects. In the absence of Transfer Learning, EEGNet emerges as the top-performing model. Remarkably, for four out of the five networks, the application of the FASTER [5] algorithm leads to a substantial and statistically significant enhancement in performance. However, the utilization of the Transfer Learning (TL) method alters this distribution. While it enhances the performance of all networks across all preprocessing steps, it introduces an intriguing reversal in the relative performance of data with and without Artifact Rejection. When TL is employed, data without Artifact Rejection consistently outperforms the same data with Artifact Rejection. This reversal in performance might be attributed to the network's ability to capitalize on a larger dataset. Neural networks often excel at learning subtle yet crucial features, and these subtle details may be inadvertently filtered out during the FASTER method. Therefore, the presence of more extensive, unfiltered data provides the network with the opportunity to capture these finer features, ultimately leading to superior performance. Finally, we conducted a study of the effect of frequency filtering. When training our networks only on the subject-wise data, the only prominent frequency ranges are from 0.1 Hz in the case of the examined CNN-s. The EEGNet and the Shallow CNN networks, however, get the highest accuracy from 5 to 75 Hz if offset-based learning is conducted.

Acknowledgements

This work is prepared with the professional support of the Doctoral Student Scholarship Program of the Co-operative Doctoral Program of the Ministry of Culture and Innovation financed from the National Research, Development and Innovation Fund.

References

[1] G. Schalk, D. Mcfarland, T. Hinterberger, N. Birbaumer, and J. Wolpaw, "BCI2000: a general-purpose Brain-Computer Interface (BCI) system," *IEEE Trans. Biomed. Eng.*, vol. 51, p. 1034, July 2004.

[2] V. J. Lawhern, A. J. Solon, N. R. Waytowich, S. M. Gordon, C. P. Hung, and B. J. Lance, "EEGNet: A Compact Convolutional Network for EEG-based Brain-Computer Interfaces," *Journal of Neural Engineering*, vol. 15, p. 056013, Oct. 2018. arXiv:1611.08024 [cs, q-bio, stat].

[3] X. Zhao, H. Zhang, G. Zhu, F. You, S. Kuang, and L. Sun, "A multi-branch 3D convolutional neural network for EEG-based motor imagery classification," *IEEE transactions on neural systems and rehabilitation engineering*, vol. 27, no. 10, pp. 2164–2177, 2019. Publisher: IEEE.

[4] R. T. Schirrmeister, J. T. Springenberg, L. D. J. Fiederer, M. Glasstetter, K. Eggensperger, M. Tangermann, F. Hutter, W. Burgard, and T. Ball, "Deep learning with convolutional neural networks for EEG decoding and visualization," *Human Brain Mapping*, vol. 38, no. 11, pp. 5391–5420, 2017. _eprint: https://onlinelibrary.wiley.com/doi/pdf/10.1002/hbm.23730.

[5] H. Nolan, R. Whelan, and R. B. Reilly, "FASTER: Fully Automated Statistical Thresholding for EEG artifact Rejection," *Journal of Neuroscience Methods*, vol. 192, pp. 152–162, Sept. 2010.

A. ADOLF, "Dependence of BCI performance on preprocessing steps" in *PhD Proceedings – Annual Issues of the Doctoral School, Faculty of Information Technology and Bionics, Pázmány Péter Catholic University – 2024.* G. Prószéky, G. Szederkényi Eds. Budapest: Pázmány University ePress, 2024, pp. 11–11.

Intracortical effects of infrared neural stimulation in the rat neocortex

Zsófia BALOGH-LANTOS
(Supervisor: Zoltán FEKETE)
Pázmány Péter Catholic University, Faculty of Information Technology and Bionics
50/a Práter street, 1083 Budapest, Hungary
lantos.zsofia@itk.ppke.hu

***Abstract*—Infrared neural stimulation (INS) has been explored as a means of modulating neuronal activity by adjusting tissue temperature. However, the underlying biophysics of this process remains incompletely understood. To address this, we investigated the effects of pulsed and continuous-wave INS on cortical neurons in anesthetized rats using high-density laminar electrode recordings. Analyzing responses from a large sample of single units, we found that pulsed INS predominantly increased neuronal firing, while continuous INS tended to suppress activity. Notably, elevating tissue temperature with INS significantly increased the number of affected cells, particularly inhibiting activity. Moreover, we observed differences in response between principal cells and interneurons. These findings provide insight into the intricate mechanisms underlying INS in the living brain.**

***Keywords*-infrared neuromodulation; electrophysiology; spike detection**

I. Introduction

A substantial proportion of individuals living with various neurological disorders, including Parkinson's disease and epilepsy, highlights the necessity of addressing these debilitating conditions [1]. Therefore, there is a pressing need to develop treatments targeting these diseases. INS utilizes infrared (IR) light to induce temperature changes in neural tissue, which in turn can either suppress or evoke action potentials in neurons. Despite numerous hypothesized biophysical and molecular mechanisms underlying INS, a more comprehensive understanding necessitates a synthesis of detailed theoretical models with experimental findings.

II. Methods

The experiments were designed to investigate how tissue temperature affects neuronal activity in anesthetized rats. Recordings were made using a Neuropixels probe to examine responses to pulsed and continuous IR stimulation. IR light was delivered in cycles of ON and OFF periods to achieve peak temperature and return to baseline. For the spike detection, Kilosort was used [2]. This is an automated method that uses the raw electrophysiological data to detect the spikes, allowing for more accurate waveforms. After this, the spike clusters were manually curated and separated into single-unit activity spike clusters. To analyze the data, custom MATLAB scripts were used. The average firing rate and relative firing rate of all detected cells were calculated and the position of the neurons was determined using brain sections.

Fig. 1 shows an example waveform of a single unit cluster detected by Kilosort. The figure shows several channels adjacent to each other where the same spike was detected with different amplitudes.

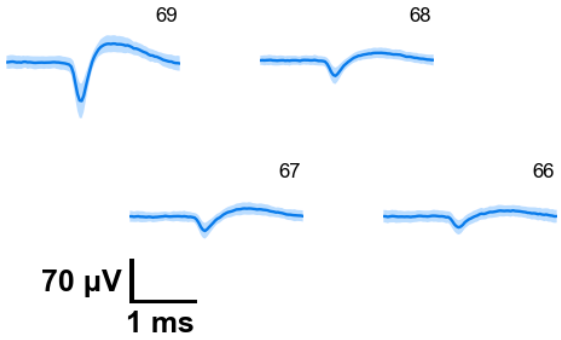

Fig. 1. Example multichannel waveform of a single unit cluster

III. Results and discussion

The objective of this study was to investigate the impact of INS on neuronal cell activity. The utilization of Neuropixels electrodes allowed data to be recorded across a range of parameters, which revealed distinct changes in neural function. Our results showed that pulsed INS predominantly increased neuronal firing, while continuous INS tended to suppress activity. Notably, increasing tissue temperature with INS significantly increased the number of affected cells, particularly those that inhibited activity. In addition, we observed differences in response between principal cells and interneurons. This study sheds light on the nuanced effects of IR stimulation on cortical neurons, providing valuable insights for future research. Additionally, it underscores the importance of combining electrophysiological and molecular approaches to understand neuronal excitability in vivo.

IV. Acknowledgement

The authors are grateful for the funding of the National Development and Innovation Office (grants NKFIH FK 134403 and TKP2021-EGA-42) and the support of the Hungarian Brain Research Program 3.0 of the Hungarian Academy of Sciences (grants NAP2022-I-8/2022 and NAP2022-I-2/2022), the scholarship of the New National Excellence Program and also the Bolyai János Research Fellowship.

References

[1] Z. Fekete, Á. C. Horváth, and A. Zátonyi, "Infrared neuromodulation: a neuroengineering perspective," *Journal of Neural Engineering*, vol. 17, no. 5, p. 051003, 2020.

[2] M. Pachitariu, N. A. Steinmetz, S. N. Kadir, M. Carandini, and K. D. Harris, "Fast and accurate spike sorting of high-channel count probes with kilosort," *Advances in neural information processing systems*, vol. 29, 2016.

Zs. BALOGH-LANTOS, "Intracortical effects of infrared neural stimulation in the rat neocortex" in *PhD Proceedings – Annual Issues of the Doctoral School, Faculty of Information Technology and Bionics, Pázmány Péter Catholic University – 2024.* G. Prószéky, G. Szederkényi Eds. Budapest: Pázmány University ePress, 2024, pp. 12–12.

Exploring the correlation between migration parameters and cell characteristics

Gréta Lilla BÁNYAI
(Supervisor: Tamás Márton GARAY)
Pázmány Péter Catholic University, Faculty of Information Technology and Bionics
50/a Práter street, 1083 Budapest, Hungary
banyai.greta.lilla@itk.ppke.hu

***Abstract*—Timelapse videomicroscopy is a widely used method for studying cell migration, offering a way to analyze cell motility independently from other factors like proliferation or invasion. However, it's crucial to process cell-tracking data carefully because many migration parameters can be calculated, each giving different information about the cells' migratory behavior. In our study, we investigated seven migration parameters and how they relate to specific characteristics of the cells. We also considered how these cells' characteristics affect the reliability of migration parameters and the differences in results from different tracking methods.**

***Keywords*-cell migration, videomicroscopy, migration parameters, cell-specific parameters, correlation**

I. Introduction

To analyze cell migration on videomicroscopic recordings, tracking of cells is essential. This can be achieved through manual, semi-automatic, or fully automated methods. Semi-automated and automated approaches present challenges due to their complexity, requiring intricate image preprocessing steps and confronting difficulties such as managing cell disappearance or division events. Following cell position detection over time, various parameters are computed, and subsequent data analysis and comparison are conducted [1]. These parameters encompass two primary categories: cell characteristic parameters derived from cell contours, and migration parameters determined based on the geometric central position of cells [2].

II. Calculation of migration parameters and cell-specific parameters

Analysis was conducted on videomicroscopic images previously recorded using an inverted phase-contrast microscope at Semmelweis University, Budapest. A total of 1287 recordings were subjected to manual and semi-automatic tracking (CellTracker). Subsequently, seven commonly utilized migration parameters were computed from cell positions at each time point using MATLAB: Mean Squared Displacement (MSD), displacement, maximal displacement as displacement-based parameters; total traveled distance, velocity, and average velocity as traveled path-based parameters; and directionality ratio. For each migration parameter, the area under the curve was computed using trapz() MATLAB built-in function, then averaged for cell lines and treatments. A relative standard deviation was also calculated to assess the repeatability of each parameter.

Three parallel control recordings were processed for each cell line using ImageJ to determine six cell-specific parameters: cell size, cell number, circularity, area coverage, colonization tendency, and maximum colony size. Additionally, average velocity was incorporated as an extra cell-specific parameter as well, considering that average cell motility might also characterize the given cell.

The relationship between migration parameters and cell-specific parameters was assessed utilizing Pearson's correlation, using corrplot() MATLAB function.

III. Results and conclusion

In our study, the relationship between cell-specific parameters and migration parameters was investigated to explore the migration of cell lines with specific properties and determine the appropriate processing of recordings, as well as the calculation of relevant migration parameters.

The analysis demonstrated correlations between cell-specific parameters and migration characteristics, with stronger associations with colonization tendency in semi-automatic tracking compared to manual tracking. Treatment-induced changes weakened some correlations, particularly between migration parameters and cell size/shape, presumably due to the effect of the treatment on the cell features. Discrepancies between tracking methods were influenced by cell parameters, particularly observed in circularity and coverage within control cases, and in cell number and coverage within treatment cases. The reliability of the migration parameters was largely independent of the cell features in the case of semi-automatic tracking, whereas in manual tracking, the correlation was consistently observed with all cell characteristic parameters. The difference in correlation strength between tracking methods might be attributed to their inherent characteristics: semi-automatic tracking relied on predefined algorithms, while manual tracking involved subjective human judgment, potentially introducing biases.

These correlations shed light on the complex interplay between cellular characteristics and migration dynamics, providing valuable insights for further research in cell biology and migration studies.

IV. Acknowledgements

Project no. TKP2021-EGA-42 has been implemented with the support provided by the Ministry of Culture and Innovation of Hungary from the National Research, Development and Innovation Fund, financed under the TKP2021 funding scheme.

References

[1] P. Masuzzo, M. Van Troys, C. Ampe, and L. Martens, "Taking aim at moving targets in computational cell migration.," *Trends in Cell Biology*, vol. 26, no. 2, pp. 88–110, 2015.

[2] C.-M. Svensson, A. Medyukhina, I. Belyaev, N. Al-Zaben, and M. T. Figge, "Untangling cell tracks: Quantifying cell migration by time lapse image data analysis.," *Cytometry A.*, vol. 93, no. 3, p. 357–370, 2018.

G. BÁNYAI, "Exploring the correlation between migration parameters and cell characteristics" in *PhD Proceedings – Annual Issues of the Doctoral School, Faculty of Information Technology and Bionics, Pázmány Péter Catholic University – 2024.* G. Prószéky, G. Szederkényi Eds. Budapest: Pázmány University ePress, 2024, pp. 13–13.

Exploring the links between grapevine physiology and the composition and functionality of grapevine microbiome in the context of drought stress

Ramóna BIRÓ-KOVÁCS
(Supervisors: Zsolt ZSÓFI, Balázs LIGETI)
Pázmány Péter Catholic University, Faculty of Information Technology and Bionics
50/a Práter street, 1083 Budapest, Hungary
biro-kovacs.ramona@itk.ppke.hu

Abstract*—: Microorganisms form the basis of the Earth's biosphere and represent a large part of the planet's biodiversity. They play a critical role in ecosystem processes and nutrient cycling, providing functions that ultimately sustain all life. Within the plant microbiome, mutualistic fungal and bacterial symbioses such as mycorrhizae, beneficial endophytes, and nitrogen-fixing bacteria are prominent examples of microorganisms that play a crucial role in nutrient acquisition and plant resistance to biotic and abiotic stresses [1]. Our results achieved with the proposed research provide unprecedented insight into the complex interaction between water stress caused by climate change and the dynamics of the microbiome and the health of the grapes, which has a direct impact on grape growing in Hungary and other countries. are increasingly facing problems related to water stress due to climate change.** ***Keywords: drought stress, Vitis vinifera, water deficit, agriculture

I. Introduction

On the world stage, the rise in temperature due to global warming has already become a reality, which has become one of the main challenges of the scientific community, has greatly reshaped or is in the process of altering all agricultural ecosystems. Since agriculture is highly dependent on climatic conditions, it can have a large impact in the short term if measures are not taken to adjust and mitigate the agricultural system. The responses of plants to abiotic stress have been investigated by many groups worldwide. Vitis vinifera is one of the most cultivated plants worldwide, which has a great impact on the economy of many countries. As in any other plant, there are numerous interacting microorganisms on the external and internal surface of the grape [2], [3]. Therefore, it is not surprising that the characterization of the grape microbiome has attracted increasing interest in recent years, in order to explore the effect these microorganism-plant relationships can have on the physiology of the grape. The overall health of grapes is greatly influenced by the diversity of microbial communities.

II. Methodology

The drought-stress experiment will be executed at the Eszterházy Vineyard in Eger operated by the Research and Development Center of the EKKE. We will manipulate grapevine water-stress levels through different irrigation, aiming to achieve 50% and 40% field capacity relative to the control with full water potential. The following physiological measurements related to metabolic activity will be taken on healthy, mature, and undamaged leaves: midday net CO_2 assimilation rate (Pn), stomatal conductance (gs), and transpiration rate (E). We will generate DNA metabarcoding data of fungi and bacteria from grapevine roots, shoots, and leaves of grapevines subjected to different levels of drought stress using our well-established workflow [4]. In addition to microbial community profiling described above, we will also characterize the composition of actively expressed grapevine and microbial genes in different plant parts under different drought stress conditions using metatranscriptomics. We will statistically compare the taxonomic and functional richness and relative abundance of microbial communities, with particular attention to various pathogenic and beneficial microbes associated with grapevine.

III. Conclusion

Wine production is a multi-billion-dollar global industry and viticulture is among the most valuable agricultural activities in Hungary and forms an important component of the cultural heritage and is even featured in our national anthem. As the sustainability and rentability of viticulture in Hungary is increasingly threathened climate change, particularly by warming-riven drought-stress, knowledge on the physiological differences among rootstocks, scions and their interactions with microorganisms is essential for responding intelligently to the above challenges. The holobiont approach of the proposed research and the used cutting-edge molecular and bioinformatic tools will provide unprecedented insights into how warming-driven drought stress shape grapevine physiology and microbiome composition and functionality, with direct implications for the viticulture industry in Hungary and elsewhere, that increasingly face problems related to water stress due to climate change.

Acknowledgment

This research is supported by the Thematic Research Excellence grant TKP2021-NKTA-16 awarded by the NKFIH.

References

[1] A. E. Arnold, L. C. Mejía, D. Kyllo, E. I. Rojas, Z. Maynard, N. Robbins, and E. A. Herre, "Fungal endophytes limit pathogen damage in a tropical tree," *Proceedings of the National Academy of Sciences*, vol. 100, no. 26, pp. 15 649–15 654, 2003.

[2] R. Cobos, A. Ibañez, A. Diez-Galán, C. Calvo-Peña, S. Ghoreshizadeh, and J. J. R. Coque, "The grapevine microbiome to the rescue: Implications for the biocontrol of trunk diseases," *Plants*, vol. 11, no. 7, p. 840, 2022.

[3] J. Geml, "Soil fungal communities reflect aspect-driven environmental structuring and vegetation types in a pannonian forest landscape," *Fungal Ecology*, vol. 39, pp. 63–79, 2019.

[4] J. Geml, L. N. Morgado, T. A. Semenova-Nelsen, and M. Schilthuizen, "Changes in richness and community composition of ectomycorrhizal fungi among altitudinal vegetation types on mount kinabalu in borneo," *New Phytologist*, vol. 215, no. 1, pp. 454–468, 2017.

R. BIRÓ-KOVÁCS, "Exploring the links between grapevine physiology and the composition and functionality of grapevine microbiome in the context of drought stress" in *PhD Proceedings – Annual Issues of the Doctoral School, Faculty of Information Technology and Bionics, Pázmány Péter Catholic University – 2024.* G. Prószéky, G. Szederkényi Eds. Budapest: Pázmány University ePress, 2024, pp. 14–14.

Learning curves of different sensor configurations during a grasping task using machine learning

Eszter BIRTALAN
(Supervisor: Miklós KOLLER)
Pázmány Péter Catholic University, Faculty of Information Technology and Bionics
50/a Práter street, 1083 Budapest, Hungary
birtalan.eszter@itk.ppke.hu

***Abstract*—Tactile sensors have proven to be a useful addition for learning in-hand manipulation and grasping tasks, however, their exact placement on both real-life and simulated hand models varies greatly between papers. This research aims to find conclusive results on how sensor density and positioning affects the learning curves of specific grasping tasks. This may substantially decrease the time spent with either real-life or in-simulation experiments of newly developed hand prostheses.**

***Keywords*-reinforcement learning; proximal policy optimization; tactile sensors;robotic grasping; prosthetic hand**

I. Introduction

Recent studies effectively utilize imitation learning to accelerate the learning process and humanize robot movements by gathering motion data from human subjects performing various grasping or manipulation tasks [3]. This can be extremely beneficial for engineers; however, it also introduces an additional bias into training by incorporating outside data as opposed to relying solely on data generated by the simulation. Imitation learning alone does not result in perfectly executed robot movement however, and further training is required, which is often achieved through reinforcement learning or deep reinforcement learning due to promising results reported in recent research [1], [2]. The addition of tactile sensors into this training pipeline enhances performance but also introduces a novel type of uncertainty related to the number and positioning of the sensors [4]. Studying the effects of tactile sensor density and placement when using reinforcement learning to learn grasping tasks therefore would be a useful expansion of the field. Due to the bias that surfaces when using imitation learning, it is necessary for the learning process to be completed using only the data generated during simulation. This puts a heavy emphasis on a reward function suitable for driving the desired behavior.

II. Methods

To investigate the effects of sensor placement a PyBullet environment was created with a rigid 3D hand model, custom tactile sensors, and various objects for the hand to lift in the air. The sensors were arranged in 3 different configurations, not including the controls. Version 1 has one sensor with a wide sensing field placed on each index of the hand, version 2 has three sensors with smaller sensing fields placed horizontally along the midline of each index, and version 3 has nine sensors placed in a matrix on the index. All the variations also include four sensors on the palm, placed near the first index of each finger. To facilitate learning this difficult and complex task the hand begins in an advantageous, partially closed position above the object. The position of the hand becomes gradually more open as the previous, easier task is successfully completed. This results in a curriculum learning scheme, which has been shown to aid the learning of complex tasks.

Results have shown that both the three- and nine-sensor configurations lagged behind the one-sensor configuration in terms of performance. Reasons for this may include not appropriate cover of the sensing areas or the increased observation space resulting in a large increase in complexity. Simulations run with tactile data were shown to have a steeper initial learning curve than simulations run without it. To further facilitate learning a soft body-based inner covering has been made in simulation. The soft cover is able to increase the contact surface between hand and object, thus contributing to better grasp quality. In order to properly simulate the soft-covered hand model in PyBullet, further experiments are needed to identify the proper physical parameters.

Acknowledgements

Project no. TKP2021-NKTA-66 has been implemented with the support provided by the Ministry of Culture and Innovation of Hungary from the National Research, Development and Innovation Fund, financed under the TKP2021 funding scheme.

Project no. ÚNKP-23-3-I-PPKE-94 has been implemented with the support provided by the Ministry of Culture and Innovation of Hungary from the National Research, Development and Innovation Fund

Project no. 2023-2.1.2-KDP-2023-00011 has been implemented with the support provided by the Ministry of Culture and Innovation of Hungary from the National Research, Development and Innovation Fund, based on the grant award certificate issued by the National Research, Development and Innovation Office.

References

[1] M. Q. Mohammed, K. L. Chung, and C. S. Chyi, "Review of Deep Reinforcement Learning-Based Object Grasping: Techniques, Open Challenges, and Recommendations," *IEEE Access*, vol. 8, pp. 178450-178481, 2020, doi: 10.1109/ACCESS.2020.3027923.

[2] P. Amaral, F. Silva, and V. Santos, "Recognition of Grasping Patterns Using Deep Learning for Human–Robot Collaboration," *Sensors*, vol. 23, no. 21, p. 8989, 2023. doi: 10.3390/s23218989.

[3] J. Choi, H. Kim, Y. Son, C. -W. Park, and J. H. Park, "Robotic Behavioral Cloning Through Task Building," *2020 International Conference on Information and Communication Technology Convergence (ICTC)*, Jeju, Korea (South), 2020, pp. 1279-1281. doi: 10.1109/ICTC49870.2020.9289148.

[4] A. Melnik, L. Lach, M. Plappert, T. Korthals, R. Haschke, and H. Ritter, "Using Tactile Sensing to Improve the Sample Efficiency and Performance of Deep Deterministic Policy Gradients for Simulated In-Hand Manipulation Tasks," *Frontiers in Robotics and AI*, vol. 8, p. 538773, 2021. doi: 10.3389/frobt.2021.538773. PMID: 34268337; PMCID: PMC8275974.

E. BIRTALAN, "Learning curves of different sensor configurations during a grasping task using machine learning" in *PhD Proceedings – Annual Issues of the Doctoral School, Faculty of Information Technology and Bionics, Pázmány Péter Catholic University – 2024.* G. Prószéky, G. Szederkényi Eds. Budapest: Pázmány University ePress, 2024, pp. 15–15.

Methods for investigating the mechanisms underlying novel hippocampal spatial representations in calcium imaging experiments

Martin BLAZSEK
(Supervisors: Judit MAKARA, Balázs UJFALUSSY)
Pázmány Péter Catholic University, Faculty of Information Technology and Bionics
50/a Práter street, 1083 Budapest, Hungary
blazsek.martin.janos@itk.ppke.hu

***Abstract*—The hippocampus is a part of the brain's navigation and memory systems, creating a cognitive map based on external cues and internally generated cognitive signals. Hippocampal pyramidal cells play a key role in spatial representation by forming place fields. How this representation is formed and maintained is still yet to be fully understood. One fruitful research direction has been the application of calcium imaging techniques *in vivo*, using calcium-sensitive fluorescent dyes to signal neural activity. This review briefly summarizes its uses in hippocampal spatial representation research, especially when used in conjunction with two-photon microscopy.**

***Keywords*-calcium imaging, two-photon microscopy**

I. Introduction

The hippocampus plays a key role in cognitive processes such as navigation and memory formation. Hippocampal pyramidal cells called place cells are selectively active at specific locations in the environment [1]. The area of the environment to which a given place cell is tuned is called the place field (Fig. 1). Place cells tile the environment with their place fields. The hippocampal spatial map is highly dynamic, with cells encoding information about novelty, changes in salient cues, attention and reward. The driving force behind these dynamic changes in coding is mostly unknown but synaptic plasticity is believed to play a role. This brief review focuses on how Ca^{2+} fluorescence imaging has been applied to hippocampal research.

II. Ca^{2+} fluorescence imaging

In vivo Ca^{2+} fluorescence imaging is an experimental technique that typically uses proteins called genetically encoded Ca^{2+} indicators. These proteins comprise two main parts: a Ca^{2+} sensor domain and a fluorescent protein domain. In the presence of Ca^{2+} the sensor domain causes the fluorescent domain to undergo structural changes leading to the emission of photons with a wavelength characteristic to the fluorescent domain. Ca^{2+} imaging is often coupled to two-photon (2P) microscopy, which uses a focused laser beam to excite the target with exactly two concurrent low-energy photons.[2].

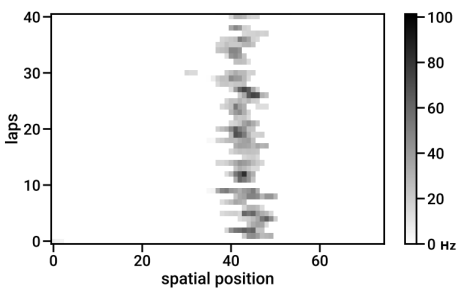

Fig. 1. Firing rate of a place-tuned pyramidal cell in CA1. Darker colors indicate higher firing rates. Note, that the cell fires at the same spatial location as the animal traverses a linear environment multiple times (i.e the cell has a place field).

III. Example studies using Ca^{2+} imaging in rodent hippocampal spatial representation research

Dombeck et al.[3] applied *in vivo* 2P Ca^{2+} imaging for the first time to measure the activity of CA1 pyramidal neurons of mice navigating a virtual environment using the GCaMP3 calcium indicator. They describe their technique in detail from the surgical procedures involving chronic implantation to the identification of regions of interests (ROIs) and subsequent data analysis including the identification of place cells and their respective place fields.

Dong et al.[4] has used *in vivo* 2P Ca^{2+} imaging to investigate the differences between the CA1 and CA3 regions of the hippocampus in mice. They found that place fields in CA3 tend to be more spatially stable, with CA1 place fields more likely to undergo drift over repeated exposures to the same environment.

Priestley et al.[5] also used *in vivo* 2P Ca^{2+} imaging to record the activity of CA1 pyramidal cells. They showed that place fields that appeared during the recording, i.e novel place fields, have properties that suggest that synaptic plasticity mechanisms play a role in their formation.

IV. Acknowledgements

This research was funded by the ERC (CoG #771849), the HHMI (International Senior Research Scholar grant #55008740), the NAP3.0 program, and the NKFIH (#K-124824).

References

[1] O'Keefe, J. & Nadel, L. The hippocampus as a cognitive map. (Oxford university press,1978)
[2] Grienberger, C. & Konnerth, A. Imaging calcium in neurons. *Neuron*. **73**, 862-885 (2012)
[3] Dombeck, D., Harvey, C., Tian, L., Looger, L. & Tank, D. Functional imaging of hippocampal place cells at cellular resolution during virtual navigation. *Nature Neuroscience*. **13**, 1433-1440 (2010)
[4] Dong, C., Madar, A. & Sheffield, M. Distinct place cell dynamics in CA1 and CA3 encode experience in new environments. *Nature Communications*. **12**, 2977 (2021)
[5] Priestley, J., Bowler, J., Rolotti, S., Fusi, S. & Losonczy, A. Signatures of rapid plasticity in hippocampal CA1 representations during novel experiences. *Neuron*. **110**, 1978-1992 (2022)

M. BLAZSEK, "Methods for investigating the mechanisms underlying novel hippocampal spatial representations in calcium imaging experiments" in *PhD Proceedings – Annual Issues of the Doctoral School, Faculty of Information Technology and Bionics, Pázmány Péter Catholic University – 2024.* G. Prószéky, G. Szederkényi Eds. Budapest: Pázmány University ePress, 2024, pp. 16–16.

The effect of population size on adaptive aneuploidy

Camilla CANCRINI
(Supervisor: Andrea CILIBERTO)
Pázmány Péter Catholic University, Faculty of Information Technology and Bionics
50/a Práter street, 1083 Budapest, Hungary
cancrini.camilla@itk.ppke.hu

***Abstract*—The objective of my project is to develop a mathematical framework for describing and predicting the behavior of cells in response to induced missegregation. This topic is of the utmost importance since such events occur to cells treated with antimitotics, a family of drugs frequently employed to treat cancer. Antimitotics alter microtubule dynamics, which hinders cancer cells' capacity to divide. These drugs activate the mitotic checkpoint, which prevents cells from entering mitosis and channels them towards cell death. However, it can happen that cells eventually bypass this checkpoint barrier and start to multiply at high rates of chromosome missegregation. While some cells die, others are capable of reproducing once more and producing resistant offspring via adaptive aneuploidies. The model aims to produce a phase-space diagram, that I will refer to as *survival map*, that will show whether cells become resistant to induced missegregation or go extinct. The major interest is to predict when cancer cells may become extinct. The fate of the population will depend on the initial population size (N_0) and missegregation rate (p) which are two parameters that can be modulated experimentally.**

***Keywords*-Initial population size; Missegregation; Adaptative Aneuploidy; Mathematical Model**

I. Introduction

Missegregation refers to the faulty segregation of chromosomes during cell division. Such errors can result in very different outcomes: cells can undergo apoptosis (i.e. programmed cell death) or become aneuploid (cells with incorrect number of chromosomes). Aneuploid cells show very different behaviors depending on the context. In non-stressful conditions, aneuploidy is traditionally considered harmful because of abnormalities in gene dosage, and is generally linked to altered phenotypes and reduced cell survival ([6],[7]). However, under stress specific aneuploidies can enable cells to survive by providing unexpected selective/proliferative advantages ([2],[3]). Given these opposite outcomes, it is not trivial to understand whether increasing or decreasing the extent of aneuploidies may rescue or hamper cell growth. Even when specific aneuploidies may rescue growth, simply increasing chromosome missegregation does not guarantee the acquisition of the optimal aneuploid state. Other karyotypes may be acquired, all of them decreasing fitness. In my project, I want to investigate what are the most important parameters for achieving the rescuing karyotype under stressful conditions, and how to modulate them to determine the fate of the population. To do this, I combine experiments and modeling. Concerning the experimental work, I use haploid budding yeast cells bearing a mutated variant of TUB2, known as *tub2-401*. These cells exhibit compromised microtubule polymerization ability at 18°C, leading to arrest by the mitotic checkpoint. Consequently, cells undergo cell division with chromosome missegregation. For what concerns the model, instead, I started supposing that cells' fate under missegregative-stressful condition only depends on two specific parameters: the initial population size (N_0) and the missegregation rate (p). During these years, it has been important to me to find strategies to modulate experimentally such parameters. I spent the first year of my PhD setting up an experimental protocol for the modulation of N_0 whereas during my second year I focused on p modulation. This involved creating a revertant strain from *tub2-401*, *tub2-MVYC*, to reduce missegregation. Finally, this year I firstly measured the specific missegregation rate values for the two strains at 18°C and then started to investigate the interplay between p and N_0. Specifically, I fixed the missegregation rate focusing on *tub2-401* cells at 18°C and studied the effect of changing the population size. The data suggest that, given a specific missegregation rate, initial population size determines the evolutionary path that leads to a specific aneuploidy which rescues chromosome missegregation and cellular growth. This was paired with a mathematical model aimed at reproducing experimental results. Exploiting measured parameter values, the model suggested interpretations of the observed dynamics.

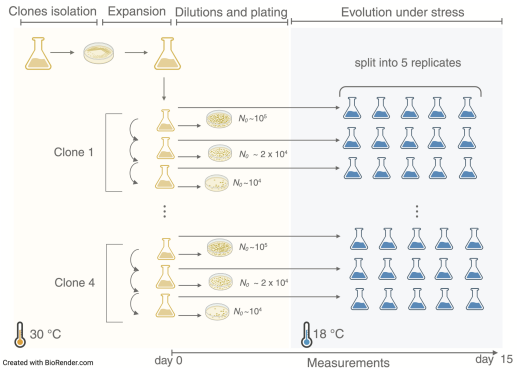

Fig. 1 : **Experimental set up.** Missegregation rate was fixed by evolving *tub2-401* cells at 18°C. Different initial population sizes were obtained through serial dilutions.

References

[1] Gomulkiewicz R, Holt RD., "When does evolution by natural selection prevent extinction?", *Evolution.* 1995; 49(1):201-207. doi:10.1111/j.1558-5646.1995.tb05971.x

[2] Ippolito MR, Martis V, Martin S, et al. , "Gene copy-number changes and chromosomal instability induced by aneuploidy confer resistance to chemotherapy.", *Dev Cell.* 2021; 56(17):2440-2454.e6. doi:10.1016/j.devcel.2021.07.006.

[3] Lukow DA, Sheltzer JM. , "Chromosomal instability and aneuploidy as causes of cancer drug resistance.", *Trends Cancer.* 2022; 8(1):43-53. doi:10.1016/j.trecan.2021.09.002

[4] Pavani M, Bonaiuti P, Chiroli E, et al., "Epistasis, aneuploidy, and functional mutations underlie evolution of resistance to induced microtubule depolymerization.", *EMBO J.* 2021.

[5] Pompei S, Cosentino Lagomarsino M., "A fitness trade-off explains the early fate of yeast aneuploids with chromosome gains.", *Proc Natl Acad Sci U S A.* 2023;120(15):e2211687120. doi:10.1073/pnas.2211687120

[6] Santaguida S, Vasile E, White E, Amon A., "Aneuploidy-induced cellular stresses limit autophagic degradation.", *Genes Dev.* 2015; 29(19):2010-2021. doi:10.1101/gad.269118.115.

[7] Torres EM, Sokolsky T, Tucker CM, et al., "Effects of aneuploidy on cellular physiology and cell division in haploid yeast.", *Science.* 2007; 317(5840):916-924. doi:10.1126/science.1142210.

C. CANCRINI, "The effect of population size on adaptive aneuploidy" in *PhD Proceedings – Annual Issues of the Doctoral School, Faculty of Information Technology and Bionics, Pázmány Péter Catholic University – 2024.* G. Prószéky, G. Szederkényi Eds. Budapest: Pázmány University ePress, 2024, pp. 17–17.

Structural and functional investigation of the wild type and mutant EVH1 domain of the HOMER1 protein

Fanni FARKAS
(Supervisor: Zoltán GÁSPÁRI)
Pázmány Péter Catholic University, Faculty of Information Technology and Bionics
50/a Práter street, 1083 Budapest, Hungary
farkas.fanni@itk.ppke.hu

***Abstract*—The postsynaptic density (PSD) is a complex network which includes millions of proteins positioned beneath the postsynaptic membrane. Homer and Shank scaffold proteins act as one of the most important components of the PSD, whose interactions are crucial for the proper formation of the protein network. Homer1 interacts with mGluR1α5 subunits via their carboxy-terminals as well, with this interaction facilitate the regulation of their postsynaptic localization, translation, and intracellular signaling. Mutations in these proteins have been associated with various neurodegenerative diseases, such as autism or schizophrenia. The focus of my research is a detailed structure and function analysis of the Homer1 protein utilizing NMR spectroscopy and other biophysical methods.**

***Keywords*-PSD; HOMER1; EVH1; mutants; NMR; interaction**

I. Introduction

Under the postsynaptic membrane of neurons, a protein rich complex structure is found, called postsynaptic density (PSD). This protein rich complex structure is characterized by numerous interactions which play a crucial role in various cognitive functions, including learning and memory formation [1]. In case of some neurodevelopmental disorders, such as autism spectrum disorder (ASD) and schizophrenia, alterations were found in the pathology of the postsynaptic density proteins at excitatory synapses. These alterations can cause impairments in cognition, learning and memory [2]. PSD contains millions of proteins and Homer and Shank scaffold proteins play a significant role in structure formation of this complex network. The EVH1 domain of Homer plays a crucial role in protein interactions. It interacts with the Shank and Drebrin proteins and with mGluR1α5 subunits via their carboxy-terminals [3]. To understand the working of this continuously changing, dynamic structure NMR spectroscopy is the best technique. It is used to investigate the three-dimensional structure and dynamics of proteins at the atomic level. However, it requires specific conditions such as a highly concentrated protein sample, low pH, and minimal buffer components, as additives can cause extra signals which obscures the protein signals.

II. Method

To produce the recombinant Homer protein (EVH1 domain) and its two mutant variants (M65I and S97L) commercially available BL21 *E. coli* cells ere used. These bacteria cells were grown in LB media in case of unlabelled proteins, in case of ^{13}C, ^{15}N isotope labelled ones, minimal media was used. These labelling was needed for NMR measurements. After protein production bacteria cell wall was brake by using ultrasonic homogenization method. For protein purification the following steps were used: first immobilized metal affinity chromatography (IMAC) utilizing a Fast Protein Liquid Chromatography (FPLC) system. Next step was a buffer exchange followed by an Ion Exchange Chromatography (IEC) step using an S column. For last purification step, size exclusion chromatography (SEC) was performed to optimize the buffer conditions (pH, NaCl level, etc.) to make the sample suitable for NMR analysis. After these purification steps SDS-PAGE was used to analyse the result. For last step the NMR-compatible sample was sent to Debrecen for NMR measurements. Functional analysis was performed, such as Thermal Shift Assay and Biolayer Interferometry. For bivalent HOMER, nucleotide sequence and plazmids was designed and ordered, and early protein purification steps were performed.

III. Results

The production and purification for both unlabelled and labelled proteins were successful, highly concentrated sample was sent for NMR measurements to Debrecen. The obtained spectra analyzation was started. Functional analysis shows promising results, but further investigations are needed. For Bivalent HOMER protein the designed primers are worked, PCR and cloning was successful as well. Early purification steps seems usable as well but further optimizations are needed.

Acknowledgements

I would like to express my gratitude to Dr. Zoltan Gaspari and Dr. Balint Peterfia for the invaluable guidance and support provided throughout my research endeavor. I am very grateful for your time, patience, and encouragement, which have played a significant role in this research. Project no. TKP2021-EGA-42 has been implemented with the support provided by the Ministry of Culture and Innovation of Hungary from the National Research, Development and Innovation Fund, financed under the TKP2021 funding scheme.

References

[1] Y. Vyas and J. M. Montgomery, "The role of postsynaptic density proteins in neural degeneration and regeneration," *Neural Regeneration Research*, vol. 11, no. 6, p. 906, 2016.

[2] A. Banerjee, J. A. Luong, A. Ho, A. O. Saib, and J. E. Ploski, "Overexpression of homer1a in the basal and lateral amygdala impairs fear conditioning and induces an autism-like social impairment," *Molecular autism*, vol. 7, no. 1, pp. 1–15, 2016.

[3] M. Sheng and E. Kim, "The postsynaptic organization of synapses," *Cold Spring Harbor perspectives in biology*, vol. 3, no. 12, p. a005678, 2011.

F. FARKAS, "Structural and functional investigation of the wild type and mutant EVH1 domain of the HOMER1 protein" in *PhD Proceedings – Annual Issues of the Doctoral School, Faculty of Information Technology and Bionics, Pázmány Péter Catholic University – 2024.* G. Prószéky, G. Szederkényi Eds. Budapest: Pázmány University ePress, 2024, pp. 18–18.

The possible molecular mechanisms shaping postsynaptic long-term potentiation governed by the ratio of different AMPA receptor subunits

Gábor FARKAS
(Supervisor: Szabolcs KÁLI)
Pázmány Péter Catholic University, Faculty of Information Technology and Bionics
50/a Práter street, 1083 Budapest, Hungary
farkas.gabor@itk.ppke.hu

***Abstract*—A sophisticated network of intracellular signaling pathways in the spine heads of postsynaptic dendrites remarkably takes part in shaping synaptic plasticity - the cellular-level basis of learning and information storage in the brain. Using computational tools to investigate networks of biochemical cascades is a well-established research method. The underlying molecular mechanisms of long-term potentiation (LTP) were studied with a detailed, experimental data-driven computational model. According to our findings, the ratio of different AMPA receptor subunits significantly influences the possible molecular-level changes that shape synaptic plasticity.**

***Keywords*-synaptic plasticity, postsynaptic LTP, molecular mechanisms, AMPAR subunits**

I. Introduction

Long-term potentiation (LTP) is the activity-driven strengthening of the efficacy of synaptic transmission. Besides the biophysical features of neurons, intracellular biochemical signaling pathways also contribute to the formation of complex neuronal functions such as activity-dependent synaptic plasticity. The experimental measurement of the interactions between biochemical cascades is a difficult task, thus computational modelling combined with experimental data is a good approach to examine these interactions and make predictions. The effects of different plasticity induction protocols, the roles of signaling pathways, and individual molecular species were investigated using a computational model located in a hippocampal CA1 pyramidal cell spine head.

II. Methods

A computational model of plasticity-related intracellular signaling pathways was created based on the model described in [1]. The model was used to fit experimental data gathered from papers in which LTP was examined. The model simulations were run using the reaction-diffusion submodule [2] of the NEURON simulator. The Neuroptimus optimization software tool [3] was used to optimize the model parameters. The Neuroscience Gateway (NSG) [4] provided high-performance supercomputers were utilized to carry out the computationally heavy optimizations. Since the resulting models fit the experimental data sufficiently, they were used for further investigations of the underlying molecular mechanisms.

III. Results

After the analysis of the model fittings, it was found that the ratio of the GluR1 and GluR2 AMPA receptor subunits significantly influences the possible molecular mechanisms

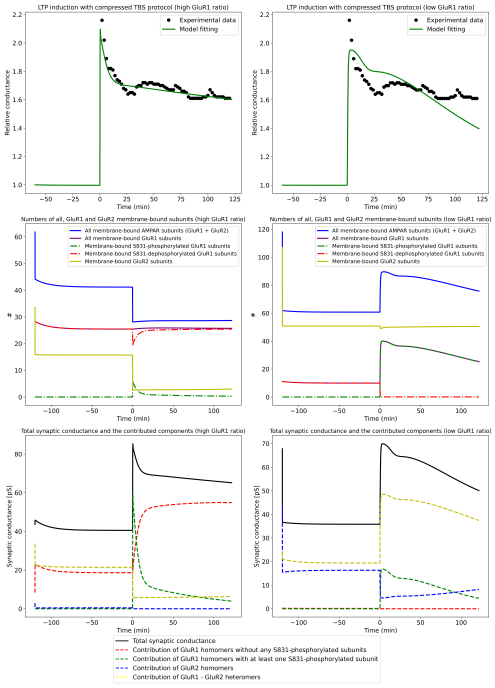

Fig. 1. Different molecular mechanisms shape postsynaptic LTP in a GluR1 ratio-dependent manner.

that determine the changes underlying altered synaptic conductance, which is a measurement of synaptic response to a plasticity induction stimulus. The possible actions and effects of individual biomolecules participating in particular mechanisms were also explored. The left side figures in Figure 1. illustrate the model fitting to experimental data, the time courses of the changes in the number of different AMPAR subunits, and the contributions of different AMPA tetramers to total synaptic conductance, in the case of high GluR1 ratio (0.78). The right side figures show the model fitting and the same changes in the case of low GluR1 ratio (0.31).

References

[1] T. Mäki-Marttunen, N. Iannella, A. Edwards, G. Einevoll, and K. Blackwell, "A unified computational model for cortical post-synaptic plasticity," *eLife*, vol. 9, p. e55714, 07 2020.
[2] R. Mcdougal, M. Hines, and W. Lytton, "Reaction-diffusion in the neuron simulator," *Frontiers in Neuroinformatics*, 11 2013.
[3] M. Mohacsi, M. Torok, S. Sáray, and S. Kali, "A unified framework for the application and evaluation of different methods for neural parameter optimization," pp. 1–7, 07 2020.
[4] S. Sivagnanam, A. Majumdar, K. Yoshimoto, V. Astakhov, A. Bandrowski, M. Martone, and N. Carnevale, "Introducing the neuroscience gateway," *CEUR Workshop Proceedings*, vol. 993, 01 2013.

G. FARKAS, "The possible molecular mechanisms shaping postsynaptic long-term potentiation governed by the ratio of different AMPA receptor subunits" in *PhD Proceedings – Annual Issues of the Doctoral School, Faculty of Information Technology and Bionics, Pázmány Péter Catholic University – 2024.* G. Prószéky, G. Szederkényi Eds. Budapest: Pázmány University ePress, 2024, pp. 19–19.

Cardiac response of patients with complete and incomplete spinal cord injury to functional electrical stimulation driven cycling training

Amelita FODOR
(Supervisor: József LACZKÓ)
Pázmány Péter Catholic University, Faculty of Information Technology and Bionics
50/a Práter street, 1083 Budapest, Hungary
fodor.amelita@itk.ppke.hu

***Keywords*-FES cycling; spinal cord injury; cardiac response**

I. Introduction

Functional Electrical Stimulation (FES) leg cycling has garnered attention as a rehabilitation method for individuals with neurological conditions, including spinal cord injury (SCI). This study aimed to explore the cardiac responses to FES leg cycling in both incomplete and complete SCI patients, offering insights into the acute cardiovascular effects of this intervention.

II. Methods

Thirty-one SCI patients participated in the study, with 12 classified as complete (iSCI) and 19 as incomplete (cSCI). Training sessions were conducted twice a week, with each session comprising a 30-minute FES leg cycling. Blood pressure, heart rate, and performance metrics were monitored throughout the sessions. Statistical analysis included Pearson's correlation coefficient and Student's t-test.

III. Results

Distinct patterns in cardiac responses were observed between iSCI and cSCI groups. Complete SCI patients exhibited an initial increase in blood pressure during stimulation, followed by a plateau and subsequent decrease. In contrast, iSCI patients showed a rapid increase in blood pressure, reaching a maximum midway through the session before declining. Pulse values mirrored these trends, with significant differences between the groups, particularly in maximum pulse values. However, correlations between intra-session changes indicated convergence in cardiac responses, particularly evident between the fifth and tenth sessions in both groups. Performance therefore significantly higher among iCSI's group.

IV. Conclusion

The study underscores the importance of considering injury severity when evaluating cardiac responses to FES leg cycling in SCI patients. Incomplete SCI patients demonstrated greater variability in responses, likely due to variable motor functions below the injury level. Conversely, complete SCI patients exhibited more consistent adaptations to training, suggesting potential cardiovascular benefits over time. These findings highlight the potential of FES leg cycling as a rehabilitation intervention to improve cardiac responses in complete SCI patients, warranting further research to optimize protocols for individuals with SCI.

Acknowledgements

I would like to express my gratitude to Lilla Botzheim and Mariann Mravcsik for additional supervision of my research; the Wigner Research Centre for Physics, the National Institute for Medical Rehabilitation, and University of Pécs for providing me instrumental and professional support and knowledge to my studies. This research was supported by the National Research, Development and Innovation Fund, Hungary, Grant number: TKP2021-EGA-35.

A. FODOR, "Cardiac response of patients with complete and incomplete spinal cord injury to functional electrical stimulation driven cycling training" in *PhD Proceedings – Annual Issues of the Doctoral School, Faculty of Information Technology and Bionics, Pázmány Péter Catholic University – 2024.* G. Prószéky, G. Szederkényi Eds. Budapest: Pázmány University ePress, 2024, pp. 20–20.

A cellular automaton approach to simulate the growth of yeast cell colonies

Bence GAIZER
(Supervisors: Attila CSIKÁSZ-NAGY, János JUHÁSZ)
Pázmány Péter Catholic University, Faculty of Information Technology and Bionics
50/a Práter street, 1083 Budapest, Hungary
gaizer.bence.tamas@itk.ppke.hu

***Abstract*—One of the most common methods of microbiological research is the cultivation of cell colonies on agar plates. During these experiments, researchers can examine the functionality of cells, including their reaction to environmental effects, their use of different resources and interaction between varying strains. These experiments are time-consuming and resource-intensive, therefore we aim to develop a computer simulation model to reduce the need for physical experiments. Traditional agent-based models, while effective, suffer from high computational demands as the number of simulated cells increases. To overcome this limitation, we propose a cellular automaton-based approach that uses state aggregation to enhance efficiency, especially with large cell populations.**

***Keywords*-cell colony simulation; cellular automaton; microbial simulation; computer simulation, multicellular systems**

I. Introduction

State aggregation is a common computational method, used to reduce complexity of a model by grouping entities of similar states, tracking aggregated information instead of details on each individual agent. It scales very well with the number of entities, which is advantageous in case of cell colony simulation, where the number of cells falls commonly in the millions and over.

There are weaknesses of state aggregated models as well. The number of states differentiated increases computational requirements, therefore good performance can be reached by discretising states with a resolution low as possible; however a low resolution would mean the loss of precision.

In our model, there are three states by which entities are differentiated: two spatial dimensions and an abstract variable describing how far a cell progressed in the cell cycle towards mitosis. The former two naturally arrange the model in a spatial grid, with the third forming a vector, representing the number of cells in each maturity level. Figure 1 shows a schematic representation of our state aggregation implementation.

II. Development targets

The main challenge of development is finding balance between computational performance and precision. Several of the fundamental mathematical concepts employed in the model have limitations regarding parameters of their implementation, setting a minimal viable configuration for accurate modelling of the biological system.

Another ambition of our work is the introduction of objective physical parameters, wherever it is possible. This might enable us to make parameter more efficient by measurement of well-defined properties in simple experiments, providing accurate seed data.

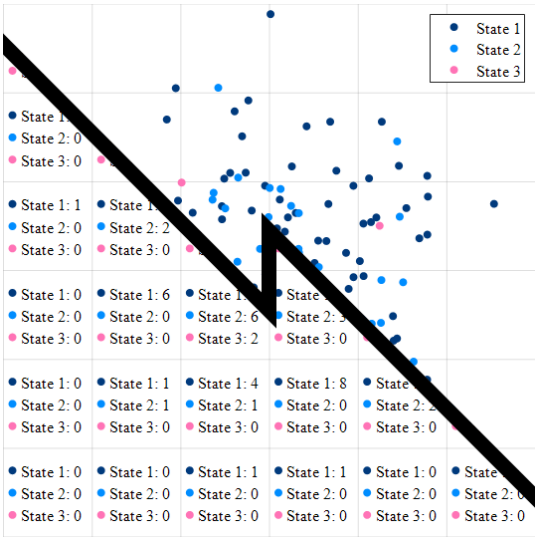

Fig. 1. Top right: in an agent-based model, entities are stored individually, with its associated properties. Bottom left: In a state aggregated model, number of entities is stored for each spatial segment, grouped by their respective discrete state

III. Results

First prototypes of the algorithm showed promising results, proving the viability of the method. The use of physical parameters was successfully implemented, backed by several benchmark tests. It was also established that changing time- and spatial resolution of the simulation within reasonable limits does not influence the simulation results to a significant extent.

however in the current stage the computational performance is not suitable for validation of results or parameter estimation. Our current focus is on optimization of the program code, also taking into consideration implementation in a higher level programming language.

Acknowledgements

Special thanks to Tünde Gaizer, who provided the experimental result necessary for building the model.

The research presented in this paper was supported by OTKA K 134489 project of the National Research, Development and Innovation Office.

References

[1] Gaizer, T., Juhász, J., Pillér, B. et al. *Integrative analysis of yeast colony growth.* Commun Biol 7, 511 2024.

B. GAIZER, "A cellular automaton approach to simulate the growth of yeast cell colonies" in *PhD Proceedings – Annual Issues of the Doctoral School, Faculty of Information Technology and Bionics, Pázmány Péter Catholic University – 2024.* G. Prószéky, G. Szederkényi Eds. Budapest: Pázmány University ePress, 2024, pp. 21–21.

A 2-state phenomenological model quantifies budding yeast cell-cycle arrest and re-entry dynamics

Valentina GUARINO
(Supervisor: Andrea CILIBERTO)
Pázmány Péter Catholic University, Faculty of Information Technology and Bionics
50/a Práter street, 1083 Budapest, Hungary
guarino.valentina@itk.ppke.hu

***Abstract*—Recent studies [1] have uncovered an intriguing link between cell growth, defined as the increase in cell mass and cell volume, and cell-cycle progression in proliferating cells. This interconnection affects cell size and cell density homeostasis, which are normally maintained by tightly regulating the biosynthetic machinery[2]. For example, a prolonged G1 phase can lead to excessive volume growth and cytoplasmic dilution due to excessive growth time, as demonstrated in budding yeast. This extended growth phase disrupts density homeostasis and impairs proper cell-cycle progression, triggering senescence-like phenotypes and therefore influencing the dynamics of cell-cycle re-entry. Cellular senescence, characterized by permanent cell-cycle arrest and enlarged cell size, is a well-known hallmark of cancer [3]. Given the relevance of these features for understanding cancer senescence, we need a quantitative framework, rooted on budding yeast but easily generalizable, to understand the dynamics of key cell's features such as density, mass and volume during a prolonged cell-cycle arrest.**

***Keywords*-Yeast; cell-cycle arrest; mathematical model**

I. Background

Controlling cell-cycle progression is essential for maintaining proper cellular function and tissue homeostasis and the precise regulation of cell cycle timing within tissues is critical and can influence processes such as aging and senescence. Recent studies have revealed the strong interplay between cell growth and cell-cycle progression in budding yeast, leading to a loss of the biosynthetic scaling between volume and mass during cell-cycle arrest. Some previous mechanistic modeling efforts explained these behaviors in relation to the molecular processes happening inside the cell[4] but their generalization is not trivial expecially for model systems whose experimental insights are at preliminary states, e.g. mammalian cell lines. We proposed a generalizable deterministic 2-state phenomenological model that, by describing the dynamical evolution of population-level quantities obtained by the integration of cellular-level ones, can accurately reproduce the experimental dynamics observed in previous works[1], already validated with mechanistic models.

II. Model

We set up the quantitative framework by assuming two possible cells' phenotypes, that is the cycling and the arrested one. These phenotypes can evolve under two different regimes, that is an *arrested* regime, describing a cell-cycle arrest state, and a *release* regime, describing the arrest release arrest and the progression into cell-cycle. For each phenotype, the model predicts the dynamical behavior of the number of cells, volume, mass and density both on a cellular level and on a population level by integrating deterministic ODEs.

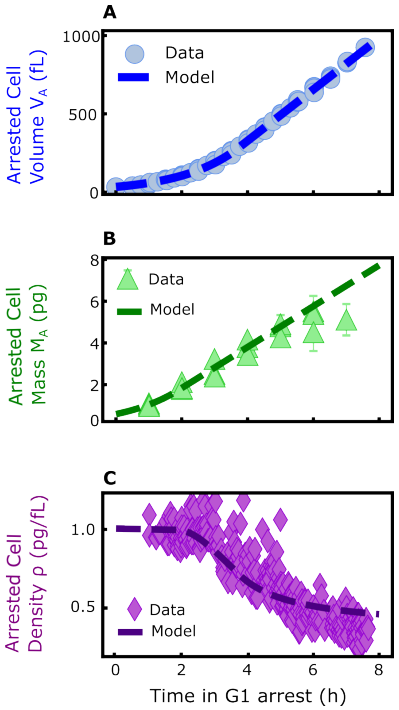

Fig. 1. Our preliminary results demonstrates that a simple phenomenological model is able to reproduce the dynamics of phenotypic quantities under G1 cell-cycle arrest. Figure A and Figure B show the fit of the data[1] respectively for cells volume and mass during arrest. Figure C shows the density prediction. The model can fully reproduce density dilution during arrest.

Acknowledgment

I gratefully acknowledge additional supervision of my research by Marco Cosentino-Lagomarsino.

References

[1] N. G. et al., "Excessive cell growth causes cytoplasm dilution and contributes to senescence," *Cell*, vol. 176, no. 5, pp. 1083–1097, 2019.
[2] N. G. et al., "Relevance and regulation of cell density," *Trends Cell Biol.*, vol. 30, no. 3, pp. 213–225, 2020.
[3] C. L. et al., "Cdk4/6 inhibitor-mediated cell overgrowth triggers osmotic and replication stress to promote senescence," *Molecular Cell*, vol. 83, no. 22, pp. 4062—-4077, 2023.
[4] R. R. et al., "Physical basis of the cell size scaling laws," *eLife*, vol. 12, 2023.

V. GUARINO, "A 2-state phenomenological model quantifies budding yeast cell-cycle arrest and re-entry dynamics" in *PhD Proceedings – Annual Issues of the Doctoral School, Faculty of Information Technology and Bionics, Pázmány Péter Catholic University – 2024.* G. Prószéky, G. Szederkényi Eds. Budapest: Pázmány University ePress, 2024, pp. 22–22.

The role of emotions and emotion regulation in chess games: A neuropsychodynamic approach

Júlia Ágnes HORVÁTH

(Supervisors: Katalin CSIGÓ, György CSEREY)
Pázmány Péter Catholic University, Faculty of Information Technology and Bionics
50/a Práter street, 1083 Budapest, Hungary
horvath.julia.agnes@itk.ppke.hu

***Abstract*—Utilizing a neuropsychodynamic approach, this paper examines how emotional regulatory processes influence executive functioning and strategic thinking in chess, the neurobiological correlates of these processes, and the implications for understanding the process of thinking, adding the new aspect of personality dynamics to the former.**

***Keywords*-emotion regulation; professional chess; Rorschach, neuropsychology, cognitive neuroscience**

I. Emotion regulation in chess

Chess players use the phrase "tilting", when a person makes a mistake during the game and the emotional reaction impacts their functioning. It raises the question if simply controlling emotions is satisfactory for staying in focus during the game – further research on emotional control and emotional flexibility is needed.

Chess requires a high level of cognitive capabilities including memory, visual memory and strategic planning. Research has shown that cognitive abilities have a genetic component[1]. Studies have indicated that even personality traits have a genetic basis, and these traits can affect a chess player's approach to training and competition [2]. In a study [3], the personality traits of young chess players were assessed to determine differences between players and non-players as well as among different levels of chess skill. Children who play chess tend to score higher on Big Five's Openness and Extraversion but lower on Agreeableness compared to those who do not play chess. More successful players also displayed higher levels of Conscientiousness and Emotional Stability [3].

II. Neurobiological Implications

From a neurobiological perspective, emotion regulation is difficult to outline because of its complexity. Emotion processing and regulation is proven to be supported by several structures. Hänggi et al. [4] investigated the neuroanatomical differences between expert chess players and control subjects using various neuroimaging techniques. They found reduced cortical thickness in chess players in some areas (Figure 1). The findings showed thinner cortex areas predominantly in the left and right occipito-temporal junction, an area playing a prominent role in visual representation. Thinner cortical areas were also shown in the precuneus, and supramarginal gyrus, when compared to control subjects [4].

III. Rorschach inkblot test as a psychodynamic addition

The Rorschach test attempts to capture these emotionally charged situations through colorful stimuli and spots; the column of determinants partially reveals how responses to these colorful spots can overwhelm the individual emotionally [5]. It holds great potential to compare how a chess player operates during a game, and if it is in line with their Rorschach performance in terms of emotion regulation. From this perspective, board VIII, which is intended to examine reactions to emotional appeals, could be particularly interesting.

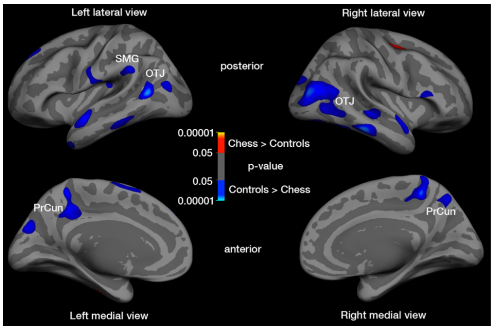

Fig. 1. An exploratory whole brain analysis revealed areas of reduced cortical thickness in chess players. Based on [4].

IV. Conclusion

By integrating neuropsychodynamic approaches, this article highlights the complexity of mental processes in chess and underscores the importance of emotion regulation in achieving a professional rank in the game. Further research should explore longitudinal studies incorporating physiological measurements to track emotional and cognitive changes in chess players, enhancing our understanding of this mechanism.

Acknowledgements

Project no. TKP2021-NVA-27 has been implemented with the support provided by the Ministry of Culture and Innovation of Hungary from the National Research, Development and Innovation Fund, financed under the TKP2021 funding scheme.

References

[1] N. L. Segal, *Born together-reared apart: The landmark Minnesota twin study*. Harvard University Press, 2012.
[2] D. J. Smits and P. Boeck, "From bis/bas to the big five," *European journal of personality*, vol. 20, no. 4, pp. 255–270, 2006.
[3] M. Bilalić, P. McLeod, and F. Gobet, "Personality profiles of young chess players," *Personality and Individual Differences*, vol. 42, no. 6, pp. 901–910, 2007.
[4] J. Hänggi, K. Brütsch, A. M. Siegel, and L. Jäncke, "The architecture of the chess player's brain," *Neuropsychologia*, vol. 62, pp. 152–162, 2014.
[5] L. Giromini, D. J. Viglione Jr, A. Zennaro, and F. Cauda, "Neural activity during production of rorschach responses: An fmri study," *Psychiatry Research: Neuroimaging*, vol. 262, pp. 25–31, 2017.

J. HORVÁTH, "The role of emotions and emotion regulation in chess games: A neuropsychodynamic approach" in *PhD Proceedings – Annual Issues of the Doctoral School, Faculty of Information Technology and Bionics, Pázmány Péter Catholic University – 2024.* G. Prószéky, G. Szederkényi Eds. Budapest: Pázmány University ePress, 2024, pp. 23–23.

Fluid dynamics optimization for miniaturized in vitro permeation test systems

Dorottya KOCSIS
(Supervisor: Franciska ERDŐ)
Pázmány Péter Catholic University, Faculty of Information Technology and Bionics
50/a Práter street, 1083 Budapest, Hungary
kocsis.dorottya@itk.ppke.hu

***Abstract*—In vitro permeation tests are essential to characterize the dermal pharmacokinetics of semisolid topical drugs. The conventional technique is the static Franz diffusion cell, where the fluid flow below the skin is not continuous. On the other hand, different so-called flow-through devices have been developed ensuring physiologically more relevant dynamic fluid flow. Since there is no consensus in the literature on the ideal in vitro permeation test systems and parameters, we aimed to 1) compare three different devices, and 2) optimize the flow rate while using different barrier models.**

***Keywords*-skin-on-a-chip; in vitro permeation test**

I. Summary

Applying innovative test systems in dermatopharmacology offers cost-effective, reproducible, and physiologically relevant experimental models. Microfluidic diffusion chambers are ideal for transdermal drug penetration studies using various barrier models, such as synthetic membranes, in vitro 2D and 3D cell cultures, and ex vivo skin samples. These techniques require fewer tissue samples, fewer sacrificed animals, and smaller amounts of cell cultures or engineered 3D bioprinted tissues compared to traditional in vitro permeation test devices [2]. Conversely, the LiveBox2 setup, designed by IvTech Ltd. (Ospedaletto, Italy), simulates physiological barriers, advancing 2D in vitro models to 3D cell cultures in a dynamic environment. Since dermal barrier modelling in the LiveBox2 has not been performed yet, we aimed to validate and compare it with two in-house developed microfluidic diffusion chambers, a single-channel (sMDC) and a multichannel (mMDC) construct, while optimizing fluid dynamics.

For evaluation, the transdermal delivery of a hydrophilic model drug (caffeine) was tested on four different barrier models. 1) Cellulose-acetate membrane was selected as a control because it is widely used in in vitro release studies. 2) Polyester (PET) membrane was used because it is a common base for cell culture inserts. 3) The third model was a collagen-containing alginate disc, which is an important scaffold in bioprinting. 4) Finally, rat skin permeability was included in the study, as ex vivo measurements are the gold standard. Different flow rates were compared, such as 4 µL/min, 40 µL/min, and 100 µL/min.

All devices provided qualitatively consistent results. Each setup has its advantages: the sMDC requires the smallest samples, the mMDC is the easiest to assemble, and the LiveBox2 is the easiest to clean. Regarding the barrier models, the two membranes showed similar characteristics. The permeability of the blank alginate disc was similar to the membranes, while the permeability of rat skin was generally lower. Higher flow rates maintained higher concentration gradients, i.e., more drug penetrated through the barriers at 40 µL/min than at 4 µL/min. However, at 100 µL/min, the penetrated drug concentrations were reduced, indicating the diffusion-inhibitory effect of higher shear stress on the microfluidic channel wall, confirmed by computational fluid dynamics calculations. The skin-on-a-chip microfluidic devices and the LiveBox2 are all successfully applicable for transdermal penetration studies. However, careful selection of skin model and flow rate is crucial.

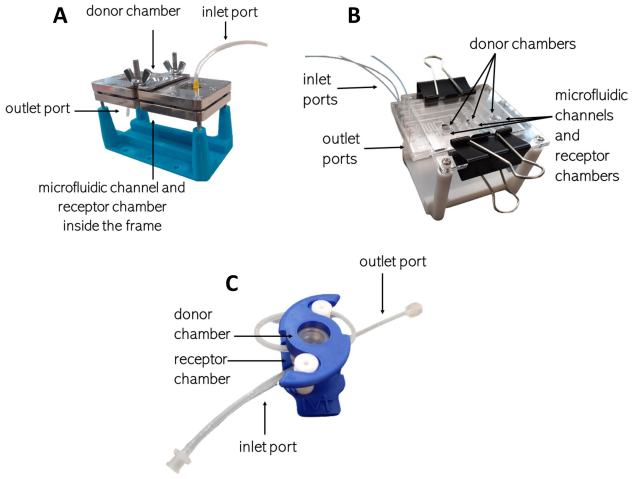

Fig. 1. Diffusion systems: A) Franz-diffusion cell, B) single-channel microfluidic device (sMDC), C) multichannel microfluidic device (mMDC), D) LiveBox2.

Acknowledgements

The author thanks Franciska Erdő for the supervision, Anna Sebestyén, Dániel Sztankovics and Dorottya Moldvai for the help with the alginate studies and András József Laki, Mária Laki, Kristóf Iván, Márton Bese Naszlady for the fabrication of the microfluidic devices. This research was supported by the ÚNKP-23-3 New National Excellence Program (Grant ÚNKP-23-3-II-PPKE-28) and by the project TKP2021-EGA-42 of the Ministry for Culture and Innovation from the source of the National Research, Development and Innovation Fund.

References

[1] D Kocsis, S Dhinakaran, D Pandey, A Laki, M Laki, D Sztankovics, M Lengyel, J Vrábel, MB Naszlady, A Sebestyén, J Ponmozhi, I Antal, F Erdő, "Fluid Dynamics Optimization of Microfluidic Diffusion Systems for Assessment of Transdermal Drug Delivery—An Experimental and Simulation Study", submitted.

[2] B Lukács, Á Bajza, D Kocsis, A Csorba, I Antal I, K Iván, AJ Laki, F Erdő, "Skin-on-a-Chip Device for Ex Vivo Monitoring of Transdermal Delivery of Drugs—Design, Fabrication, and Testing", *Pharmaceutics*, vol. 11, no. 9, p. 445, 2019.

D. KOCSIS, "Fluid dynamics optimization for miniaturized in vitro permeation test systems" in *PhD Proceedings – Annual Issues of the Doctoral School, Faculty of Information Technology and Bionics, Pázmány Péter Catholic University – 2024.* G. Prószéky, G. Szederkényi Eds. Budapest: Pázmány University ePress, 2024, pp. 24–24.

Structure of yeast colonies with different growth strategies

Valentina MADÁR
(Supervisor: Attila CSIKÁSZ-NAGY)
Pázmány Péter Catholic University, Faculty of Information Technology and Bionics
50/a Práter street, 1083 Budapest, Hungary
madar.valentina@itk.ppke.hu

***Abstract*—During evolution, multicellularity and directed growth have evolved along numerous pathways. This altered lifestyle strategy provided ecological advantages over unicellular forms of life [1]. In our research, we model this evolutionary strategy shift using baker's yeast *(Saccharomyces cerevisiae).* This species has already been described as capable of forming facultative multicellular structures in nutrient-deficient environments. In our research, we modify this facultativity to obligate multicellularity.**

Previous studies have demonstrated that knockout of the ACE2 (Activator of CUP1 Expression 2) gene leads to significant phenotypic changes. In its absence, the daughter cell fails to fully separate from the mother cell, resulting in their remaining together in a clonal multicellular structure [2]. The BUD8 and BUD9 (BUD site selection) genes determine the bipolar budding pattern of yeast cells. In the absence of one of them, this pattern is disrupted, and the mother cell only produces a daughter cell at one pole [3]. Combining this with the knockout of ACE2, we obtain a directed growth of a multicellular structure. We perform these modifications in several yeast strains and examine the physiological changes compared to the unicellular ancestor. Through these experiments, we get closer to understanding this phenomenon of evolution and comprehend the ecological advantages or disadvantages associated with such structural changes.

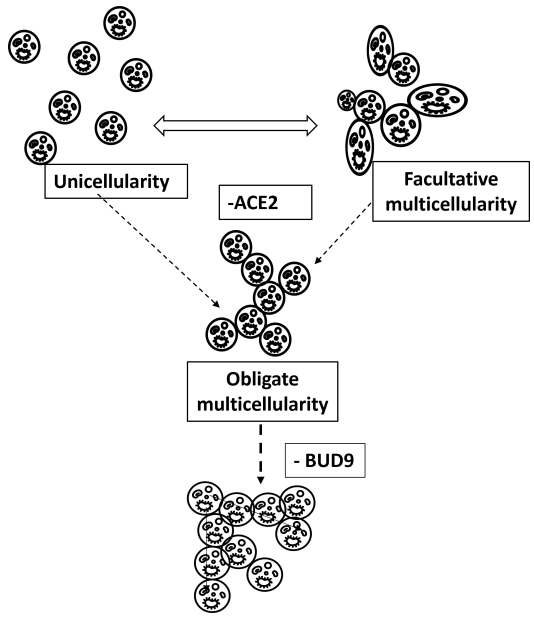

Fig. 1. Graphical abstract

***Keywords*-yeast; multicellularity; differentiation;**

I. Introduction

Colonies formed by yeast cells are influenced by numerous environmental conditions. Within a colony, different groups and layers of cells receive varying amounts of nutrients and oxygen, affecting their function. These differences induce metabolic changes that enable the formation of different cell types. In a yeast colony, there are cells undergoing aerobic respiration, fermentation, and dormancy, and over time, an increasing number of dead cells appear within the colony [4].

The positions of these cell states vary by strain [5]. A smooth-surfaced laboratory strain shows a different colony structure compared to a rougher-morphology wild strain. These strains exhibit different growth patterns, and this structure-function relationship is significant.

In this project, we create new genome-level changes in these already different strains to study their effects on structure and function. One gene that has a significant impact on morphology is ACE2. This transcription factor positively influences the digestion of the post-division septum. If knocked out, the daughter cell cannot separate from the mother cell, creating clonal multicellular structures [2].

Another gene, BUD9, helps establish the typical bipolar budding pattern in the cell. In its absence, cells become unipolar, producing daughter cells only at one pole [3]. By combining these two gene knockouts, we can create a multicellular yeast strain with directed growth, capable of forming colonies with different structures and functions.

So far, our experiments have revealed the altered structure and detected the presence of dead cells as one function. Future experiments will focus on uncovering additional functions.

Acknowledgements

This research was supported by the New National Excellence Program grant ÚNKP-23-3-1-PPKE-46 of the Ministry for Culture and Innovation from the source of the National Research, Development and Innovation Fund and by grant K 134489 from the Hungarian Scientific Research Fund.

References

[1] A. H. Knoll, "The multiple origins of complex multicellularity," *Annual Review of Earth and Planetary Sciences*, vol. 39, pp. 217–239, 2011.
[2] W. C. Ratcliff, J. D. Fankhauser, D. W. Rogers, D. Greig, and M. Travisano, "Origins of multicellular evolvability in snowflake yeas," *Nat Commun*, vol. 20, no. 6, p. 6102, 2015.
[3] A.-B. Krappmann, N. Taheri, M. Heinrich, and H.-U. Mösch, "Distinct domains of yeast cortical tag proteins Bud8p and Bud9p confer polar localization and functionality," *Mol Biol of the Cell*, vol. 18, no. 9, pp. 3323–3339, 2007.
[4] L. Váchová and Z. Palková, "How structured yeast multicellular communities live, age and die?," *FEMS Yeast Research*, p. 18, 2018.
[5] M. Čáp, L. Štěpánek, K. Harant, L. Váchová, and Z. Palková, "Cell differentiation within a yeast colony: Metabolic and regulatory parallels with a tumor-affected organism," *Molecular Cell*, pp. 436–448, 2012.

V. MADÁR, "Structure of yeast colonies with different growth strategies" in *PhD Proceedings – Annual Issues of the Doctoral School, Faculty of Information Technology and Bionics, Pázmány Péter Catholic University – 2024.* G. Prószéky, G. Szederkényi Eds. Budapest: Pázmány University ePress, 2024, pp. 25–25.

Harmonization of structural brain MR images

Vilmos MADARAS
(Consultant: Béla WEISS, Supervisor: Csaba BENEDEK)
Pázmány Péter Catholic University, Faculty of Information Technology and Bionics
50/a Práter street, 1083 Budapest, Hungary
madaras.vilmos@itk.ppke.hu

***Abstract*—In this paper, we evaluate the performance of three harmonization methods (ComBat, CovBat, and ComBat-GAM) on image quality metrics from MRI scans of varying quality. For this purpose, Support Vector Machines with linear and radial basis function kernels, Random Forest, and Extreme Gradient Boosting models were trained to predict the original data batch of the samples on unharmonized and harmonized features. The results show that the selection of relevant covariates significantly impacts harmonization effectiveness.**

***Keywords*-MRI, image quality metrics, harmonization, ComBat, CovBat, ComBat-GAM**

I. Introduction

Medical imaging, especially structural MRI, is a widely used technique for examining changes in the brain, enabling the non-invasive identification of brain pathologies. Guided by clinical questions, artificial intelligence can aid in decision-making, however, developing accurate models requires large datasets. Collecting data from multiple batches has shown promise in providing increased sample sizes, but it may also introduce site-related non-biological variability, known as batch effects. Image harmonization techniques aim to mitigate these effects while retaining variations deriving from biological differences (e.g. sex and age). This paper focuses on three harmonization techniques when applied to images of varying quality.

II. Materials and Methods

62 image quality metrics were extracted from 2072 structural brain MRI scans from 3 databases. Support Vector Machines (SVM) with linear and radial basis function kernels, Random Forest, and Extreme Gradient Boosting were fitted to predict the original database of the samples from these metrics. Harmonization methods included ComBat [1], a widely validated state-of-the-art harmonization method, CovBat [2], which extends ComBat by addressing covariance differences as well, and ComBat-GAM [3] as it introduces nonlinearity through a Generalized Additive Model. Harmonization efficacy was assessed by comparing model predictions before and after applying three different harmonization models, each incorporating a unique set of covariates: a) no additional information, b) image quality category, c) age and gender, and d) all three. Harmonization, when applied, preceded any preprocessing steps. Data were standardized using the training set's mean and standard deviation.

III. Results

Without batch effect mitigation, models accurately predicted test samples, showing strong site-related signals in features. Nonlinear models performed well regardless of harmonization. In the case of the linear model, the effectiveness of harmonization depended significantly on the covariates preserved. Considering more covariates result in greater residual batch effects. Retaining changes related to image quality causes the smallest decrease in effectiveness. Preserving age and gender-related changes alone significantly reduces harmonization performance, with minimal deviation from considering all three covariates. Additionally, ComBat-GAM was found to be slightly less effective in eliminating linear site-related signals from the samples when covariates were considered. ComBat and CovBat perform similarly with image quality metrics.

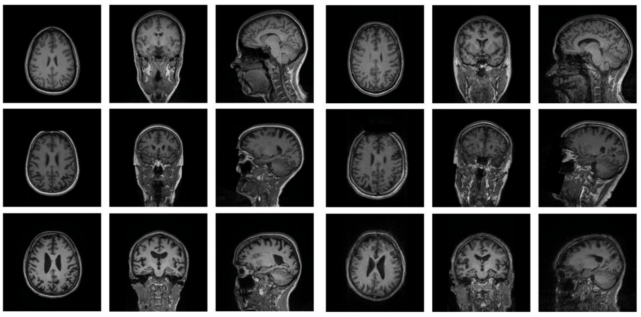

Fig. 1. Examples of T1-weighted MR image slices from the (top row) MR-ART, (middle row) UKBB, and (bottom row) OASIS-3 databases, (on the left) three clinically usable and (on the right) three clinically unusable scans are shown [4]

Acknowledgments

The author is grateful to HUN-REN SZTAKI and HUN-REN TTK Brain Imaging Centre, particularly to Béla Weiss and Csaba Benedek for the opportunity to work on this project.

References

[1] Fortin, Jean-Philippe et al. "Harmonization of multi-site diffusion tensor imaging data." NeuroImage vol. 161 (2017): 149-170. doi:10.1016/j.neuroimage.2017.08.047
[2] Chen, Andrew A et al. "Mitigating site effects in covariance for machine learning in neuroimaging data." Human brain mapping vol. 43,4 (2022): 1179-1195. doi:10.1002/hbm.25688
[3] Pomponio, Raymond et al. "Harmonization of large MRI datasets for the analysis of brain imaging patterns throughout the lifespan." NeuroImage vol. 208 (2020): 116450. doi:10.1016/j.neuroimage.2019.116450
[4] Vakli, Pál et al. "Automatic brain MRI motion artifact detection based on end-to-end deep learning is similarly effective as traditional machine learning trained on image quality metrics." Medical image analysis vol. 88 (2023): 102850. doi:10.1016/j.media.2023.102850

V. MADARAS, "Harmonization of structural brain MR images" in *PhD Proceedings – Annual Issues of the Doctoral School, Faculty of Information Technology and Bionics, Pázmány Péter Catholic University – 2024.* G. Prószéky, G. Szederkényi Eds. Budapest: Pázmány University ePress, 2024, pp. 26–26.

The effects and mitigation of the object centering bias in common datasets

Zsófia MOLNÁR
(Supervisor: András HORVÁTH)
Pázmány Péter Catholic University, Faculty of Information Technology and Bionics
50/a Práter street, 1083 Budapest, Hungary
molnar.zsofia@itk.ppke.hu

***Abstract*—The accurate detection and segmentation of synaptic clefts is a crucial step for various neurobiological experiments, as the length and shape of synaptic clefts can serve as complex indicators of neural connectivity and other factors. This research focuses on developing a machine learning-based tool employing novel approaches for synaptic cleft segmentation. The primary challenges lie in representing synaptic clefts due to their relatively small width, as well as accounting for the effects of 3D orientation. The current version of the pipeline, although in early development, includes the essential steps of data preparation, model training, prediction, reconstruction, and evaluation. Future work will involve benchmarking this solution against existing methods to validate its efficacy.**

I. Background

Understanding the neural processes involved in learning and memory is crucial in neurobiological research. Synaptic clefts, the gaps between neurons facilitating neurotransmitter release, play a vital role in neural communication and are implicated in various neurological disorders. This study, based on data from the Cerebral Cortex Research Group, aims to develop a machine learning tool for accurate synaptic cleft detection and shape regression. Traditional methods struggle with the complex nature of synaptic structures, motivating the need for new techniques.

Existing approaches to synaptic cleft detection vary from manual annotation to automated methods [1], but they often lack precision, especially in handling 3D structures. Current gaps include errors in spatial representation and length measurement. This project addresses these issues by introducing a 3D representation-based approach, utilizing convolutional neural networks with tailored loss functions and augmentation strategies. These advancements hold promise for expanding neurological research capabilities, facilitating the creation of more experiments and generating more reliable results.

II. Architecture Overview

The dataset from the Cerebral Cortex Research Group underwent center-line labeling to establish ground truth values. Images were partitioned for training, validation, and testing, with preprocessing steps including grayscale conversion and binary mask generation to isolate synaptic cleft regions. To optimize resource usage, images were tiled with a specified stride, ensuring full dataset coverage without disrupting labeled regions.

The training process utilized DeepLabV3Plus [2] with a ResNet34 [3] encoder. Sequential tiled images were processed to capture temporal dependencies, with data augmentation techniques applied within the training pipeline. Furthermore, a distance-based label mapping technique was utilized to extend cleft boundaries, while a custom loss function prioritized minimizing false negatives. Training was conducted using the Adam optimization algorithm with fixed hyperparameters.

III. Results and Future Work

The study shows promising results in synaptic cleft detection and shape regression using a 3D representation-based approach with convolutional neural networks. Experiments reveal insights into optimizing model performance and efficiency, emphasizing the advantages of 3D representations for accurate segmentation. An example of 2D and 3D displays of 3D model-based predictions is shown in Figure 1.

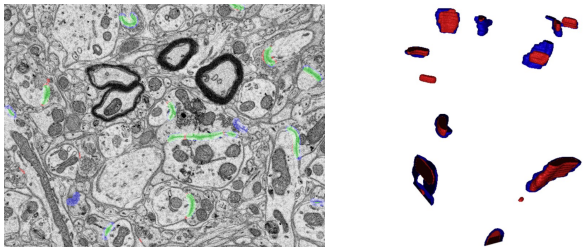

Fig. 1: Display of 3D architecture-based prediction results in 2D and 3D environments. Blue areas indicate ground truth values, red areas indicate predicted values, and green areas on the 2D display indicate the perfectly matching overlap between ground truth and predicted areas.

Feedback from neurobiologists confirms the model's efficacy in identifying previously unlabeled synaptic clefts, suggesting its potential impact on research practices.

Future work involves refining the approach, benchmarking against standards, and developing comprehensive software tools for synaptic research, including 3D visualization capabilities.

IV. Acknowledgments

Our sincere gratitude is extended to Prof. Gabor Nyiri, the head of the Cerebral Cortex Research Group at KOKI, and his colleagues, for generously providing and labeling the dataset used in this study.

References

[1] Hong, Bei, Jing Liu, Weifu Li, Chi Xiao, Qiwei Xie, and Hua Han. "Fully automatic synaptic cleft detection and segmentation from EM images based on deep learning." In *International Conference on Brain Inspired Cognitive Systems*, pp. 64-74. Springer, 2018.

[2] Chen, Liang-Chieh, Yukun Zhu, George Papandreou, Florian Schroff, and Hartwig Adam. "Encoder-decoder with atrous separable convolution for semantic image segmentation." In *Proceedings of the European Conference on Computer Vision (ECCV)*, pp. 801-818. 2018.

[3] He, Kaiming, Xiangyu Zhang, Shaoqing Ren, and Jian Sun. "Deep residual learning for image recognition." In *Proceedings of the IEEE Conference on Computer Vision and Pattern Recognition*, pp. 770-778. 2016.

Zs. MOLNÁR, "Examination of neurons and their connections using artificial intelligence" in *PhD Proceedings – Annual Issues of the Doctoral School, Faculty of Information Technology and Bionics, Pázmány Péter Catholic University – 2024.* G. Prószéky, G. Szederkényi Eds. Budapest: Pázmány University ePress, 2024, pp. 27–27.

Evaluation of heart sound detection methods on fetal phonocardiogram data

Kristóf MÜLLER
(Supervisor: Dr. Miklós KOLLER)
Pázmány Péter Catholic University, Faculty of Information Technology and Bionics
50/a Práter street, 1083 Budapest, Hungary
muller.kristof@itk.ppke.hu

***Abstract*—The basis of most classical phonocardiogram analysis and classification methods is an accurate enough heart sound detection or segmentation method. This usually is a multi-step process with high interdependence. Motivated by this we evaluated the accuracy of the most widely used heart sound detection methods on a fetal phonocardiogram dataset. For evaluation we used the positive predictive value, F1-score, and mean absolute difference.**

I. Introduction

Phonocardiogram (PCG) analysis can be used to detect heart defects, which usually appear as signature noises called murmurs. The heart sounds (S1 and S2) also can contain useful information for diagnosing other problems. Most PCG processing methods use a simple processing flow (Figure 1) of preprocessing, segmentation, feature extraction and classification. This motivates an accurate localization method of heart sounds since the accuracy of later steps highly depend on it. In our case we evaluated the accuracy of different heart sound detection methods on fetal phonocardiograms (fPCG).

II. Methods

The evaluation of a detection method is not trivial, thus we implemented a framework with different performance scores. Since the detection algorithms can produce labels which have a small time difference to the manual labels and can still be deemed accurate, we introduced a tolerance parameter similar to [1]. Each detection was classified true positive if it was inside the time tolerance of a corresponding manual label, else it was considered as false positive. This way not all popular performance metrics can be evaluated. The authors in [1] used positive predictive value (PPV) and F1-score which are what we decided to use as well. We also introduced a the mean of absolute differences (MAE) of the detections and the manual labels. The main focus of our work was evaluating specifically the accuracy of detecting the first heart sound. The tested methods were:

- local maximum detection on the envelope of the signal, with preset minimum distances between peaks (labeled as “naive”)
- adaptive local maximum detection on the homomorphic envelope, with a basic heart sound differentiation method (labeled as “adaptive”)
- Hidden Semi-Markov Model based on [2] (labeled as “HSMM”)

III. Results

We benchmarked the previously mentioned detection methods on an fPCG database consisting of 50 manually labeled 1-minute-long recordings from multiple subjects. The previously mentioned performance metrics were calculated for the S1 detections. These results are shown in Table I.

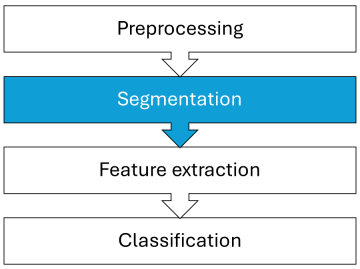

Fig. 1. Simple processing flow of most classical methods

Method	PPV (%)	F1 (%)	MAE (ms)
Naive	96.1	95.9	14.3±8.5
Adaptive	79.9	82.3	33.1±25.2
HSMM	83.5	83.4	19.2±10.4

TABLE I
Benchmark results of the tested methods

IV. Conclusions

We can see that the naive method outperformed the other two methods in every metric. This can be attributed to that the signals in this dataset were good quality and the number of parameters to finetune in this method is minimal. However it is important to note that this method only works well with low noise signals and does not differentiate between heart sounds. The HSMM method on the other hand performed well enough, but the algorithm and the parameters need to be finetuned for a better segmentation of fetal heart sounds. Although the adaptive method is less accurate, this is most likely caused by an inaccurate differentiation between the heart sounds, and it is much faster compared to the HSMM method.

Acknowledgements

This work was supported by the TKP2021-NVA-27 grant, funded by the Ministry of Culture and Innovation with support from the National Research Development and Innovation Fund under the TKP2021 program. I would like to thank Janka Hatvani and Márton Áron Goda for their help during this work.

References

[1] F. Renna, J. Oliveira, and M. T. Coimbra, “Deep convolutional neural networks for heart sound segmentation,” *IEEE Journal of Biomedical and Health Informatics*, vol. 23, no. 6, pp. 2435–2445, 2019.
[2] D. B. Springer, L. Tarassenko, and G. D. Clifford, “Logistic regression-hsmm-based heart sound segmentation,” *IEEE Transactions on Biomedical Engineering*, vol. 63, no. 4, pp. 822–832, 2016.

K. MÜLLER, “Evaluation of heart sound detection methods on fetal phonocardiogram data” in *PhD Proceedings – Annual Issues of the Doctoral School, Faculty of Information Technology and Bionics, Pázmány Péter Catholic University – 2024.* G. Prószéky, G. Szederkényi Eds. Budapest: Pázmány University ePress, 2024, pp. 28–28.

Exploration of kayaker performance via integrated electromyography

Gábor NAGY
(Supervisors: György CSEREY, László GRAND)
Pázmány Péter Catholic University, Faculty of Information Technology and Bionics
50/a Práter street, 1083 Budapest, Hungary
nagy.gabor@itk.ppke.hu

***Abstract*—We measure kayaker performance using onboard accelerometers, segment the motion using data obtained from inertial measurement units (IMU) and gather EMG readings from key muscle groups in a demanding on-water setting. We compared stroke duration to on-water acceleration integral and found a similar relationship with output force as in our earlier on-ergometer study. Higher cadence, lower stroke duration, and higher acceleration integral are physically more demanding and require higher muscle intensities across all measured muscle groups. Thus, the proposed accelerometer-based measurement procedure is suitable for athlete performance measurement.**

***Keywords*-kayaker performance, EMG sensors, IMU sensor, accelerometer**

I. Introduction

The advances in wireless sensors technologies in recent years in Inertial Measurement Units (IMU) and wireless electromyography (EMG) sensors let researchers use these advanced technologies to study motion in a more convenient, non-intrusive ways. [2] To aid the efforts of athletes and their trainer's studies focused largely on-ergometer based studies biomechanical models and wired EMG sensors. [1] Comparative kinematic studies have been developed without integrating EMG signals for on-water and on-ergometer kayaking. [4] This study aims to provide a report on the ongoing efforts to create a reliable framework for IMU and EMG recording and setup a methodology that can be used for longitudinal and inter-subject comparative studies of kayaker biomechanics, muscle usage on-water.

II. Methods

A total of 3 skilled right handed kayakers, all men, actively participated in the study on two different days. A wireless inertial motion capture system (Xsense) was utilized to record on water kayaker motion and wireless EMG sensors (Cometa) were used to acquire EMG signals from strategically chosen muscles to capture a comprehensive representation of the muscular activity involved in the kayaking exercise. We employed the EMG sensors on-board accelerometer to measure boat and paddle acceleration. In total three types of paddling scenarios were investigated to acquire a large number variable samples. EMG readings were preprocessed with adhering to standard guidelines and min-max normalized. [2]

III. Results

On water a stroke is divided into two phases: underwater phase, and air-work or recovery phase. Both phases can be identified from the accelerometer employed on the boat. Integrating the positive pull part is an important speed-dimension quantity used by trainers that could be interpreted as the increasing of speed by the actual pulling. [5] Instead of measuring the paddle force directly we rely on the pull phase x-axis acceleration integral as the proxy of paddle force that propels the kayak. There is a strong negative correlation (-0.5474) between the stroke duration (higher cadence) and the acceleration integral which is similar to on-ergometer force measurements and shows intrapersonal differences. [3] We find with t-test that maintaining higher acceleration integrals are more physically demanding than to maintain lower acceleration integrals, which is reflected in higher muscle intensities and muscle usage. We will focus our efforts on biomechanical modeling in our future studies and to collect more samples from diverse groups of athletes to improve the validity of the results.

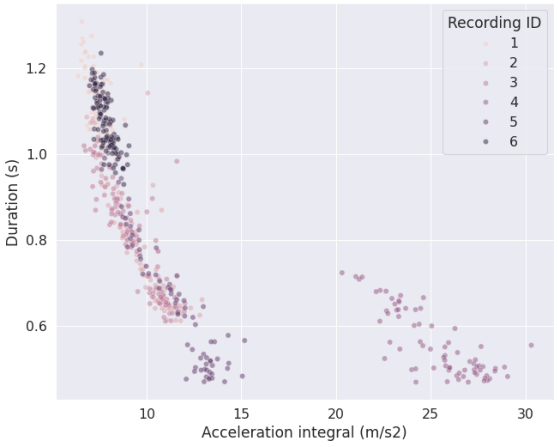

Fig. 1. Relationship between acceleration integral and stroke duration for subject C

References

[1] Bjerkefors A., Tarassova O., Rosén J. S., Zakaria P., Arndt A. *Three-dimensional kinematic analysis and power output of elite flat-water kayakers.* Sports Biomechanics, 17, 1–14. (2017)

[2] Tapia B., Soto I., Martinez D., Candolfi N. *Myoelectric Interfaces and Related Applications: Current State of EMG Signal Processing – A Systematic Review.* IEEE Access. PP. 1-1. (2020)

[3] Nagy G., Komka Zs., Szathmáry G., Katona P., Gannoruwa L., Erdős G., Tarjányi P., Tóth M., Krepuska M., Grand, L., *Multimodal Approach for Kayaking Performance Analysis and Improvement* International Journal of Computer Science in Sport, Vol 19, pages 50-79, 10.2478/ijcss-2020-0010

[4] Klitgaard K., Hauge, C., Oliveira A. S., Heinen F. *A kinematic comparison of on-ergometer and on-water kayaking.* European journal of sport science, 21(10), 1375–1384. (2021)

[5] Vadai, G., Makan G., Gingl Z., Mingesz R., Mellar, J., Szepe T. Csamango, A. *On-water measurement and analysis system for estimating kayak paddlers' performance.* 36th International Convention on Information & Communication Technology Electronics & Microelectronics (MIPRO), 2013. 131-136.

G. NAGY, "Exploration of kayaker performance via integrated electromyography" in *PhD Proceedings – Annual Issues of the Doctoral School, Faculty of Information Technology and Bionics, Pázmány Péter Catholic University – 2024.* G. Prószéky, G. Szederkényi Eds. Budapest: Pázmány University ePress, 2024, pp. 29–29.

Interaction between the GKAP scaffold and DLC2 hub proteins: an integrative modeling approach

Eszter NAGY-KANTA
(Supervisor: Zoltán GÁSPÁRI)
Pázmány Péter Catholic University, Faculty of Information Technology and Bionics
50/a Práter street, 1083 Budapest, Hungary
nagy-kanta.eszter@itk.ppke.hu

I. Introduction

Scaffold proteins of the post-synaptic density (PSD) have been shown to have a high relevance in different neuronal disorders, as they participate in the regulation and modulation of protein-level processes of learning and memory. GKAP (guanylate-kinase associated protein) is an important scaffold protein in the PSD, accumulating essential signal transmission proteins like the NMDA receptors-PSD-95-Shank-Homer scaffold complex, but also connecting to the dynein motor via dynein light chain 2 (DLC2) molecule [1]. Most of GKAP is predicted to be disordered. DLC2 has been identified as a dominant player that can form multivalent complexes with many disordered proteins, promoting their dimerization. GKAP contains two linear motifs which are involved in DLC2-binding, and DLC2 is capable of binding two ligands simultaneously, therefore the most likely stoichiometry of their complex is 2:2 (i.e. 2 GKAP monomers and 2 DLC2 dimers) [2]. Here, we describe the multivalent GKAP-DLC2 interaction with NMR titration measurements and molecular dynamics calculations.

II. Methods

We were using plasmid vector technology in *E. coli* bacteria for protein expression, and affinity chromatography, ion exchange chromatography and size-exclusion chromatography for the purification of the dynein binding region of GKAP. ^{15}N- and ^{13}C isotopic labeling was used for the interacting partners. NMR measurements were executed at 298K on a Bruker 800 MHz spectrometer, with the help of Permi Perttu and his colleagues, at the University of Jyväskylä, Finland.

III. Results and Discussion

The segment spanning residues 655-711 in the rat GKAP protein is predicted to be intrinsically disordered by various methods. Our experimental results (^{1}H-^{15}N-HSQC signal dispersion, secondary chemical shift values) confirm these predictions. Considering the titration NMR spectra, our results suggest that both binding sites participate in the binding of DLC2, but GKAP retains partial flexibility even in bound form. We evaluated the molecular dynamics simulations regarding their consistency with the experimental observations. None of the previously described DLC2 complex structures have similar amino acid compositions in the binding motif sequences. Furthermore, only one study have been performed before, where the flexibility of a disordered, bivalent DLC2 partner protein segment has been characterized with NMR experiments [3]. Our results are in accordance with theirs.

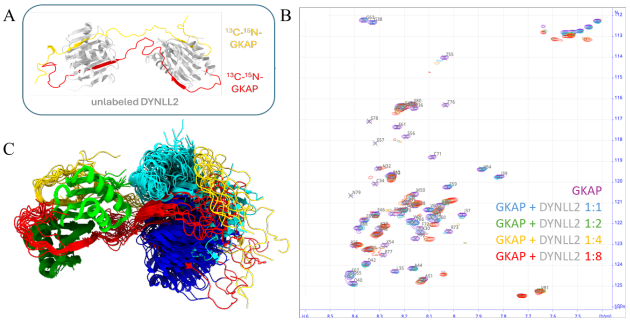

Fig. 1. NMR and molecular dynamics (MD) analysis of the bivalent DLC2-binding segment of the intrinsically disordered protein GKAP. **(A)** The experimental desing of the NMR titration measurements illustrated with the initial structure of the molecular dynamics simulations. **(B)** ^{1}H-^{15}N-HSQC spectra of the titration points with the stoichiometry of 1:1 (blue), 1:2 (green), 1:4 (yellow) and 1:8 (red). Amide NH peaks chemical shift assignment of the free GKAP is visible on the spectrum. **(C)** One example of the molecular dynamics calculations representing the complex structure. The calculations support the hypothesis that both binding sites participate in the binding, and GKAP retains partial flexibility even in bound form. Structural illustrations were created with ChimeraX.

IV. Acknowledgements

Project no. TKP2021-EGA-42 has been implemented with the support provided by the Ministry of Culture and Innovation of Hungary from the National Research, Development and Innovation Fund, financed under the TKP2021 funding scheme. The author thanks Zoltán Gáspári, Permi Perttu, Helena Tossavainen, Bálint Ferenc Péterfia, Fanni Farkas, József Hegedüs, Anna Sánta, Melinda Keresztes, Viktor Farkas and Tünde Juhász for their contribution to this work.

References

[1] S. Naisbitt, J. Valtschanoff, D. W. Allison, C. Sala, E. Kim, A. M. Craig, R. J. Weinberg, and M. Sheng, "Interaction of the postsynaptic density-95/guanylate kinase domain-associated protein complex with a light chain of myosin-V and dynein.," *The Journal of neuroscience : the official journal of the Society for Neuroscience*, vol. 20, pp. 4524–34, jun 2000.

[2] E. Moutin, V. Compan, F. Raynaud, C. Clerté, N. Bouquier, G. Labesse, M. L. Ferguson, L. Fagni, C. A. Royer, and J. Perroy, "The stoichiometry of scaffold complexes in living neurons - DLC2 functions as a dimerization engine for GKAP.," *Journal of cell science*, vol. 127, pp. 3451–62, aug 2014.

[3] P. N. Reardon, K. A. Jara, A. D. Rolland, D. A. Smith, H. T. M. Hoang, J. S. Prell, and E. J. Barbar, "The dynein light chain 8 (LC8) binds predominantly "in-register" to a multivalent intrinsically disordered partner.," *The Journal of biological chemistry*, vol. 295, pp. 4912–4922, apr 2020.

E. NAGY-KANTA, "Interaction between the GKAP scaffold and DLC2 hub proteins: an integrative modeling approach" in *PhD Proceedings – Annual Issues of the Doctoral School, Faculty of Information Technology and Bionics, Pázmány Péter Catholic University – 2024.* G. Prószéky, G. Szederkényi Eds. Budapest: Pázmány University ePress, 2024, pp. 30–30.

Extracellular vesicles promote migration despite BRAF inhibitor treatment

Afrodité NÉMETH
(Supervisor: Tamás Márton GARAY)
Pázmány Péter Catholic University, Faculty of Information Technology and Bionics
50/a Práter street, 1083 Budapest, Hungary
nemeth.afrodite@itk.ppke.hu

***Abstract*—Melanoma is the deadliest form of skin cancer, with incidences growing faster than any other malignancy. It possesses a high capacity for metastasis formation and the potential to develop resistance against targeted therapies. Approximately half of the melanoma patients harbor BRAF mutations, making BRAF-targeted therapies (e.g. vemurafenib, dabrafenib) widely used in clinical practice. However, after the promising initial responses resistance occurs in most of the patients. Resistance can arise through various mechanisms, such as sustained MEK phosphorylation. For this reason, MEK inhibitors are frequently used in conjunction with BRAF inhibitor therapies. Extracellular vesicles (EVs), are important factors in intercellular communication. They are pivotal in the formation of metastases and the development of resistance in cancer. In our previous experiments, we examined the influence of EVs on cancer cell migration, as this process is a critical early step of metastasis formation. Now the commonly used BRAF inhibitors (vemurafenib, dabrafenib), MEK inhibitor (trametinib), BRAF (dabrafenib) and MEK (trametinib) inhibitors combined treatments were investigated against the migration-promoting effect of EVs. The applied cell lines vemurafenib, dabrafenib, trametinib, and the combined dabrafenib and trametinib sensitivity were evaluated. The isolated EVs were utilized to assess the EVs' capability to transfer resistance and their potential to mitigate the effects of inhibitors on cell migration. The effectiveness of EVs from resistant cell line in mitigating the inhibition induced by vemurafenib and dabrafenib surpassed the EVs of the sensitive cells. Conversely, trametinib and the combination treatment of dabrafenib and trametinib were effective in neutralizing the migration-promoting effect of EVs. In summary, our results enhance our understanding of resistance mechanisms to targeted therapies.**

***Keywords*-extracellular vesicles, melanoma, vemurafenib, dabrafenib, trametinib, single cell migration**

I. Introduction

BRAF mutations, found in about half of the melanoma cases, predominantly consist of the BRAF V600E mutation, which comprises over 90% of total mutations. For this reason, BRAF-targeted therapies as vemurafenib and dabrafenib are often used in clinical practices. Vemurafenib specifically targets BRAF V600E, while dabrafenib interacts with various forms of BRAF. Despite initial positive responses, many patients develop resistance to these therapies, often due to persistent MEK phosphorylation. Hence, combination treatments involving MEK inhibitors like trametinib are commonly administered [1]. Extracellular vesicles (EVs) play crucial roles in intercellular communication and contribute to metastasis formation [2]. We explored whether the migration-promoting effect of EVs could be inhibited by vemurafenib, dabrafenib, trametinib, and their combination. This investigation aids in understanding the mechanisms underlying drug resistance.

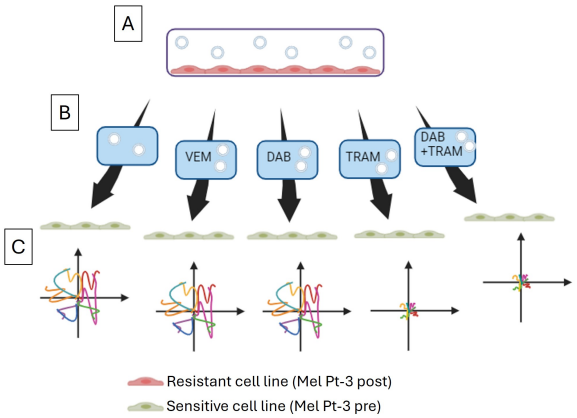

Fig. 1. Graphical abstract.: EVs derived from the more resistant cell lines could more prominently diminish the migration inhibitory effect of BRAF inhibitors (vemurafenib (VEM), dabrafenib (DAB)), albeit they were ineffective against the MEK inhibitor trametinib (TRAM) and the combined treatment of BRAF and MEK inhibitors. A) EVs were produced and isolated; B) Cells were treated with EVs, EVs + (VEM), EVs + (DAB) + EVs + (TRAM), EVs + DABR and TRAM; C) Single-cell migration was followed by video microscopy

II. Summary

The Mel Pt-3 pre cell line was more sensitive to BRAFi, MEKi and BRAFi-MEKi combined treatment than the Mel Pt-3 post cells. All of the combination treatments acted synergistically, which means that the two drugs are more effective together than they would have been individually. EVs were found to counteract the migration-inhibiting effects of BRAF inhibitors (vemurafenib, dabrafenib), but they showed no impact against the MEK inhibitor trametinib and the combination treatment of dabrafenib and trametinib. Our findings suggest that EVs play a significant role in resistance development, although combination therapy may effectively counteract the migration-promoting effect of EVs

III. Acknowledgements

Project no. TKP2021-EGA-42 has been implemented with the support provided by the Ministry of Culture and Innovation of Hungary from the National Research, Development and Innovation Fund, financed under the TKP2021 funding scheme.

References

[1] L. Skudalski, R. Waldman, P. E. Kerr, and J. M. Grant-Kels, "Melanoma: An update on systemic therapies," *Journal of the American Academy of Dermatology*, 2022.
[2] B. H. Sung, "Extracellular vesicles: Critical players during cell migration," *Developmental Cell*, 2021.

A. NÉMETH, "Extracellular vesicles promote migration despite BRAF inhibitor treatment" in *PhD Proceedings – Annual Issues of the Doctoral School, Faculty of Information Technology and Bionics, Pázmány Péter Catholic University – 2024.* G. Prószéky, G. Szederkényi Eds. Budapest: Pázmány University ePress, 2024, pp. 31–31.

Amide Proton Transfer Imaging of Brain Metastasis and Stereotactic Radiosurgery Scars: Preliminary Findings

Bence NÉMETH
(Supervisor: András HORVÁTH)
Pázmány Péter Catholic University, Faculty of Information Technology and Bionics
50/a Práter street, 1083 Budapest, Hungary
nemeth.bencze@itk.ppke.hu

***Keywords*-tumor imaging, Amide proton transfer imaging, quantitative image analysis**

***Abstract*—Amide proton transfer weighted (APTw) imaging shows promise in classifying gliomas and differentiating tumor from edema. This study explores the value of APTw imaging and standard MRI sequences in detecting brain metastasis, tumor recurrence, or necrosis after stereotactic radiosurgery (SRS). In this prospective study, we applied APTw imaging alongside standard MRI techniques to patients with primary tumors of melanoma or lung cancer. Results showed altered APT signals in metastasis residuum.**

I. Introduction

Standard MRI protocols include T2-weighted, native and contrast-enhanced T1-weighted FLAIR, DWI, and ADC maps. APTw imaging, detecting endogenous mobile proteins via amide proton saturation, is now used clinically. This study assesses APTw's efficacy in detecting brain metastasis and distinguishing it from post-SRS changes.

II. Methods

A. Population

From 22 recruited patients, 8 were included. Exclusions were due to metastasis analysis issues or different tumor types. Treatments included radiotherapy, chemotherapy, immunotherapy, or surgical resection. APTw imaging and standard MRI sequences were used.

B. Imaging Techniques

APTw imaging was performed on a 3 Tesla GE Premier scanner using a 2D single-shot spin EPI sequence. Other sequences included DWI, FLAIR, native T1w, ceT1, and T2w.

C. Data Preprocessing

Tissue groups were manually segmented to investigate voxel intensities. The tumor class included intracranial metastases from lung cancer and melanoma. Non-tumor class included post-resectional changes, non-specific white matter lesions, normal white matter, and grey matter.

D. Data Analysis

Voxel intensities were analyzed using unpaired t-tests, SNR, CNR, and random forests. The Wasserstein metric compared intensity distributions. ROI masks were manually segmented on ceT1 and FLAIR sequences.

E. Discrimination Capacity of the Sequences

Wasserstein distance, t-values, SNR, and CNR were calculated on voxel intensities. Random forest models were trained to classify voxels and identify important MRI sequences and APT measurements for classification.

III. Results

APTw imaging showed significant alterations in metastasis residuum and scar tissue locations, differentiating melanoma and lung cancer metastases. APTw had higher SNR and CNR than traditional sequences, showing superior discriminability for tumor detection.

A. Correlation of Voxel Intensities

Significant interactions were found between APT and other MRI parameters, with APTw providing distinct signal changes for metastasis and post-operative scars.

B. Wasserstein Distance and Feature Importance

APTw imaging had a higher capacity to differentiate between tumor and non-tumor clusters compared to other sequences. Feature importance analysis of Random Forest and XGBoost classifier showed APTw's key role in distinguishing metastasis types.

IV. Discussion

APTw imaging demonstrated higher discriminative power than traditional MRI biomarkers, effectively distinguishing between tumor and non-tumor voxels and different metastasis types.

V. Conclusion

APTw imaging shows potential for brain metastasis detection. Larger studies are needed to confirm these findings and explore clinical applications.

VI. Acknowledgements

We thank the study participants and Prof. Dr. Lars Michels, University Hospital Zürich, for his invaluable guidance. Special thanks to GE for the research agreement to implement the CEST APT sequence.

References

[1] Heo, H.Y., Jones, C.K., Hua, J., Yadav, N., Agarwal, S., Zhou, J., van Zijl, P.C., Pillai, J.J., *Whole-brain amide proton transfer (APT) and nuclear overhauser enhancement (NOE) imaging in glioma patients using low-power steady-state pulsed chemical exchange saturation transfer (CEST) imaging at 7T*, J Magn Reson Imaging, vol. 44, pp. 41–50, 2016a.

B. NÉMETH, "Amide proton transfer imaging of brain metastasis: Quantitative image analysis in assesment of brain tumor treatments" in *PhD Proceedings – Annual Issues of the Doctoral School, Faculty of Information Technology and Bionics, Pázmány Péter Catholic University – 2024.* G. Prószéky, G. Szederkényi Eds. Budapest: Pázmány University ePress, 2024, pp. 32–32.

Comprehensive account of cortical functional architecture in the cat visual cortex

Ábel PETIK
(Supervisors: Dániel HILLIER, István ULBERT)
Pázmány Péter Catholic University, Faculty of Information Technology and Bionics
50/a Práter street, 1083 Budapest, Hungary
petik.abel@itk.ppke.hu

***Abstract*—Functional ultrasound imaging is a relatively new imaging modality, that allows the capturing of neural activity in 3D at unprecedented spatial resolution. I have applied this technique to create a map of orientation preference in the early visual cortex of a cat. I have found that the orientation-specific component of the stimulus evoked response used to construct such a map is slow and sustained in comparison to the early-onset non-specific response.**

***Keywords*-functional ultrasound imaging; orientation preference; functional mapping**

I. Introduction

Vision is arguably the most important sense in our everyday lives. Therefore, any impairment of this sensory system significantly reduces an individual's quality of life [1]. Despite its importance, our understanding of how vision functions and what goes wrong when it fails is still quite limited. This is why I have undertaken the task of unravelling the processes of vision in the brain with unprecedented resolution and detail. My goal is to use this knowledge to develop potential new treatments and visual prosthetic devices.

I apply functional ultrasound imaging (fUSI) to map the functional organization of the initial levels of visual processing in the cat visual cortex at high resolution [2].

II. Methods

The functional mapping experiment was carried out using fUSI in an anaesthetised cat. In preparation for the imaging experiment a cranial window was created in the animal's skull to aid the propagation of the ultrasound waves to the target brain tissue. A 12 MHz ultrasound transducer was mounted on the head of the animal using a custom motorised holder. Imaging framerate was set to 2 Hz throughout the experiment.

Visual stimuli were presented on a large screen in front of the animal. They consisted of drifting black and white gratings. Four different grating orientations were used as depicted by the coloured bars in Figure 1, each drifting in a direction perpendicular to the grating orientation, reversing the movement direction every 0.5 seconds. Each stimulus orientation was presented 10 times, with each repetition consisting of a 5 second pre-baseline period, when the screen was grey, then 15 seconds of stimulation, lastly 7 seconds of post-baseline.

The analysis steps of the created recording are the following. First, a baseline correction and a temporal filtering is applied on each repetition. Then the repetitions corresponding to the same stimulus orientation are averaged together to increase signal-to-noise ratio. Lastly, the orientation preference of each voxel is determined by comparing the signal amplitude of the response given to each orientation in a predefined time window.

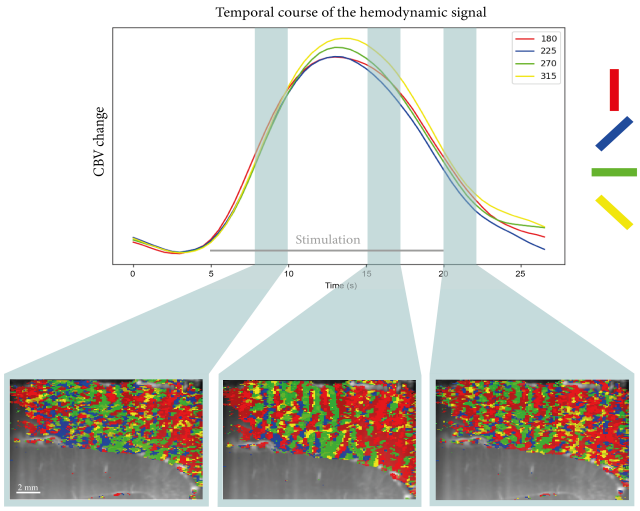

Fig. 1. Comparison of orientation preference maps calculated from signals taken from different time windows.

III. Discussion

Based on the data presented in Figure 1 we can say that the early-onset component of the response is orientation non-specific, since the signal corresponding to the four orientations rises at the same rate, and the orientation map constructed from the 7.5 - 10 seconds time window after stimulation onset is the least structured. This is in contrast to the map created from the data between 15 - 17.5 seconds, which displays an almost columnar organisation. Also note, that in this time window the responses plotted in the top panel show a clear separation, a preference for the 315° orientation in this case. The last time window is comparable to the first.

The construction of such functional maps will help in elucidating how the visual cortex is altered in individuals with vision loss.

Acknowledgements

Supported by grants 2019-2.1.7-ERA-NET-2021-00047, ELKH-POC-2021-026, the Lendület Programme of the Hungarian Academy of Sciences to Daniel Hillier, grant no.129120 implemented with the support by the Ministry of Culture and Innovation of Hungary.

References

[1] H. Vu, J. Keeffe, C. McCarty, and H. R. Taylor, "Impact of unilateral and bilateral vision loss on quality of life," *British journal of ophthalmology*, vol. 89, no. 3, pp. 360–363, 2005.

[2] E. Macé, G. Montaldo, I. Cohen, M. Baulac, M. Fink, and M. Tanter, "Functional ultrasound imaging of the brain," *Nature Methods*, vol. 8, pp. 662–664, Aug. 2011.

Á. PETIK, "Comprehensive account of cortical functional architecture in the cat visual cortex" in *PhD Proceedings – Annual Issues of the Doctoral School, Faculty of Information Technology and Bionics, Pázmány Péter Catholic University – 2024.* G. Prószéky, G. Szederkényi Eds. Budapest: Pázmány University ePress, 2024, pp. 33–33.

Exploring the impact of toxin production in *Saccharomyces cerevisiae* populations

Bíborka PILLÉR
(Supervisor: Attila CSIKÁSZ-NAGY)
Pázmány Péter Catholic University, Faculty of Information Technology and Bionics
50/a Práter street, 1083 Budapest, Hungary
piller.biborka@itk.ppke.hu

***Abstract*—Microbial populations thriving in natural habitats form intricate communities comprising numerous strains, each with the potential to mutually influence one another. One noteworthy interaction arises from the secretion of toxins by "killer" active yeast strains, a phenomenon of considerable importance in food and beverage fermentation. These toxins play a pivotal role in controlling microbial dynamics during fermentation processes, ensuring desired outcomes. Our research aims to investigate the distinctive growth characteristics of various toxin-producing strains of *Saccharomyces cerevisiae*. We want to observe yeast culture growth, both in isolation and within mixed populations, to determine the impact of different toxin-producing strains on the growth of other laboratory strains. To facilitate this investigation, we carefully selected multiple *Saccharomyces cerevisiae* strains and labeled them with fluorescent proteins. Employing a PCR-based method, we identified the specific types of toxins produced by each strain. Subsequent evaluations involved assessing the toxin-producing capabilities of each selected strain on different solid media and within liquid cultures. Our preliminary findings indicate the significant influence of varying conditions on toxin production efficiency and the susceptibility of other strains to these toxins.**

***Keywords*-yeast growth; toxin production, mixed populations**

I. Introduction

The *Saccharomyces* genus comprises a wide range of species, each exhibiting variations in habitat, fermentation abilities, metabolite production, resilience to environmental conditions, and toxin generation. Among these species, *Saccharomyces cerevisiae*, commonly referred to as Baker's yeast, holds significant importance in both research and industry [1]. Wine yeast strains derived from *S. cerevisiae*, isolated from various regions globally, demonstrate unique characteristics that are highly dependent on the varying environmental conditions [2].

At the beginning of the fermentation process, various strains that are present in grapes and in the surrounding environment play a part [3]. However, as the process progresses, these strains diminish in dominance, with *Saccharomyces* taking on the primary role [3]. While it's widely recognized that *Saccharomyces* strains can outcompete non-*Saccharomyces* strains, questions arise about the dynamics when multiple *Saccharomyces* strains are co-cultivated, especially when certain strains possess killer activity.

Interactions between yeast strains have been observed since the 1970s [1]. While cooperation is common as strains collaborate to produce essential substances for survival, the predominant interaction is competition for nutrients [4]. One form of competition stems from the production of toxins [5] by killer active yeast strains, a phenotype resulting from infection by dsRNA viruses known as L-A and M [6]. In a mixed colony, a strain with toxin production capability gains an advantage over others. Currently, there are four distinct types of killer strains, namely K1, K2, K28, and Klus, each exhibiting similarities but also significant differences [6]. This toxin production plays a crucial role in the fermentation of food and beverages, as well as in medical research [5].

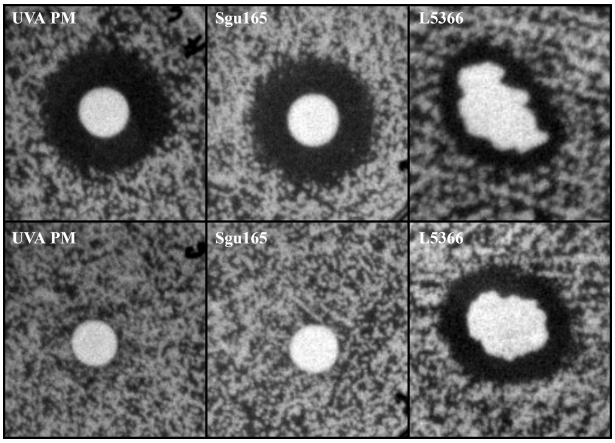

Fig. 1: The pH dependence of toxin production. The images of the upper row show the size of the inhibition zones on pH 4 and the bottom images the results of pH 4.6

Acknowledgements

We acknowledge support by the Hungarian National Research, Development and Innovation Office (NKFI/NRDI) through the Hungarian Scientific Research Fund (OTKA K 134489) and the Thematic Excellence Programme grant no. TKP2021-EGA-42 financed under the K20 and TKP2021 funding schemes.

References

[1] M. Cavaliere, S. Feng, O. S. Soyer, and J. I. Jiménez, "Cooperation in microbial communities and their biotechnological applications," *Environmental Microbiology*, vol. 19, no. 8, pp. 2949–2963, 2017.

[2] T. Gaizer, J. Juhász, B. Pillér, H. Szakadáti, C. I. Pongor, and A. Csikász-Nagy, "Integrative analysis of yeast colony growth," *Communications Biology*, vol. 7, no. 1, p. 511, 2024.

[3] F. Zamora, M. V. Moreno-Arribas, and M. C. Polo, "Wine chemistry and biochemistry," 2009.

[4] J. Friedman and J. Gore, "Ecological systems biology: The dynamics of interacting populations," *Current Opinion in Systems Biology*, vol. 1, pp. 114–121, 2017.

[5] V. Palpacelli, M. Ciani, and G. Rosini, "Activity of different 'killer' yeasts on strains of yeast species undesirable in the food industry," *FEMS Microbiology Letters*, vol. 84, no. 1, pp. 75–78, 1991.

[6] J. Quintero-Blanco, J. Jimenez, and A. Garzón, "A simple multiplex reverse transcription-pcr method for the diagnosis of la and m totiviruses in saccharomyces cerevisiae," *Applied and Environmental Microbiology*, vol. 88, no. 4, pp. e02213–21, 2022.

B. PILLÉR, "Exploring the impact of toxin production in *Saccharomyces cerevisiae* populations" in *PhD Proceedings – Annual Issues of the Doctoral School, Faculty of Information Technology and Bionics, Pázmány Péter Catholic University – 2024.* G. Prószéky, G. Szederkényi Eds. Budapest: Pázmány University ePress, 2024, pp. 34–34.

Biomechanical changes in gait of incomplete spinal cord injured patients after FES cycling therapy

Balázs RADELECZKI
(Supervisor: József LACZKÓ)
Pázmány Péter Catholic University, Faculty of Information Technology and Bionics
50/a Práter street, 1083 Budapest, Hungary
radeleczki.balazs@itk.ppke.hu

Restoration of lost walking functions after spinal cord injury is one of the main goals of spinal cord injury (SCI) treatments and research. According to the literature, approximately 2/3 of the participants had incomplete spinal cord injury (iSCI) [1], [2]. The members of iSCI patient group, had some remaining functions, below the level of injury. Therefore, partial functionalities of the legs are observed, and the remaining neural connections could be utilized for gait rehabilitation. The improvement of iSCI gait training techniques would have a beneficial influence on the personal life of the patients and on social and economic systems.

There are studies which apply additional electrical stimulation (ES) with enhanced involvement of the remaining neural system of the participant during the leg cycling [3].

The paper of Zhou et al. shows that the involvement of cyclic movements of the upper limbs with simultaneous FES assisted leg cycling can improve the walking of iSCI participants compared to traditional FES assisted leg cycling [4]. This exercise is called hybrid FES cycling. Their results proved that a significantly better improvement in walking ability can be achieved with hybrid FES cycling compared to traditional FES cycling.

In this exploratory work, we would like to present the effect of hybrid FES cycling on walking abilities of two iSCI participants. The training duration was 12 weeks. It contained three biomechanical assessments. The training program started and finished with these assessments and there were also assessments after every three weeks of the training.

We assessed conventional gait parameters with motion capture system, but we additionally measured muscle activation intervals (MAI) of the leg muscles to follow the state of the muscles. We also used 3D force plates to measure center of pressure (CoP) curves which potentially gives information about the dynamics of the gait during the clinical rehabilitation. We assume that hybrid FES cycling training has a beneficial effect on gait characteristics, biomechanical gait parameters as step time, step length, walking speed, COP curves and also MAI.

For participant 3 (p03): Comparing the pretraining assessment with the assessment of 6 weeks later, the step time decreased and remained about the same in the 12th weeks. Step length increased substantially during the first 6 weeks an further increased slightly for the 12th week. The same was found for walking speed. The average (across 12 steps) length of CoP curve showed similar changes. The standard deviation (across 12 steps) decreased at the 6th and later at the 12th week regarding all measured parameters.

For participant 7: p07 had the better starting condition. He was able to walk alone small distances without any assistive

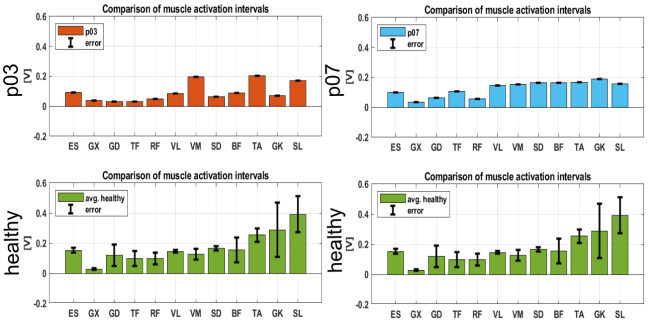

TABLE I
PARTICIPANTS' HEALTH CONDITION AT THE BEGINNING OF THE GAIT ASSESSMENT PROGRAM

Participant	Age	Gender	Level of injury	Training start after injury	Initial supplementary device
p03	63	male	C0-C2, T11-L3	4 months	walker, 1 left knee brace
p07	46	male	C4-C8	9 months	none

TABLE II
PARTICIPANTS' BIO-MECHANICAL PARAMETER CHANGES DURINT THE 12 WEEK LONG TRAINING PROGRAM

	P03			P07		
	0. week	6. week	12. week	0. week	6. week	12. week
L. mean CoP [cm]	38,7±9,9	13,1±2,3	12,1±2,3	16,3±3,9	16,1±3,5	12,2±0,8
R. mean CoP [cm]	23±4,4	13,8±1,1	11,1±0,4	17,3±2,8	16±2	15±1,8
Mean step time [sec]	2,03±0,43	0,64±0,04	0,57±0,03	0,64±0,04	0,63±0,02	0,62±0,02
Average step length [mm]	0,39±0,03	0,56±0,03	0,57±0,03	0,61±0,05	0,64±0,03	0,66±0,03
Average speed [mm/sec]	0,2±0,03	0,89±0,04	1,00±0,06	0,97±0,05	1,02±0,03	1,08±0,06

devices. According to the kinematic data assessment the walking speed had minor decrease. The step length is increased monotonically along the twelve weeks long program. Totally the, the average walking speed has increased monotonically as well. The CoP curves continuously decreased for both the left and right legs but at the end of the program, the right leg has longer mean CoP curve and standard deviation than the left.

The results of the study supports the idea that the hybrid FES cycling rehabilitation method has a beneficial effect on the walking abilities of iSCI participants compared that of conventional rehabilitation. The actual results of the MAI calculations requires further validation and fine tuning.

REFERENCES

[1] V. K. Noonan, "A look at spinal cord injury in canada: Rick hansen spinal cord injury registry (rhscir)–2021 sci data summary," *Topics in Spinal Cord Injury Rehabilitation*, vol. 29, no. Supplement, pp. 165–170, 2023.

[2] N. S. C. I. Center, "Spinal cord injury facts and figures at a glance," *The journal of spinal cord medicine*, vol. 37, no. 3, pp. 355–356, 2014.

[3] S. Piazza, D. Torricelli, J. Gómez-Soriano, D. Serrano-Muñoz, G. Ávila-Martín, I. Galán-Arriero, J. L. Pons, and J. Taylor, "Assessing sensorimotor excitability after spinal cord injury: a reflex testing method based on cycling with afferent stimulation," *Medical & Biological Engineering & Computing*, vol. 56, pp. 1425–1434, 2018.

[4] R. Zhou, L. Alvarado, R. Ogilvie, S. L. Chong, O. Shaw, and V. K. Mushahwar, "Non-gait-specific intervention for the rehabilitation of walking after sci: role of the arms," *Journal of Neurophysiology*, vol. 119, no. 6, pp. 2194–2211, 2018.

B. RADELECZKI, "Biomechanical changes in gait of incomplete spinal cord injured patients after FES cycling therapy" in *PhD Proceedings – Annual Issues of the Doctoral School, Faculty of Information Technology and Bionics, Pázmány Péter Catholic University – 2024.* G. Prószéky, G. Szederkényi Eds. Budapest: Pázmány University ePress, 2024, pp. 35–35.

Binding site mutations of the Shank1 PDZ domain in cancer and ASD

Anna SÁNTA
(Supervisor: Zoltán GÁSPÁRI)
Pázmány Péter Catholic University, Faculty of Information Technology and Bionics
50/a Práter street, 1083 Budapest, Hungary
santa.anna@itk.ppke.hu

***Abstract*—Shank proteins are important scaffolds in the postsynaptic density, whose loss of function was known to be one of the causes autism spectrum disorders (ASD). In recent years, Shank was discovered to be an oncogene, found in various different types of cancer. In this study, effects of ASD- and cancer-associated point mutations of the Shank1 PDZ domain were investigated.**

***Keywords*-postsynaptic density; protein interaction; Shank; cancer; autism spectrum disorder, oncogene; PDZ domain**

I. Introduction

The postsynaptic density (PSD) is a membraneless organelle located in glutamatergic synapses in the brain. Inside the PSD is a complex, dense network of proteins, dynamically rearranging upon stimuli. Shank proteins are a family of scaffolding proteins, shepherding others in the network, ensuring correct localization of proteins to allow for various pathways to function. [1] Loss of Shank proteins results in deformed dendrite morphology, and a weaker synapse - a phenotype seen both in Shank-knockout ASD mice models and Shank-deficit disorders (eg. Phelan-McDermid syndrome) in humans. [2] [3] Recently, Shank genes were identified as oncogenes. Shank proteins play a role in facilitating dendrite growth via the mTOR pathway, however they are not normally expressed in the periphery, therefore their presence causes abnormal cell growth. [4] All members of the Shank family are characterized by a similar multidomain structure. One of these domains, the PDZ is a highly conserved and remarkably promiscuous protein-protein interaction domain, with dozens of known binding partners. [5] To investigate the possible pathways affected in Shank-associated diseases, five missense mutations of the Shank1 PDZ domain were picked and analyzed with experimental and bioinformatics methods.

II. Materials and methods

Proteins were produced and purified as described earlier. [6] The TECAN Spark 20M plate reader was used for fluorescence polarization (FP) experiments. Biolayer interferometry (BLI) was performed on a Fortebio BLItz device. Models were created with UCSF Chimera. Docking experiments were carried out in AutoDock CrankPep. [7]

III. Results

All but one of the point mutations affect binding affinity to GKAP negatively. Changes in sidechain interactions responsible for this were identified. Binding of five other peptides of known Shank1 PDZ interaction partners were modelled by docking simulations.

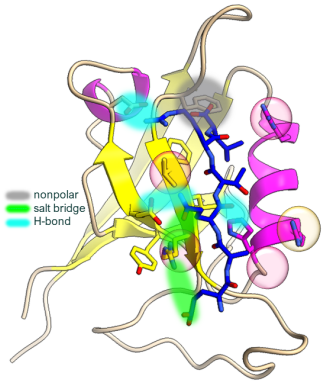

Fig. 1. Structure of the Shank1 PDZ (β-sheets and α-helices are colored yellow and magenta respectively) in complex with a GKAP C-terminal hexapeptide (blue). Important sidechain interactions are highlighted, legend included. The image was created in UCSF Chimera.

IV. Discussion

The cancer associated mutations affect binding affinity differently than the ASD-related one. Some interactions might be affected less by the mutations than the GKAP interaction, suggesting a complex effect on the interaction network.

Acknowledgements

The author thanks supervisor Zoltán Gáspári for his guidance, senior research fellow Bálint Péterfia for his laboratory expertise, and Zsófia Kálmán for help with bioinformatics.

References

[1] M. Sheng and E. Kim, "The Shank family of scaffold proteins," *Journal of Cell Science*, vol. 113, pp. 1851–1856, June 2000.
[2] A. Ö. Sungur, R. K. W. Schwarting, and M. Wöhr, "Early communication deficits in the Shank1 knockout mouse model for autism spectrum disorder: Developmental aspects and effects of social context," *Autism Research: Official Journal of the International Society for Autism Research*, vol. 9, pp. 696–709, June 2016.
[3] C. S. Leblond *et al.*, "Meta-analysis of SHANK Mutations in Autism Spectrum Disorders: A Gradient of Severity in Cognitive Impairments," *PLoS Genetics*, vol. 10, p. e1004580, Sept. 2014.
[4] B. Chen, H. Zhao, M. Li, Q. She, W. Liu, J. Zhang, W. Zhao, S. Huang, and J. Wu, "SHANK1 facilitates non-small cell lung cancer processes through modulating the ubiquitination of Klotho by interacting with MDM2," *Cell Death & Disease*, vol. 13, p. 403, Apr. 2022.
[5] M. Ali, M. M. McAuley, S. Lüchow, S. Knapp, A. C. Joerger, and Y. Ivarsson, "Integrated analysis of Shank1 PDZ interactions with C-terminal and internal binding motifs," *Current Research in Structural Biology*, vol. 3, pp. 41–50, 2021.
[6] A. Sánta, A. Czajlik, G. Batta, B. Péterfia, and Z. Gáspári, "Resonance assignment of the Shank1 PDZ domain," *Biomolecular NMR assignments*, vol. 16, pp. 121–127, Apr. 2022.
[7] Y. Zhang and M. F. Sanner, "AutoDock CrankPep: combining folding and docking to predict protein–peptide complexes," *Bioinformatics*, vol. 35, pp. 5121–5127, Dec. 2019.

A. SÁNTA, "Binding site mutations of the Shank1 PDZ domain in cancer and ASD" in *PhD Proceedings – Annual Issues of the Doctoral School, Faculty of Information Technology and Bionics, Pázmány Péter Catholic University – 2024.* G. Prószéky, G. Szederkényi Eds. Budapest: Pázmány University ePress, 2024, pp. 36–36.

Examination of protein phase separation via *in vitro* and *in silico* methods

András László SZABÓ
(Supervisor: Zoltán GÁSPÁRI)
Pázmány Péter Catholic University, Faculty of Information Technology and Bionics
50/a Práter street, 1083 Budapest, Hungary
szabo.andras.laszlo@itk.ppke.hu

***Abstract*—Protein phase separation is a biochemical process that involves the reversible formation of so called membraneless organelles (MLOs). It is usually initiated by interactions between multivalent proteins, referred to as scaffolds or drivers. Phase separation is known to contribute to various cellular processes such as the organization of postsynaptic densities (PSDs). My work can be partitioned into a computational and an experimental part. The latter utilizes techniques from the fields of fluorescent microscopy and microfluidics in order to observe the phase separation of PSD proteins, while the former aims to reveal correlations between the phenomenon and certain types of sequence motifs.**

***Keywords*-protein phase separation; charged sequence motifs; microfluidics; fluorescent microscopy**

I. Introduction

PSDs are multilayered cellular components that are located on the internal surface of postsynaptic membranes. The dynamic changes in their structure exhibit strong correlations to synaptic strength and plasticity, which in turn are pillars of higher biological functions such as memory and learning. [1] The computational part of my work so far showed that liquid-liquid phase separation (LLPS) correlates with the presence of several charged sequence motifs such as single α-helices (SAHs). The experimental part of my work aims to develop a diffusion-based technique for the detection of protein phase separation that relies on the characteristics of laminar flow within microfluidic devices. This technique has previously been utilized by Arosio et al. for the distinction of solute nanobodies and α-Synuclein fibrils. [2]

II. Methods

All charged residue repeats were identified by the FT-CHARGE algorithm that calculates the charge correlation function of different segments, analysing the charge patterns of its Fourier transform afterwards. The characteristic frequency range of SAHs is 1/9 to 1/6. [3] Custom window functions were used to survey sequences for additional motifs with high charge-densities. Several online databases were considered during the creation of a LLPS-related subset of the human proteome. A recent investigation of RNA-binding sites and disordered regions prompted the creation of a new dataset with more thourough annotations.

As for the experimental part of my work, the size approximation of solute particles requires three major steps. The first step is to apply a fluorescent marker to the individual particles. The second step is to run the fluorescent sample through a microfluidic device with several measurement points along its length. The final step is fitting Gaussian functions to the measured profiles, from which diffusion coefficients and particle sizes are then approximated.

III. Results

As part of my computational studies, a high-throughput approach was developed for the recognition of specific sequence motifs, and several types of charged sequence motifs were shown to correlate with LLPS. The preliminary experiments with fluorescent particles on the nanometer scale show encouraging results that can be seen as a proof of concept for the technique of diffusion-based size approximation.

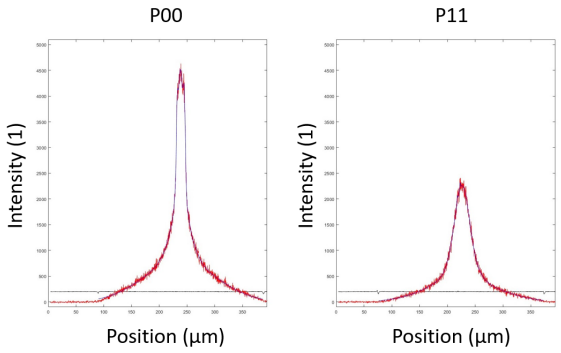

Fig. 1. Fluorescent profiles (red) at the beginning of the device (P00) and at its end (P11). In both cases, a linear combination of Gaussian functions (blue) was fitted to the curve inside the 300 um wide channel.

IV. Acknowledgements

Project no. TKP2021-EGA-42 has been implemented with the support provided by the Ministry of Culture and Innovation of Hungary from the National Research, Development and Innovation Fund, financed under the TKP2021 funding scheme.

V. Publications

A. L. Szabó, A. Sánta, R. Pancsa, and Z. Gáspári, "Charged sequence motifs increase the propensity towards liquid-liquid phase separation," *FEBS Letters*, vol. 596, no. 8, p. 1013-1028, 2022.

References

[1] Z. Feng, X. Chen, M. Zeng, and M. Zhang, "Phase separation as a mechanism for assembling dynamic postsynaptic density signalling complexes," *Current Opinion in Neurobiology*, vol. 57, pp. 1–8, Aug. 2019.

[2] P. Arosio, T. Müller, L. Rajah, E. V. Yates, F. A. Aprile, Y. Zhang, S. I. Cohen, D. A. White, T. W. Herling, E. J. De Genst, and et al., "Microfluidic diffusion analysis of the sizes and interactions of proteins under native solution conditions," *ACS Nano*, vol. 10, no. 1, p. 333–341, 2015.

[3] Z. Gáspári, D. Süveges, A. Perczel, L. Nyitray, and G. Tóth, "Charged single alpha-helices in proteomes revealed by a consensus prediction approach," *Biochimica Et Biophysica Acta*, vol. 1824, pp. 637–646, Apr. 2012.

A. SZABÓ, "Examination of protein phase separation via in vitro and in silico methods" in *PhD Proceedings – Annual Issues of the Doctoral School, Faculty of Information Technology and Bionics, Pázmány Péter Catholic University – 2024.* G. Prószéky, G. Szederkényi Eds. Budapest: Pázmány University ePress, 2024, pp. 37–37.

Application of generative models in modelling the visual system

Péter József SZABÓ
(Supervisors: Gergő ORBÁN, András HORVÁTH)
Pázmány Péter Catholic University, Faculty of Information Technology and Bionics
50/a Práter street, 1083 Budapest, Hungary
peter.jozsef.szabo@itk.ppke.hu

***Abstract*—Generative models play a crucial role as a modeling framework to explain the responses of the visual system. These models are advantageous due to their superb attribute of replicating the causal structure of the world. Additionally, these models are actively researched in the Machine Learning community, and already reached remarkable performance, and have well-established frameworks.**

This work provides a historical overview of the most remarkable generative models that were used as a framework for providing explanations of the human visual system. Starting with the Sparse Coding Model, proposed by Olhausen and Field et al. [1] where the sparsity as a constraint for the latent representation was introduced, followed by the Sparse-Coding Variational Autoencoder proposed by Barello et al. [2] that introduces the Variational Autoencoder Framework to provide remedy for the computation limitations of the Sparse Coding Model, and finally introducing Top-Down Variational Autoencoder proposed by Csikor et al. [3] that extends the framework with hierarchical, top-down connections. These models serve as a basis of the future work, which is detailed in the final section.

I. Introduction

Generative Models have contributed to neuroscience by providing explanations of observed natural response properties. These models are advantageous due to their superb attribute of replicating the causal structure of the real-world.

An image that is falling on the retina originates from multiple sources of the world (such as light source, reflection, pose etc.). These sources are normally latent, not directly available on the pixel space, but coded non-linearly. During perception the goal is to identify these latent sources that generate the sensory stimuli. Perception can be formulated as a statistical inference problem, which aims to summarize the knowledge about the real-world and provide an explanation of how the observations are produced.

The statistical inference problem can be described mathematically as applying the Bayes rule to obtain the posterior over latent sources given the sensory data.

The goal is to model the distribution of the natural stimuli in the real-world.

II. Current and Future work

In the current work, the model proposed by Barello et al.[2] is implemented and can be publicly reached on GitHub[1]. The schematic architecture of the model can be seen on Figure a).

The future plans include the implementation of the TDVAE proposed by Csikor F. et al [3], and the investigation of the impact of a larger patch size.

Future testing on publicly available data is planned, such as on the standardized high-density high throughput data publicly available by Allen Institute. Their cutting-edge technology now allows the registration of thousands of neurons even from higher hierarchical parts of the visual system. They also offer private services for laboratories for validation of specific hypotheses, and with the help of my supervisor, this could be a future possibility.

References

[1] B. Olshausen and D. Field, "Emergence of simple-cell receptive field properties by learning a sparse code for natural images," *Nature*, vol. 381, pp. 607–9, 07 1996.
[2] G. Barello, A. Charles, and J. Pillow, "Sparse-coding variational auto-encoders," *bioRxiv*, 08 2018.
[3] F. Csikor, B. Meszéna, and G. Orbán, "Top-down perceptual inference shaping the activity of early visual cortex," *bioRxiv*, 2023.

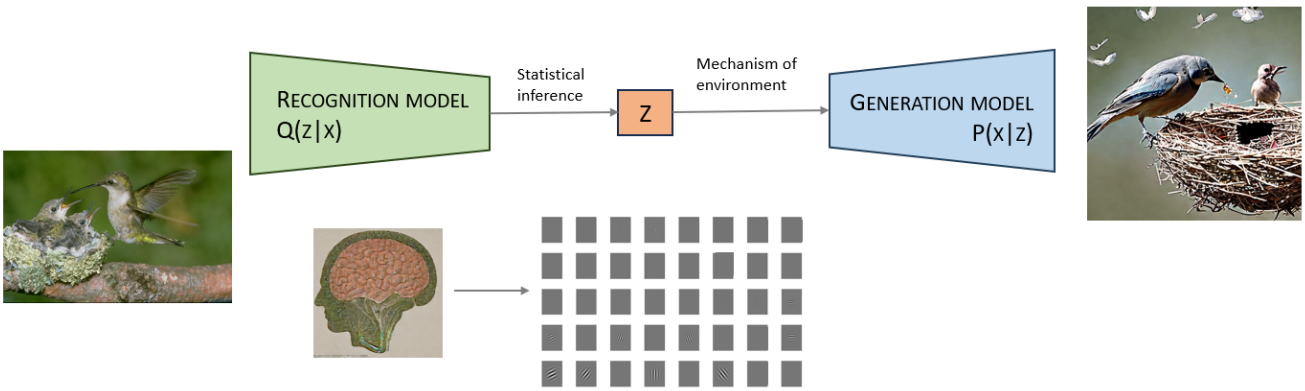

Fig. 1. The Variational Autoencoder Framework. The Recognition model performs the statistical inference using a variational distribution parameterized by the Generative Model. It is in correspondence with the visual system. Both produce a sparse coding of the natural stimuli of the real world. The Generative Model summarizes the mechanism of the environment, where an image, falling on the retina, is generated by multiple sources in the world that are normally latent or hidden from the observer.

[1] https://github.com/Fjuzi/VisionModell

P. SZABÓ, "Application of generative models in modelling the visual system" in *PhD Proceedings – Annual Issues of the Doctoral School, Faculty of Information Technology and Bionics, Pázmány Péter Catholic University – 2024.* G. Prószéky, G. Szederkényi Eds. Budapest: Pázmány University ePress, 2024, pp. 38–38.

Neuropsychodynamic approach to affordance perception and projection in psychological assessment

Péter SZABÓ
(Supervisors: Katalin CSIGÓ, György CSEREY)
Pázmány Péter Catholic University, Faculty of Information Technology and Bionics
50/a Práter street, 1083 Budapest, Hungary
szabo.peter@itk.ppke.hu

***Abstract*—The aim of this paper is to bridge the gap between the psychodynamic concept of projection and the cognitively oriented notion of affordances. This integrative approach addresses a niche in modern psychology lacking proper attempts to reconcile psychodynamic and cognitive psychology.**

***Keywords*-affordance; projection; neuropsychodynamic**

I. Affordances

Affordances are interactional possibilities perceived before object representation [1]. A handle is perceived as something that affords grasping and a chair that affords sitting. More abstractly, affective significance of arousing stimuli could also be considered as an affordance for inviting functionally flexible behaviour. Neuroscientifically, affordances might be related to canonic and mirror neurons [2]. Neuroscientific data suggest that affordance perception is tied to the monitoring of motion possibilities, and social intentions [3], the latter outlining affective significance.

II. Projection

Projection is the process of consciously perceiving something as external while originating from internal unconscious sources [4]. In cognitive terms projection is the unconscious inference of prior experiences, thoughts and affects onto the yet-to-be-explored environment. In projective techniques, like the Rorschach Test, the subject is presented with ambiguous stimuli, like a non-figurative inkblot. This ambiguity provokes the subject to act in a way they generally would in ambiguous situation. This observation then is translated into the subject's psychological analysis [5].

III. Affordances and projection

Every Rorschach card have parts affording something in particular, but they are not obvious, leaving space for projection. It is suggested that certain cards, even if unconsciously, evoke associations related to specific psychological topics. This affordance of the card is called the "demand character", because it invites certain psychologically relevant associations [6]. Investigation of the associational processes evoked by the demand character would provide insight into the organisation of the psyche. Turning affective stimuli into Rorschach-like cards would create potent test stimuli evoking diagnostically valuable responses.

Fig. 1. A Rorschach-like card generated by DALL-E for illustrative purposes. The red stains can evoke assoications related to blood, agression, violence.

IV. Summary

This short article walked through the conceptual relation between affordance perception and projection and their interaction in assessment using projective techniques.

Acknowledgements

Project no. TKP2021-NVA-27 has been implemented with the support provided by the Ministry of Culture and Innovation of Hungary from the National Research, Development and Innovation Fund, financed under the TKP2021 funding scheme.

References

[1] J. J. Gibson, *The ecological approach to visual perception: classic edition*. Psychology press, 2014.
[2] J. Grèzes, J. L. Armony, J. Rowe, and R. E. Passingham, "Activations related to "mirror" and "canonical" neurones in the human brain: an fmri study," *Neuroimage*, vol. 18, no. 4, pp. 928–937, 2003.
[3] L. Fogassi, P. F. Ferrari, B. Gesierich, S. Rozzi, F. Chersi, and G. Rizzolatti, "Parietal lobe: from action organization to intention understanding," *Science*, vol. 308, no. 5722, pp. 662–667, 2005.
[4] G. O. Gabbard. American Psychiatric Pub, 2014.
[5] J. E. Exner Jr, *The Rorschach: A comprehensive system: Basic foundations, Vol. 1*. John Wiley & Sons, 1993.
[6] F. Mérei, "A rorschach táblák felszólító jellege," *Magyar Pszichológiai Szemle*, vol. 16, no. 3-4, pp. 115–125, 1947.

P. SZABÓ, "Neuropsychodynamic approach to affordance perception and projection in psychological assessment" in *PhD Proceedings – Annual Issues of the Doctoral School, Faculty of Information Technology and Bionics, Pázmány Péter Catholic University – 2024.* G. Prószéky, G. Szederkényi Eds. Budapest: Pázmány University ePress, 2024, pp. 39–39.

Drug target affinity prediction using deep learning

János SZALMA

(Supervisors: Attila CSIKÁSZ-NAGY, Erzsébet FICHÓ)
Pázmány Péter Catholic University, Faculty of Information Technology and Bionics
50/a Práter street, 1083 Budapest, Hungary
janos.szalma@itk.ppke.hu

***Abstract*—Accurate prediction of drug-target binding affinity is crucial in drug discovery to identify new drugs and therapeutic targets. Traditional methods like molecular dynamics and docking simulations are computationally intensive and often limited by the availability of 3D protein-ligand structures. To overcome these challenges, we propose a deep learning-based method leveraging extensive datasets and focusing on affinity data. Our method rigorously applies cold protein and cold drug splits to evaluate its generalization capability. In the warm start scenario, our model achieves a Pearson R value of 0.87, while under the cold protein scenario, the Pearson R value slightly decreases to 0.79, indicating the model's robustness with unseen proteins. The cold drug scenario results in a Pearson R value of 0.68, showing the model's ability to handle novel compounds. The most challenging cold both scenario yields a Pearson R value of 0.42, reflecting the difficulty of predicting interactions for entirely new drugs and proteins. Our approach offers a promising solution for improving drug-target interaction predictions, ultimately accelerating the drug discovery process.**

***Keywords*-deep-learning; affinity prediction; drug discovery**

I. Introduction

Accurately predicting how chemicals bind to proteins is a crucial part of discovering new drugs. This process helps identify new treatments, reduce failures in clinical trials, and ensure drug safety. Traditional methods, such as molecular dynamics and docking simulations, are commonly used to find potential protein-ligand interactions. Recently, sequence-based techniques have gained popularity in computational biology, avoiding the use of the rarely available 3D structures[1]. Advances in deep learning have led to the development of neural network models that can extract features from protein sequences and drug molecules, represented as SMILES (Simplified Molecular Input Line Entry System). These models can learn about the characteristics of target proteins and drugs more effectively. By leveraging large datasets and advanced neural network architectures, these methods can provide accurate predictions quickly and efficiently, making them a valuable tool in the drug discovery process.

Methods

We use an extensive database of binding affinity measurements as our primary data source. To evaluate the model's ability to generalize to new drugs and targets, we implement cold protein and cold drug splits. In the cold drug split, some drugs in the test set are not present in the training set, allowing us to assess the model's performance on novel compounds. Similarly, the cold protein split includes proteins in the test set that were not seen during training, testing the model's ability to handle new targets. The most challenging scenario, the cold drug-protein split, involves entirely new drug-protein pairs that were absent in the training data, representing a comprehensive test of the model's generalization capabilities.

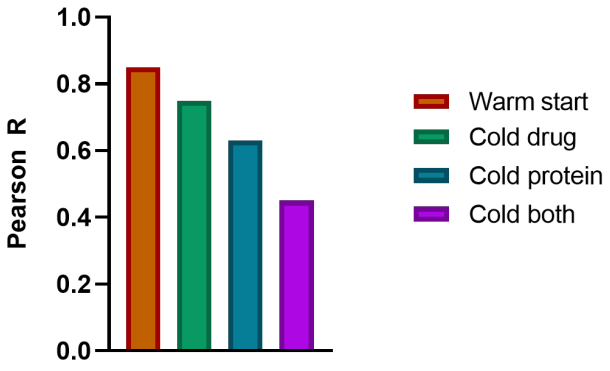

Fig. 1. Model performance for all four validation configurations

We log-transform the binding affinity values to ensure that the data distribution is more suitable for machine learning models. Entries with missing data are removed to maintain data quality, and we filter out interactions where the binding affinity values are outliers or fall below a certain threshold. To model drug-like molecules we use the SMILES representation canonized by the RDKit canonization algorithm. In the case of the protein targets an amino-acid string based representation is utilized. After that these representations are converted into a vector space by employing neural networks based on the language modelling paradigm. The embedding vectors are fed into an interaction network with a neural network head predicting the binding affinity scores. The system is trained using a weighted mean squared error loss function.

Results

Figure 1 illustrates the Pearson R values for our method under different evaluation scenarios. In the warm start scenario, the model achieves the highest Pearson R value of approximately 0.87, indicating a strong linear correlation between predicted and actual binding affinities. In the cold protein scenario, the performance decreases slightly, with a Pearson R value of around 0.79. For the cold drug scenario, the model attains a Pearson R value of about 0.68. The most challenging scenario, cold both (cold drug and cold protein), shows the lowest Pearson R value of approximately 0.42, reflecting the difficulty of generalizing to entirely new drugs and proteins.

Acknowledgments

This work was done using the resources of Cytocast Hungary Kft.

References

[1] Gawehn, E., Hiss, J. A., & Schneider, G. (2016). Deep learning in drug discovery. *Molecular Informatics, 35*(1), 3-14.

J. SZALMA, "Drug target affinity prediction using deep learning" in *PhD Proceedings – Annual Issues of the Doctoral School, Faculty of Information Technology and Bionics, Pázmány Péter Catholic University – 2024.* G. Prószéky, G. Szederkényi Eds. Budapest: Pázmány University ePress, 2024, pp. 40–40.

Exploring universal principles of cellular growth regulation in eukaryotes using budding yeast

Giorgio TALLARICO
(Supervisor: Andrea CILIBERTO)
Pázmány Péter Catholic University, Faculty of Information Technology and Bionics
50/a Práter street, 1083 Budapest, Hungary
tallarico.giorgio@itk.ppke.hu

***Abstract*—While bacterial models have provided insights in growth physiology and cellular resource allocation, limited research exists for eukaryotic cells. This study proposes a combination of mathematical modelling and experimental approaches for enabling a quantitative description of cellular growth and its regulation. Preliminary results shows that the budding yeast *Saccharomyces cerevisiae* follows a similar proteome allocation pattern as predicted by the mathematical models developed for bacteria and this seems to be the result of the TOR pathway sensing and regulation.**

***Keywords*-Yeast; growth laws**

I. Background

In bacteria, recent work has shown how growth physiology can be described by simple mathematical relationships (sometimes termed "growth laws") which formalize complex emerging principles that connect environmental cues to growth and cell composition. These models are based on a broad description of cells, typically organizing proteins into groups based on their function (e.g., ribosomal proteins grouped as the "R class" or "R sector") or shared regulation [1]. Such descriptions naturally reflect the idea that allocating excessive resources to one function can adversely impact others [2], [3].

These models have been instrumental in explaining how cells optimize the allocation of cellular resources to physiological processes and pathways, thereby influencing the molecular composition of the cell in response to specific environmental conditions, such as bacterial response to antibiotic drugs [2], and how they strive to minimize disruption [3]. For example, the linear relationship found between specific growth rate and ribosome content under translation inhibition can be explained by a simple model in which the whole proteome is divided in two distinct classes and the regulation of these two classes arises from the consideration that the sum of their mass fractions is constant [2].

While there is a wealth of literature on bacterial growth laws [2], [3], the available body of research on eukaryotic cells is comparatively small. However, some seminal experimental studies have shown clear evidence of growth laws in both yeast and cancer cells [4], [5] but at the same time, these studies often lack the experimental data required to validate their quantitative models or are more phenomenologically oriented. My PhD project aim is to perform "knowledge transfer" of powerful tools that emerge from work in bacteria to eukaryotic cells, in particular to the budding yeast *Saccharomyces cerevisiae*. The potential results of this project could be also relevant in the field of cancer research, because having a robust quantitative theory for cell growth and proteome allocation for eukaryotic cells could unveil key trade-offs involved in how normal and cancer cells allocate their resources in response to drugs and help designate better treatments.

Recent studies have revealed the conservation of growth laws in eukaryotes, particularly in yeast [4], [6], [7]. This discovery has significant implications for our understanding of cellular processes, especially ribosome biogenesis and its regulation. It suggests that despite variations in regulatory pathways and cellular architecture among different organisms, the regulation of ribosome biogenesis follows similar patterns. In bacteria, these mathematical laws are known to be implemented through the relief of repression of rRNA synthesis by the alarmone ppGpp [2], triggered by the accumulation of uncharged tRNAs [8]. In contrast, in yeast and higher eukaryotes, this regulation could potentially be mediated by the TOR pathway, which controls ribosome biogenesis [9] and monitors the level of free amino acids among its various functions [10], [11].

Acknowledgment

I gratefully acknowledge additional supervision of my research by Marco Cosentino-Lagomarsino.

References

[1] S. Hui, J. M. Silverman, S. S. Chen, D. W. Erickson, M. Basan, J. Wang, T. Hwa, and J. R. Williamson, "Quantitative proteomic analysis reveals a simple strategy of global resource allocation in bacteria," *Molecular Systems Biology*, vol. 11, Feb. 2015.

[2] M. Scott, C. W. Gunderson, E. M. Mateescu, Z. Zhang, and T. Hwa, "Interdependence of cell growth and gene expression: Origins and consequences," *Science*, vol. 330, pp. 1099–1102, Nov. 2010.

[3] A. Bren, D. S. Glass, Y. K. Kohanim, A. Mayo, and U. Alon, "Tradeoffs in bacterial physiology determine the efficiency of antibiotic killing," Mar. 2022.

[4] E. Metzl-Raz, M. Kafri, G. Yaakov, I. Soifer, Y. Gurvich, and N. Barkai, "Principles of cellular resource allocation revealed by condition-dependent proteome profiling," *eLife*, vol. 6, Aug. 2017.

[5] K. Kochanowski, T. Sander, H. Link, J. Chang, S. J. Altschuler, and L. F. Wu, "Systematic alteration of in vitro metabolic environments reveals empirical growth relationships in cancer cell phenotypes," *Cell Reports*, vol. 34, p. 108647, Jan. 2021.

[6] J. Xia, B. J. Sánchez, Y. Chen, K. Campbell, S. Kasvandik, and J. Nielsen, "Proteome allocations change linearly with the specific growth rate of saccharomyces cerevisiae under glucose limitation," *Nature Communications*, vol. 13, May 2022.

[7] T. V. Karpinets, D. J. Greenwood, C. E. Sams, and J. T. Ammons, "Rna:protein ratio of the unicellular organism as a characteristic of phosphorous and nitrogen stoichiometry and of the cellular requirement of ribosomes for protein synthesis," *BMC Biology*, vol. 4, Sept. 2006.

[8] C. Wu, R. Balakrishnan, N. Braniff, M. Mori, G. Manzanarez, Z. Zhang, and T. Hwa, "Cellular perception of growth rate and the mechanistic origin of bacterial growth law," *Proceedings of the National Academy of Sciences*, vol. 119, May 2022.

[9] J. Urban, A. Soulard, A. Huber, S. Lippman, D. Mukhopadhyay, O. Deloche, V. Wanke, D. Anrather, G. Ammerer, H. Riezman, J. R. Broach, C. De Virgilio, M. N. Hall, and R. Loewith, "Sch9 is a major target of torc1 in saccharomyces cerevisiae," *Molecular Cell*, vol. 26, p. 663–674, June 2007.

[10] Y. Inoue and W. Nomura, "TOR signaling in budding yeast," in *The Yeast Role in Medical Applications*, InTech, Jan. 2018.

[11] A. J. Valvezan and B. D. Manning, "Molecular logic of mtorc1 signalling as a metabolic rheostat," *Nature Metabolism*, vol. 1, p. 321–333, March 2019.

G. TALLARICO, "Exploring universal principles of cellular growth regulation in eukaryotes using budding yeast" in *PhD Proceedings – Annual Issues of the Doctoral School, Faculty of Information Technology and Bionics, Pázmány Péter Catholic University – 2024.* G. Prószéky, G. Szederkényi Eds. Budapest: Pázmány University ePress, 2024, pp. 41–41.

Relationship between certain characteristics of visual perception and cognition in psychiatric disorders

Brigitta UNGVÁRI
(Supervisors: Katalin CSIGÓ, György CSEREY)
Pázmány Péter Catholic University, Faculty of Information Technology and Bionics
50/a Práter street, 1083 Budapest, Hungary
ungvari.brigitta@itk.ppke.hu

***Abstract*—Visual perception and cognition are tightly intertwined: understanding this relationship can help us comprehend why some visual processing deficits are more common in psychiatric disorders, thereby enhancing our understanding of them. This paper presents a brief literature review on the relationship between certain characteristics of visual perception and cognition, in relation to schizophrenia, obsessive-compulsive disorder, bipolar disorder, and major depression. Following this, we present a possible interpretation, which is the endophenotype approach. This suggests that the visual-perceptual deficits in these characteristics may be traits genetically related to the disorder. Measuring these visual functions and patterns can also serve as useful psychodiagnostic tools in the clinical practice.**

***Keywords*-visual perception; cognitive functions; eye tracking; pupil dilation; contrast sensitivity; psychiatric disorders, endophenotype**

Visual processing comprises perceptive and cognitive components that engage in a bidirectional relationship [1]. The aim of this paper is to describe three important mechanisms of the earlier perceptive phases: pupil dilation, eye movements, and contrast sensitivity. Pupil dilation reflects mental effort or cognitive load as well as the emotional component of the task. Eye movements are closely related to memory and executive functions, particularly the cognitive control and inhibitory dimensions, along with oculomotor processes.

In certain psychiatric disorders – schizophrenia, obsessive-compulsive disorder, major depression, bipolar disorder – these functions can be impaired. Pupillometric research has shown relationship between pupil dilation and schizophrenia. It correlated negatively with the negative symptoms, especially the motivational deficits [2]. In OCD, eye movement patterns can serve as a biomarker of impaired organizational strategies [3]. In free viewing tasks (where participants freely scan a visual stimulus), major depressive disorder patients have shown shorter scanpath lengths and lower saccade velocities [4]. In the antisaccade task, individuals with bipolar disorder have increased reaction time due to psychomotor disturbances [5].

These correlations can be interpreted in multiple ways, but within the endophenotype approach, these impairments can be seen as traits genetically associated with the disorders. The presented studies and results can also be possibly used in psychodiagnostics: eye movement characteristics can be indicative in diagnosing some disorders.

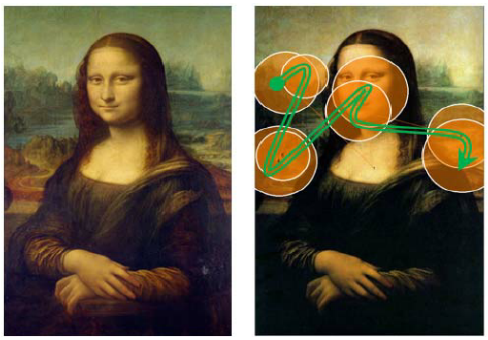

Fig. 1. Eye movement patterns in a free viewing task [6]

ACKNOWLEDGEMENTS

Project no. TKP2021-NVA-27 has been implemented with the support provided by the Ministry of Culture and Innovation of Hungary from the National Research, Development and Innovation Fund, financed under the TKP2021 funding scheme.

REFERENCES

[1] B. L. Anderson, "Mid-level vision," *Current Biology*, vol. 30, no. 3, pp. R105–R109, 2020.
[2] A. Shmukler, A. V. Latanov, M. Karyakina, V. N. Anisimov, M. A. Churikova, I. S. Sukhachevsky, and V. A. Spektor, "Eye movements and cognitive functioning in patients with schizophrenia spectrum disorders: network analysis," *Frontiers in Psychiatry*, vol. 12, p. 736228, 2021.
[3] M. Kim, W. Shin, T. H. Lee, T. Kim, W. J. Hwang, and J. S. Kwon, "Eye movement as a biomarker of impaired organizational strategies during visual memory encoding in obsessive–compulsive disorder," *Scientific Reports*, vol. 11, no. 1, p. 18402, 2021.
[4] J. Takahashi, Y. Hirano, K. Miura, K. Morita, M. Fujimoto, H. Yamamori, Y. Yasuda, N. Kudo, E. Shishido, K. Okazaki, *et al.*, "Eye movement abnormalities in major depressive disorder," *Frontiers in Psychiatry*, vol. 12, p. 673443, 2021.
[5] N. Carvalho, E. Laurent, N. Noiret, G. Chopard, E. Haffen, D. Bennabi, and P. Vandel, "Eye movement in unipolar and bipolar depression: A systematic review of the literature," *Frontiers in psychology*, vol. 6, p. 1809, 2015.
[6] G. Ahmad, "Eye fixation curves along analogical thinking in scene viewing," *International Journal of Engineering and Industries*, vol. 6, no. 1, p. 54, 2015.

B. UNGVÁRI, "Relationship between certain characteristics of visual perception and cognition in psychiatric disorders" in *PhD Proceedings – Annual Issues of the Doctoral School, Faculty of Information Technology and Bionics, Pázmány Péter Catholic University – 2024.* G. Prószéky, G. Szederkényi Eds. Budapest: Pázmány University ePress, 2024, pp. 42–42.

Kinetic discretization based population level control for gene regulatory networks

Mihály András VÁGHY
(Supervisors: Mihály KOVÁCS, Gábor SZEDERKÉNYI)
Pázmány Péter Catholic University, Faculty of Information Technology and Bionics
50/a Práter street, 1083 Budapest, Hungary
vaghy.mihaly.andras@itk.ppke.hu

This progress report is based on [1], [2]. In this paper the exogenous control of gene regulatory networks is investigated through the semi-discretized partial integro-differential equation (PIDE) describing the time-evolution of the network's probability density function. With an appropriate finite volume method the semi-discretized system is a mass-conservative linear compartmental model, and thus it preserves most qualitative properties of the solution of the PIDE, namely, it is nonnegative and mass conservative. These advantages combined with the newly investigated mesh-invariance of control allows us to efficiently determine the reachability set. The possibilities of this framework are demonstrated through an illustrative example from literature.

The dynamical model applied in this work is rooted in [3], where the evolution of the probability density function of protein concentration is approximated with a partial integro-differential equation (PIDE), derived from the master equation. This model is able to capture the characteristic random bursts of protein production as it has been observed and described in the literature [4]. An important step in the PIDE-based modeling of GRNs was [5], where the multidimensional (also called generalized) Friedman model was introduced, which is able to describe the dynamics of several genes expressing different protein types. It has been shown that such an approach is already suitable for simulation based control [6], [7]. However, an ODE-based description of the process is also preferred both for dynamical analysis and controller design. Therefore, a semi-discretization of the multidimensional PIDE model was proposed in [1] resulting in a kinetic compartmental description of the system in possibly time-varying linear ODE form.

The probability density function (PDF) of the protein level, denoted by $p(t, \boldsymbol{x})$, can be modeled with the following PIDE:

$$\frac{\partial p(t,\boldsymbol{x})}{\partial t} = \sum_{i=1}^{n} \frac{\partial}{\partial x_i}\left[\gamma_x^i(\boldsymbol{x}) x_i p(t,\boldsymbol{x})\right] + \sum_{i=1}^{n} k_m^i \int_0^{x_i} \beta_i(x_i - y_i) c_i(\boldsymbol{y_i}) p(t,\boldsymbol{y_i})\,\mathrm{d}y_i\,,$$

where $\boldsymbol{y_i} = \boldsymbol{x} + (y_i - x_i)e_i$ and the β_i functions have the following form:

$$\beta_i(x) = \omega_i(x) - \delta(x),$$

where δ is the Dirac delta function. After an appropriate finite volume discretization the following system is obtained

$$\dot{p}(t) = Gp(t) + \big(B \odot C(\boldsymbol{I})\big)p(t),$$

where $\odot$ denotes the Hadamard (or elementwise) product. The following PI controller is applied to drive the expected values of the marginal probability density functions to desired values.

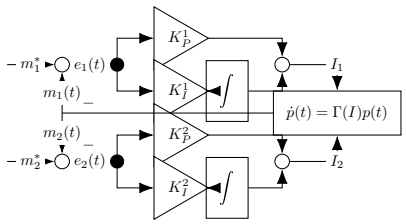

Fig. 1: PI control loop

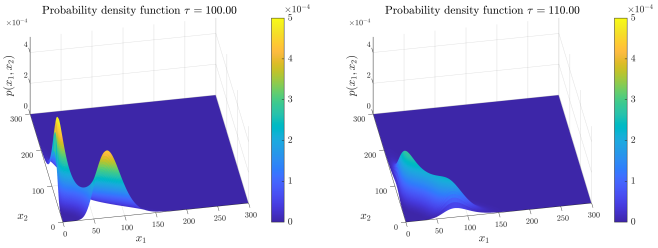

(a) Open-loop system on 300×300 mesh.

(b) Closed-loop system on 300×300 mesh.

Fig. 2: PI control of the genetic toggle switch on various mesh sizes with prescribed expected values $m_1^* = 41$ and $m_2^* = 55$.

Acknowledgements

Support of the Hungarian NRDI Office (NKFIH) through grant K 145934 and that of the ÚNKP-23-3-II-PPKE-81 National Excellence Program of the Ministry for Culture and Innovation is gratefully acknowledged.

References

[1] M. A. Vághy, I. Otero-Muras, M. Pájaro, and G. Szederkényi, "A Kinetic Finite Volume Discretization of the Multidimensional PIDE Model for Gene Regulatory Networks," *Bulletin of Mathematical Biology*, vol. 86, no. 2, 2024.

[2] M. A. Vághy, I. Otero-Muras, and G. Szederkényi, "Analysis and control of gene regulation network models using kinetic semi-discretization," in *European Control Conference - ECC*, 2024.

[3] N. Friedman, L. Cai, and X. S. Xie, "Linking Stochastic Dynamics to Population Distribution: An Analytical Framework of Gene Expression," *Physical Review Letters*, vol. 97, no. 16, 2006.

[4] V. Elgart, T. Jia, A. T. Fenley, and R. Kulkarni, "Connecting protein and mRNA burst distributions for stochastic models of gene expression," *Physical Biology*, vol. 8, no. 4, p. 046001, 2011.

[5] M. Pájaro, A. A. Alonso, I. Otero-Muras, and C. Vázquez, "Stochastic modeling and numerical simulation of gene regulatory networks with protein bursting," *Journal of Theoretical Biology*, vol. 421, pp. 51–70, 2017.

[6] P. Bokes and A. Singh, "Controlling Noisy Expression Through Auto Regulation of Burst Frequency and Protein Stability," in *Hybrid Systems Biology* (M. Češka and N. Paoletti, eds.), (Cham), pp. 80–97, Springer International Publishing, 2019.

[7] C. Fernández, H. Faquir, M. P. jaro, and I. Otero-Muras, "Feedback control of stochastic gene switches using PIDE models," *IFAC-PapersOnLine*, vol. 55, no. 18, pp. 62–67, 2022.

M. VÁGHY, "Kinetic discretization based population level control for gene regulatory networks" in *PhD Proceedings – Annual Issues of the Doctoral School, Faculty of Information Technology and Bionics, Pázmány Péter Catholic University – 2024.* G. Prószéky, G. Szederkényi Eds. Budapest: Pázmány University ePress, 2024, pp. 43–43.

NMR based investigation of the single alpha-helical region and the Actin-binding core of the postsynaptic Drebrin protein

Soma VARGA
(Supervisor: Bálint Ferenc PÉTERFIA)
Pázmány Péter Catholic University, Faculty of Information Technology and Bionics
50/a Práter street, 1083 Budapest, Hungary
varga.soma@itk.ppke.hu

***Abstract*—The postsynaptic density (PSD) of excitatory synapses is a complex network of nervous system proteins involved in postsynaptic signaling. It also modulates and regulates several functions of the nervous system, thereby responsible for a few molecular mechanisms involved in learning and memory [1]. Our research group focuses on the function of proteins in PSD organization. The Drebrin protein is an essential component of the cytoskeleton, and its presence is required for actin polymerization of synapses and recruitment of CXCR4 chemokine receptors [2], as well as for the morphogenesis of the dendritic spike. Drebrin also plays an important role in synaptic plasticity associated with hippocampal memory and establishes several key interactions with other proteins present in PSD [3]. In this work we aim to characterize the structure of three different Drebrin domains, namely the ADFH (Actin-Depolymerizing Factor Homology) domain at the N-terminal, the SAH (Single Alpha Helix) domain which was earlier predicted with bioinformatic methods [4], and the HBMs (Homer Binding Motifs) near the C terminus. We have optimized the bacterial expression of the corresponding constructs and already performed structural analysis with CD (Circular Dichroism), NMR (Nuclear Magnetic Resonance) spectroscopy and SAXS (Smal Angle X-ray Scatering).**

***Keywords*-PSD, Drebrin, SAH domain, Circular dichroism spectroscopy, solution NMR, protein structure**

I. Introduction

Drebrin modulates and regulates several functions of the nervous system, thereby responsible for a few molecular mechanisms involved in learning and memory [1]. The Drebrin protein is an essential component of the cytoskeleton, and its presence is required for actin polymerization of synapses and recruitment of CXCR4 chemokine receptors [2], as well as for the morphogenesis of the dendritic spike. Drebrin also plays an important role in synaptic plasticity associated with hippocampal memory and establishes several key interactions with other proteins present in PSD [3].
In this work we aim to characterize the structure of different Drebrin regions, namely the ADFH (Actin-Depolymerizing Factor Homology) domain and the actin-binding core at the N-terminal, the SAH (Single Alpha Helix) domain which was earlier predicted with bioinformatic methods [4], and the HBMs (Homer Binding Motifs) near the C terminus.

II. Methods

We performed the molecular cloning with pEV and pGEX4T1 vectors and the expression of the corresponding constructs with our competent DH5 alpha, XL-10 Gold and BL21 E. coli bacteria cells. Purification of the proteins were done by several chromatography methods, namely: IMAC (Immobilized Metal Affinity Chromatography), IEC (Ion Exchange Chromatography), and SEC (Size Exclusion Chromatography). NMR experiments were performed on a 800 MHz Bruker Avance spectrometer equipped with a cryoprobe.

III. Results

For characterizing the secondary protein structure of the D233 and SAH domains, CD measurements were performed. The structural characterization of the SAH domain has been continued with 2D, 3D and 4D NMR techniques (Fig.1). We reached the complete backbone assignment for the SAH and the D233 constructs as well.

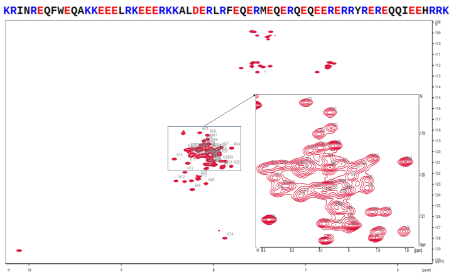

Fig. 1. Complete backbone assignment shown in the 1H-15N HSQC spectra obtained from the SAH domain. The applied assignment strategy based on the 4D i(HCA)N(CA)CONH experiment helped us to overcome the severe signal overlap.

Acknowledgements

I would like to thank my supervisor Dr. Bálint Ferenc Péterfia for his help and guidance with my laboratory work and to Dr. Zoltán Gáspári for his comprehensive help with my research and to Dr. Perttu Permi for performing the NMR measurements. The authors acknowledge the support of the National Research, Development and Innovation Office – NKFIH – through grant no. TKP2021-EGA-42.

References

[1] V. M. Ho, J.-A. Lee, and K. C. Martin, "The Cell Biology of Synaptic Plasticity," *Science*, vol. 334, pp. 623–628, Nov. 2011.
[2] M. Pérez-Martínez, M. Gordón-Alonso, J. R. Cabrero, M. Barrero-Villar, M. Rey, M. Mittelbrunn, A. Lamana, G. Morlino, C. Calabia, H. Yamazaki, T. Shirao, J. Vázquez, R. González-Amaro, E. Veiga, and F. Sánchez-Madrid, "F-actin-binding protein drebrin regulates CXCR4 recruitment to the immune synapse," *Journal of Cell Science*, vol. 123, pp. 1160–1170, Apr. 2010.
[3] Y. Hayashi, "Drebrin-Homer Interaction at An Atomic Scale," *Structure*, vol. 27, pp. 3–5, Jan. 2019.
[4] Á. Kovács, D. Dudola, L. Nyitray, G. Tóth, Z. Nagy, and Z. Gáspári, "Detection of single alpha-helices in large protein sequence sets using hardware acceleration," *Journal of Structural Biology*, vol. 204, pp. 109–116, Oct. 2018.

S. VARGA, "NMR based investigation of the single alpha-helical region and the Actin-binding core of the postsynaptic Drebrin protein" in *PhD Proceedings – Annual Issues of the Doctoral School, Faculty of Information Technology and Bionics, Pázmány Péter Catholic University – 2024.* G. Prószéky, G. Szederkényi Eds. Budapest: Pázmány University ePress, 2024, pp. 44–44.

Simulating the effects of TDP-43 expression in yeast

Áron WEBER
(Supervisors: Attila CSIKÁSZ-NAGY, Erzsébet Fichó)
Pázmány Péter Catholic University, Faculty of Information Technology and Bionics
50/a Práter street, 1083 Budapest, Hungary
weber.aron@itk.ppke.hu

***Abstract*—Amyotrophic lateral sclerosis (ALS) is a neurodegenerative disease, meaning that it is characterized by the gradual degradation and eventual death of both upper and lower motor neurons. Since these cells are responsible for voluntary movement, the patient progressively loses their ability to move, leading to their eventual death, as they become unable to breathe. The aggregation of mutant forms of TAR DNA-binding protein (TDP-43) is hypothesized to be one of the main factors behind the pathogenesis of the disease. Therefore, during my work, I have run cell simulations using data on budding yeast cells aimed to model the malicious effects of the expression of TDP-43 in this model organism. The main goal of this project was to try to further our understanding in the molecular biology of ALS, by examining which protein complexes and cellular pathways show significant changes, which can possibly be translated to human neurons as well.**

***Keywords*-neurodegenerative diseases; complexomics; computational simulation**

Summary

Amyotrophic lateral sclerosis, or ALS, is a neurodegenerative disease, that is, an illness that is characterized by the progressive degradation, and eventual death of neurons. ALS itself affect both the upper and lower motor neurons of the central nervous system. Patients affected by this disorder gradually start to lose their ability to move, ultimately leading to them succumbing to the illness. The aggregation of mutant forms of the TAR DNA-binding protein (TDP-43) has been hypothesised to play a role in the pathophysiology of ALS.
The goal of this research project was to establish the effects of the expression of TDP-43 on the complexome and cellular pathways of budding yeast, through computational cell simulations. Since there is proteomics data available on TDP-43 expression's effects in yeast [1], one can try to provide a full computational replication of this experiment, and this proteomics data can also be used as the input of the simulator algorithm. Due to these factors, running simulations in yeast is a promising first step in order to provide a frame of reference for subsequent simulations using human data.
During this project, I have run cell simulations of yeast cells expressing TDP-43, both using the data from [1] and by explicitly adding this protein to the simulation inputs, using the Cytocast Cell Simulator algoritm. To analyze the outputs of the simulations, I have used an Anderson-Darling test for the comparison of protein complex abundances to a healthy baseline, and a generalized version of the Euclidean distance for pathway graphs.
Results show that while the simulation algorithm was able to capture some effects of TDP-43 expression in yeast, these are lower in overall magnitude than those seen in the simulations using even the earliest measurements after TDP-43 expression as input. This can be mostly due to the rather crude nature of the interactor prediction algorithm, and due to the fact that the simulation algorithm is unable to simulate downstream effects on e.g. transcription or intracellular transport. Still, the significantly changed complexes and pathways show consistency with the function of TDP-43, and as such, these simulations can still provide a frame of reference for further experiments.

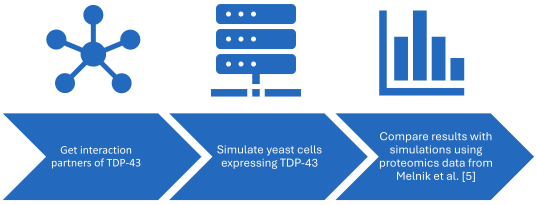

Fig. 1: Overview of the main steps of the project.

Acknowledgements

This work was done using the resources of Cytocast Hungary Kft.

References

[1] A. Melnik, V. Cappelletti, F. Vaggi, *et al.*, "Comparative analysis of the intracellular responses to disease-related aggregation-prone proteins," eng, *Journal of Proteomics*, vol. 225, p. 103 862, Aug. 2020, ISSN: 1876-7737. DOI: 10.1016/j.jprot.2020.103862.

[2] T. J. Cohen, V. M. Lee, and J. Q. Trojanowski, "TDP-43 functions and pathogenic mechanisms implicated in TDP-43 proteinopathies," *Trends in Molecular Medicine*, vol. 17, no. 11, pp. 659–667, Nov. 2011. DOI: 10.1016/j.molmed.2011.06.004.

[3] V. Khurana and S. Lindquist, "Modelling neurodegeneration in Saccharomyces cerevisiae: Why cook with baker's yeast?" *Nature Reviews Neuroscience 2010 11:6*, vol. 11, pp. 436–449, 6 Apr. 2010, ISSN: 1471-0048. DOI: 10.1038/nrn2809. [Online]. Available: https://www.nature.com/articles/nrn2809.

[4] S. Rizzetto, P. Moyseos, B. Baldacci, C. Priami, and A. Csikász-Nagy, "Context-dependent prediction of protein complexes by SiComPre," *npj Systems Biology and Applications 2018 4:1*, vol. 4, pp. 1–9, 1 Sep. 2018, ISSN: 2056-7189. DOI: 10.1038/s41540-018-0073-0.

Á. WEBER, "Simulating the effects of TDP-43 expression in yeast" in *PhD Proceedings – Annual Issues of the Doctoral School, Faculty of Information Technology and Bionics, Pázmány Péter Catholic University – 2024.* G. Prószéky, G. Szederkényi Eds. Budapest: Pázmány University ePress, 2024, pp. 45–45.

PROGRAM 2
COMPUTER TECHNOLOGY BASED ON MANY-CORE PROCESSOR CHIPS, VIRTUAL CELLULAR COMPUTERS, SENSORY AND MOTORIC ANALOG COMPUTERS

Head: Péter SZOLGAY

Advanced analysis of fiber photometry for neuroscience research

Boldizsár Zsolt BALOG
(Supervisors: Gábor NYÍRI, György CSEREY)
Pázmány Péter Catholic University, Faculty of Information Technology and Bionics
50/a Práter street, 1083 Budapest, Hungary
balog.boldizsar.zsolt@itk.ppke.hu

***Abstract*—Neuroscience experiments are crucial to the study of brain physiology and pathology. A recently developed method called fiber photometry allows the activity of specific brain nuclei or circuits to be recorded in behaving animals. This study describes the methods to prepare mice for fiber photometry experiments, methods of data acquisition and data processing.**

***Keywords*-keyword; fiber photometry; head restrained; mouse; behavior; experiment; neuroscience**

I. Introduction

The main steps of fiber photometry experiments are: transgene expression, optic fiber implantation, behavioral experimentation, histological verification and finally data analysis. To induce the expression of a neural-transmission-activated fluorophore in the target neurons, harmless viral vectors can be micro-injected into the appropriate anatomical structures. After this procedure, mice rest for a few weeks, which aids in their recovery and allows the infected cells to express the proteins. Next an implantation surgery fixes the optic fiber tips just above the regions of interest. After a second recovery period neural activity can be recorded. These behavioral experiments are followed by histological verification. If the surgeries were successful, data analysis can proceed and quantification of the results can be statistically tested, conclusions can be drawn. In the following paragraphs, I will describe the methods we used to study a subcortical brain area using fiber photometry.

II. Fiber photometry data acquisition

In vivo fiber photometry was used to record cell type specific dynamic activity using a setup built from commercially available parts including Doric Neuroscience Studio 5.4.1.23 (Doric Lenses), Fiber Photometry Console (Doric Lenses), a 2 channel LED driver (Doric Lenses), 405 nm and 465 nm connectorized LEDs (Doric Lenses), Minicube with built in amplifier (Doric Lenses), and a 400 μm fiber patch cord (FP400URT Thorlabs). Sinusoidal light intensity modulation was used to make cells expressing GCaMP8m or DA4.4 emit activity dependent fluorescent signal (excitation 465 nm, 40μW at fiber tip, 208.616 Hz modulation) and theoretically activity independent control isosbestic signal (excitation 405 nm isosbestic wavelength, 4 μW at fiber tip, 572.205 Hz modulation) simultaneously. The emitted green light was detected by a photodiode, amplified, converted to a digital signal with 12048 Hz sampling frequency, lock-in amplified by the data acquisition software and saved in a file for offline analysis.

III. Fiber photometry data processing

Data processing was done with custom written MATLAB (MathWorks) programs. Demodulated activity dependent and isosbestic signals were median filtered (window width = 0.0083 s) and decimated (100x, resulting in 120.48 Hz sampling rate). To get ΔF/F signals, the filtered isosbestic signal was then fitted linearly to the activity dependent signal using the least squares method. Bleaching and motion correction was simultaneously done by evaluating the following formula at each measurement timestamp: ΔF/F= (activity dependent - fitted isosbestic) / fitted isosbestic [1]. The readings were separated into peri-event sections with the help of the synchronization signals. To account for inter-subject and inter-session variability and to make ΔF/F and isosbestic signals comparable to each other, z-score calculation was applied for each peri-event section separately.

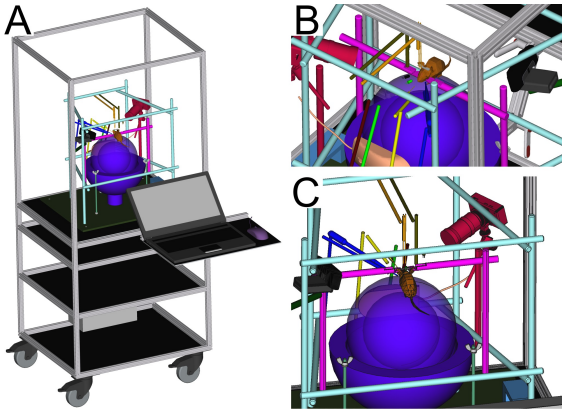

Fig. 1. CAD model of a head restrained experimental arrangement

IV. Discussion

The methods described above allowed the high-resolution study of target neurons in the subcortical region of the mouse brain. The results of the fiber photometry experiments showed the activation of the target neurons during salient, positive or negative stimuli and their effects on the release of dopamine in other brain regions. Data obtained using the above methods will be published to support results obtained using other neuroscience research methods.

References

[1] T. N. Lerner, C. Shilyansky, T. J. Davidson, K. E. Evans, K. T. Beier, K. A. Zalocusky, A. K. Crow, R. C. Malenka, L. Luo, R. Tomer, and K. Deisseroth, "Intact-Brain analyses reveal distinct information carried by SNc dopamine subcircuits," *Cell*, vol. 162, pp. 635–647, July 2015.

B. BALOG, "Advanced analysis of fiber photometry for neuroscience research" in *PhD Proceedings – Annual Issues of the Doctoral School, Faculty of Information Technology and Bionics, Pázmány Péter Catholic University – 2024.* G. Prószéky, G. Szederkényi Eds. Budapest: Pázmány University ePress, 2024, pp. 47–47.

Progress report on parameter computation, control, and state estimation of nonnegative nonlinear systems

Balázs CSUTAK
(Supervisor: Gábor SZEDERKÉNYI)
Pázmány Péter Catholic University, Faculty of Information Technology and Bionics
50/a Práter street, 1083 Budapest, Hungary
csutak.balazs@itk.ppke.hu

***Abstract*—In this progress report, I present our recent results concerning the parameter computation, robust control, and state estimation of nonlinear nonnegative models with biological and epidemiological motivation. First, I introduce a novel, optimization-based approach for finding parameter values that guarantee a predefined qualitative behavior (eg. sustained oscillations) for such systems, illustrated using three case studies. Secondly, I show our recent extensions of our previously published but continuously developed epidemic control toolbox, achieving robust asymptotic output tracking based on feedback linearization, reliable in the presence of serious model and parameter mismatch combined with inaccurate state values obtained using an 8-variable Extended Kalman Filter.**

***Keywords*-dynamical systems, nonnegative systems, kinetic systems, oscillations, nonlinear programming, epidemic, feedback linearization, robust control, Extended Kalman Filter**

I. Introduction

Kinetic models represent an important subclass of nonnegative dynamic systems, being widely applied in different fields of science. Due to the fact, that often originally non-kinetic models can be transformed to kinetic representation, these reaction networks are sometimes called the "prototype of nonlinear science", widely used for representing complex chemical, biological and even social processes (eg. epidemic models, population dynamics, vehicle traffic flows on highways, etc). Consequently, the development of mathematical methods and algorithms for the design, analysis, and control of such systems has higher relevance than ever before.

In this progress report, I highlight two such techniques we created during the last academic year: first, a method for computing the parameters of such a system to achieve prescribed qualitative behavior, already published as [1], and secondly, a direct extension of our previous work [2], in which we present a robust reference tracking control algorithm for compartmental models, a contribution to our continuously developing epidemic simulation and control framework.

To illustrate the capabilities of the proposed techniques, I apply these to different nonnegative models with increasing complexity, presented below. The features and limits of the epidemic reference tracking controller are shown using real-world data extracted from COVID-19 statistics in Sweden and Hungary.

II. Optimization-based parameter computation

We aim to compute the parameters providing the desired qualitative dynamical properties by creating an appropriate nonlinear optimization problem, having the parameters as decision variables. The resulting parameters, computed for one of our case studies, a three-species Lotka-Volterra foodchain model are shown in figure 1.

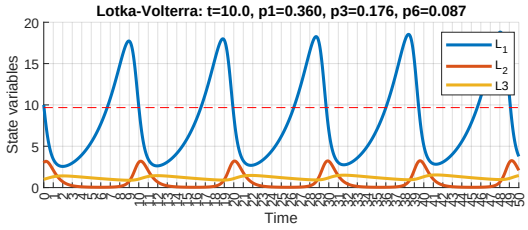

Fig. 1. Prescribed oscillation period, the computed parameters, and the corresponding trajectory for the Lotka-Volterra model with $\epsilon = 0.1$. The red dashed line shows the computed oscillation threshold τ_1.

III. Robust control with EKF state estimation

As a direct continuation of [2], in this section I present our modified control setup for the robust asymptotic output tracking controller designed for epidemic models, equipped with an Extended Kalman Filter built for the 8-compartment simulation model.

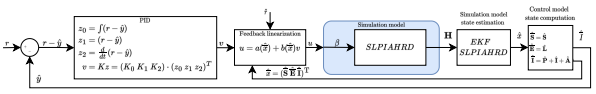

Fig. 2. Control setup: the 'true' system is simulated by a detailed 8-compartment model, the linearizing state feedback is computed using a simplified SEIR model, and the state is estimated using an 8-compartment EKF

Acknowledgements

Supported by the ÚNKP-23-3-II-PPKE-10 New National Excellence Program of the Ministry for Culture and Innovation from the source of the National Research, Development and Innovation Fund. G. Sz. acknowledges the support of the grants NKFIH-OTKA 145934 and RRF-2.3.1-21-2022-00006.

References

[1] B. Csutak and G. Szederkényi, "Optimization-based parameter computation for nonnegative systems to achieve prescribed dynamic behaviour," *Acta Polytechnica Hungarica*, vol. 21, no. 10, 2024.

[2] B. Csutak and G. Szederkényi, "Reference tracking control of a nonlinear epidemiological model with state estimation," in *9th International Conference On Control, Decision And Information Technologies*, 2023. To be published.

B. CSUTAK, "Progress report on parameter computation, control, and state estimation of nonnegative nonlinear systems" in *PhD Proceedings – Annual Issues of the Doctoral School, Faculty of Information Technology and Bionics, Pázmány Péter Catholic University – 2024.* G. Prószéky, G. Szederkényi Eds. Budapest: Pázmány University ePress, 2024, pp. 48–48.

Improving open set recognition with an approach based on multi-view learning and methods used in large language models

Lóránt Szabolcs DAUBNER
(Supervisors: Tamás ZSEDROVITS, Kálmán TORNAI)
Pázmány Péter Catholic University, Faculty of Information Technology and Bionics
50/a Práter street, 1083 Budapest, Hungary
daubner.lorant.szabolcs@itk.ppke.hu

I. Multi-View Learning

Most of the machine learning and object recognition algorithms used nowadays are single-view learning methods which means that the data is represented in a single view. In many real-world applications the information about the objects is collected from different sources (e.g. for an image meta attributes or a description could be available). This is called Multi-View Data which refers to datasets that consist of observations from multiple perspectives or produced by different methods or at different levels of processing, and each 'view' provides various but potentially complementary information about the same set of entities.

Because of the frequent occurrence of Multi-View Data quite a variety of Multi-View Learning algorithms were already developed and has been surveyed in [1] and in [2]. A crucial aspect of Multi-View Learning is how to effectively integrate the different views to improve learning performance.

II. Improving the performance of Open Set Recognition

When dealing with real-world recognition problems, we usually do not have knowledge of the entire set of possible classes. We need classification methods which can deal with the "unknown" and reject samples belonging to classes never seen during training. Scheirer et al. formalized the theory of Open Set Recognition [3].

Considering the Multi-view aspects we could improve the recognition accuracy in three ways:

- using different sources for different views (e.g. depth map)
- generating additional views from our dataset using some image captioning models
- using a fast object detection algorithm in parallel/sequentially as an additional view

To achieve this a highly accurate and fast model is required (because of the limited capacity of drones and mobile devices. Two models were examined for this purpose (YOLOv7 and BLIP-2) which are (partly) based on the recently popular and widely used transformer architecture and will be described in the following chapters.

III. About the planned algorithm

The above mentioned two algorithms are relevant from two points of view: these could be directly used in our model to enhance the recognition accuracy and parts of the architecture are important in designing our method. Figure shows the architecture of our proposed algorithm (under development) for improving OSR accuracy. BLIP-2 could be used for image-to-text generation, and thus adding new samples to our training set similarly to our former work in [4]. Although we have high performance computers with appropriate GPU capacity available for training, inference should be run in real-time with low latency on drones and mobile devices, so mobile versions and frozen parts of the discussed models are also considered.

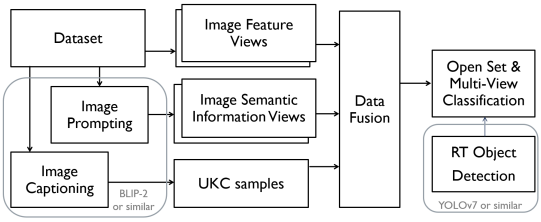

Fig. 1. Schematic view of our proposed algorithm using BLIP-2 for image-to-text generation and YOLOv7 for fast object detection

Acknowledgements

Project no. TKP2021-NVA-26 has been implemented with the support provided by the Ministry of Culture and Innovation of Hungary from the National Research, Development and Innovation Fund, financed under the TKP2021 funding scheme.

References

[1] Chang Xu and Dacheng Tao and Chao Xu, *A Survey on Multi-view Learning*. arXiv:1304.5634, 2013.
[2] Jing Zhao, Xijiong Xie, Xin Xu, Shiliang Sun, *Multi-view learning overview: Recent progress and new challenges*. Information Fusion, Volume 38, Pages 43-54, 2017.
[3] W. J. Scheirer, A. de Rezende Rocha, A. Sapkota and T. E. Boult, *Toward Open Set Recognition*. IEEE Transactions on Pattern Analysis and Machine Intelligence, Volume 35, Pages 1757-1772, 2013.
[4] Halász, A.P.; Al Hemeary, N.; Daubner, L.S.; Zsedrovits, T.; Tornai, K., *Improving the Performance of Open-Set Recognition with Generated Fake Data*. Electronics 2023, 12, 1311, 2023.
[5] J. Redmon, S. Divvala, R. Girshick and A. Farhadi, *You Only Look Once: Unified, Real-Time Object Detection*. 2016 IEEE Conference on Computer Vision and Pattern Recognition (CVPR), Las Vegas, NV, USA, Pages 779-788, 2016.
[6] Junnan Li and Dongxu Li and Silvio Savarese and Steven Hoi, *BLIP-2: Bootstrapping Language-Image Pre-training with Frozen Image Encoders and Large Language Models*. arXiv:2301.12597, 2023.

L. DAUBNER, "Improving open set recognition with an approach based on multi-view learning and methods used in large language models" in *PhD Proceedings – Annual Issues of the Doctoral School, Faculty of Information Technology and Bionics, Pázmány Péter Catholic University – 2024.* G. Prószéky, G. Szederkényi Eds. Budapest: Pázmány University ePress, 2024, pp. 49–49.

QoE in light field visualization for observers with reduced visual capabilities

Mary GUINDY
(Supervisors: Péter SZOLGAY, Vamsi Kiran ADHIKARLA)
Pázmány Péter Catholic University, Faculty of Information Technology and Bionics
50/a Práter street, 1083 Budapest, Hungary
guindy.mary.mohsen.messak@itk.ppke.hu

***Abstract*—While most research targeting the perceived quality of light field visualization involves participants with normal vision, a significant number of future users are anticipated to fail the Snellen chart screening for visual acuity. This paper elaborates on our research regarding the preferred viewing distance for potential applications of light field visualization, as perceived by users with reduced visual capabilities.**

***Keywords*-Light field visualization, viewing distance, human visual system, use-case-specific preference**

I. Related work

Numerous factors can be utilized to determine the potential use cases of light field visualization, among which is the viewing distance. The recommended maximum viewing distance (denoted as D_V) is calculated according to the angular resolution of visualization [1], based on the following equation:

$$Viewing\ distance \leq \frac{Interpupillary\ distance}{tan(Angular\ resolution)}, \quad (1)$$

where, according to the scientific community, the average interpupillary distance is approximately 6.5 cm.

II. Experimental setup

The experiment was conducted using the 640RC HoloVizio light field display, with six marked viewing distances on the floor of the laboratory: 1.39 m, 1.86 m, 2.32 m, 2.79 m, 3.25 m, and 3.72 m. Regarding the resolutions implemented in this study, two quality representations were utilized: a low resolution one (spatial resolution of 640×480 and angular resolution of 1 degree) and a high resolution one (spatial resolution of 1024×768 and angular resolution of 0.5 degrees).

For this study, six different visual stimuli were presented and participants were instructed to evaluate the quality of visualized content using the ACR scale ranging from 1 (lowest quality) to 10 (highest quality). In this study, the case of static observation was investigated with little head and body sways allowed. The participant was required to provide a rating at each of the six designated viewing distances.

The study enlisted 20 test participants: 13 males and 7 females, with an average age of 23, all of whom wore glasses with high diopter values. Additionally, the study incorporated one participant with a vision impairment exceeding 90%, who did not utilize corrective eyewear [2].

III. Results

Figure 2 depicts a total of 1440 ratings recorded by the 20 test participants for both resolutions. As illustrated in the figure, both resolutions exhibit a similar distribution, with a discernible shift in ratings. The average ratings for the low and high resolution stimuli are 5.65 and 6.53, respectively. Figure 2 depicts the rating distribution recorded at the various viewing distances. A conspicuous trend towards greater viewing distances was observed for both resolutions. While the majority of test participants exhibited a preference for greater distances, there were disparities in individual assessments.

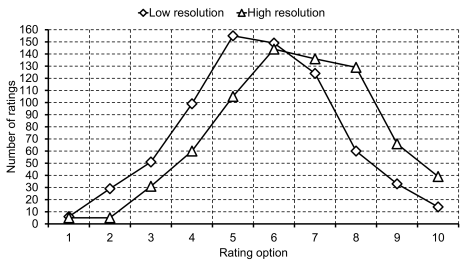

Fig. 1: Rating distribution for low and high resolution [2].

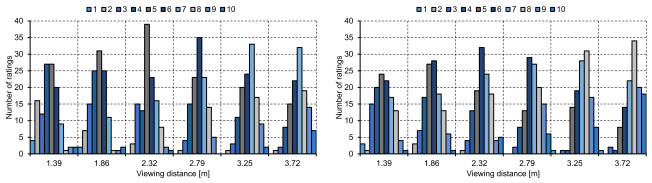

(a) Low resolution. (b) High resolution.

Fig. 2: Rating distribution for both resolutions at the different viewing distances [2].

Out of the 20 test participants, only two displayed interest in closer distances. Unlike the remaining 18 participants, whose average rating differences sometimes exceeded 5, theirs were within 1. Moreover, out of these two participants, only one distinctly favored closer distances, while the other evaluated 2.79 m with the highest scores, albeit with even smaller average rating differences.

Figure 3 illustrates the average ratings for the test participant with severe vision loss. Unlike the previous results, this

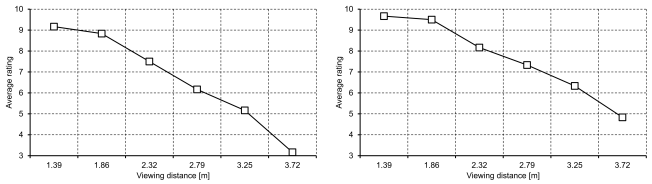

(a) Low resolution. (b) High resolution.

Fig. 3: Average ratings of the test participant with high vision loss for both resolutions at the different viewing distances [2].

M. GUINDY, "QoE in light field visualization for observers with reduced visual capabilities" in *PhD Proceedings – Annual Issues of the Doctoral School, Faculty of Information Technology and Bionics, Pázmány Péter Catholic University – 2024.* G. Prószéky, G. Szederkényi Eds. Budapest: Pázmány University ePress, 2024, pp. 50–51.

participant exhibited a distinct preference for closer viewing distances, likely due to vision impairment [2].

ACKNOWLEDGMENTS

Project no. TKP2021-NVA-27 has been implemented with the support provided by the Ministry of Culture and Innovation of Hungary from the National Research, Development and Innovation Fund, financed under the TKP2021 funding scheme. Moreover, this project has received funding from the European Union's Horizon 2020 research and innovation programme under the Marie Skłodowska-Curie grant agreement No 813170.

REFERENCES

[1] P. A. Kara, A. Barsi, R. R. Tamboli, M. Guindy, M. G. Martini, T. Balogh, and A. Simon, "Recommendations on the viewing distance of light field displays," in *Digital Optical Technologies 2021*, vol. 11788, pp. 166–179, SPIE, 2021.

[2] A. Simon, P. A. Kara, M. Guindy, X. Qiu, L. Szy, and T. Balogh, "One step closer to a better experience: Analysis of the suitable viewing distance ranges of light field visualization usage contexts for observers with reduced visual capabilities," in *Novel Optical Systems, Methods, and Applications XXV*, vol. 12216, pp. 133–143, SPIE, 2022.

Structural identifiability of delayed dynamical systems with approximation

Gergely HORVÁTH
(Supervisor: Gábor SZEDERKÉNYI)
Pázmány Péter Catholic University, Faculty of Information Technology and Bionics
50/a Práter street, 1083 Budapest, Hungary
horvath.gergely@itk.ppke.hu

***Abstract*—Various fields are affected by modelling uncertainty from economics to biology when certain aspects of the system are unknown. One practice is to include delay terms into the system as parameters, to account for the unknown phenomena. For the system to be suitable for parameter estimation, i.e., computing its innate and delay parameters, it needs to be structurally identifiable. Throughout this semester, we have thoroughly established the necessary and sufficient conditions that a system must meet to be considered structurally globally or locally identifiable. These conditions are crucial for ensuring that parameter estimation can be effectively performed on the system. Previously, our studies focused on systems incorporating a single delay term. We demonstrated how such systems can achieve the property of structural identifiability. However, in our latest work, we present a general solution that extends to systems with an arbitrary number of delay terms. This solution employs the linear chain approximation technique, which simplifies the delayed terms into linear expressions. This approximation has proven instrumental in allowing us to conclusively establish the necessary conditions for structural identifiability. By replacing complex delay terms with more manageable linear expressions, we can enhance the clarity and applicability of our identifiability conditions, paving the way for more robust and reliable parameter estimation in systems characterized by multiple delays.**

***Keywords*-delayed dynamical systems, structural identifiability, linear chain approximation**

I. Introduction

In a wide range of disciplines, from economics to biology, the uncertainty in modelling is a significant challenge, especially when certain aspects of a system remain unknown. A common approach to address this uncertainty is the integration of delay terms into the system's equations. These terms act as parameters that represent the unknown phenomena, allowing for a more accurate representation of the system's dynamics.

To effectively use these models for parameter estimation—that is, to accurately compute both the innate parameters of the system and those representing delays—the model must be structurally identifiable. Structural identifiability is a critical property that ensures the theoretical possibility of determining the model parameters uniquely from given input-output data.

When modelling, one needs to know the dynamics of the system of interest to carry out fully detailed simulations. The most common way is to use a system of ordinary differential equations to represent the phenomenon:

$$\dot{\boldsymbol{x}}(t) = f(\boldsymbol{x}(t), \boldsymbol{\theta}) \tag{1}$$

$$\boldsymbol{y}(t) = h(\boldsymbol{x}(t), \boldsymbol{\theta}) \tag{2}$$

Where $\boldsymbol{x}(t) \in \mathbb{R}^n$ is the state vector (n is the number of states), $\boldsymbol{y}(t) \in \mathbb{R}^m$ is the observed output vector (m is the number of observed measures), $\boldsymbol{\theta} \in \mathbb{R}^p$ is the parameter vector (p is the number of parameters), $f : \mathbb{R}^n \to \mathbb{R}^n$ is for the dynamics of the system, $h : \mathbb{R}^n \to \mathbb{R}^m$ is observation process. Unfortunately, on many occasions the entire dynamics are not known, therefore the known part of the system is being modelled with delay terms as well to account for the unknown parts. This gives rise to the notion of delayed differential equations (DDE) (for simplicity we assume that the output dynamics does not contain delay terms):

$$\dot{\boldsymbol{x}}(t) = f(\boldsymbol{x}(t), \boldsymbol{\theta}, \boldsymbol{\tau}) \tag{3}$$

$$\boldsymbol{y}(t) = h(\boldsymbol{x}(t), \boldsymbol{\theta}) \tag{4}$$

Here, the system's internal dynamics now contain the $\boldsymbol{\tau} \in \mathbb{R}^d$ vector, which are the already-mentioned time-delays.

The task was to determine the structural identifiability conditions for $\boldsymbol{\tau}$.

The structure of this document is carefully designed to guide the reader through the intricate aspects of modelling delayed dynamical systems and the essential concept of structural identifiability. The initial section serves as an introduction, setting the stage for the detailed analysis that follows. In the second chapter, we delve deeply into the theoretical background necessary for deriving the conditions required for structural identifiability. This chapter begins by explaining the fundamentals of delayed dynamical systems, which are crucial for understanding the complexity and behaviour of systems influenced by time lags. It then progresses to discuss the linear chain approximation method. This technique simplifies the representation of delay terms within the system, making the analysis more tractable. The chapter concludes by thoroughly defining structural identifiability, a pivotal concept that ensures that the model parameters can indeed be uniquely determined from observed data. The third chapter succinctly summarizes the problem statement this work aims to address. It clarifies the specific challenges and questions that our research seeks to resolve, setting a clear framework for the subsequent analysis. In the fourth chapter, we present our original contributions to the field. Here, we outline the specific conditions that a system must satisfy to achieve structural identifiability. This part of the document is critical as it not only proposes theoretical conditions but also demonstrates how these can be practically applied to complex systems with multiple delays. Finally, the fifth chapter concludes the work. It provides a synthesis of the findings and discusses the implications of our research. This closing chapter also suggests directions for future research, considering the limitations of the current study and the potential for discoveries in the field of delayed dynamical systems.

G. HORVÁTH, "Structural identifiability of delayed dynamical systems with approximation" in *PhD Proceedings – Annual Issues of the Doctoral School, Faculty of Information Technology and Bionics, Pázmány Péter Catholic University – 2024.* G. Prószéky, G. Szederkényi Eds. Budapest: Pázmány University ePress, 2024, pp. 52–52.

Researching the physiological effects of the morphology of umbilical cord

Imre Gergely JÁNOKI
(Supervisor: Péter FÖLDESY)
Pázmány Péter Catholic University, Faculty of Information Technology and Bionics
50/a Práter street, 1083 Budapest, Hungary
janoki.imre.gergely@itk.ppke.hu

***Abstract*—The placenta and the umbilical cord is often evaluated in a non-invasive way to assess the healthiness of the fetus, and it is part of the protocol in triage 3 birth cases with complications requiring macroscopic and microscopic examination. Moreover, correlation was found between the coiling of the umbilical cord - more precisely between the pressure in the blood vessels - and the perinatal outcome. In this article a populational measurement of macroscopic examinations are described, with an emphasis on investigating the umbilical cord after birth and estimating blood pressure in the blood vessels based on width, length and coiling. The automatization process of such evaluation is also described.**

***Keywords*-umbilical cord, coiling, pressure, NICU, UCI**

I. Introduction

There are both validated correlations and some presumptions about the morphology and macroscopic properties of the placenta and the umbilical cord, and the perinatal outcome. [1] investigated the placental structural abnormalities and when they develop. Studies [2] and [3] reviewed the literature and previous findings about linkage between abnormal umbilical cord coiling and risk factors and illnesses, such as maternal age, birth weight, birth percentile, ponderal index, abruption, preeclampsia and gestational diabetes mellitus. However, there are only a few extensive studies on umbilical cord coiling and to the best of our knowledge, no bigger, populational measurements are done so far.

II. Methods

To create a populational database, we are measuring placentas and umbilical cords from the Perinatal Intensive Care units of Semmelweis University, Hungary. First a declaration of consent is presented to the mother, and if signed, the measurements are done on a neonatal dissection table. A special stand was fabricated and attached to the dissection table (Fig. 1) holding a calibrated camera needed for later automatization. After cleaning the organs, the morphology of the placenta, then of the umbilical cord is assessed. After the separation of the cord, the membrane, the fetal surface and the maternal surface are examined in order. Finally, the placental tissue is assessed. All data are anonimously stored in REDCap [4]. As part of the automatization process, using the collected images, a prototype trained neural network was created. The UNET-based network creates a segmentation of the umbilical cord, which is then used to determine the length and the width of the umbilical cord. The first calculations for a more advanced coiling indicator - replacing the Umbilical Coiling Index (UCI) - are done based on [5].

Fig. 1. Setup for macroscopic examination of the placenta and umbilical cord, including a calibrated camera on a stand for later automatization.

Acknowledgments

The author would like to express gratitude to Eszter Zsáry, Tamás Gyuláné Marton, Izsó Izsold, Tibor Csaba Várkonyi, Miklós Szabó and Péter Földesy. The research presented here was supported by grant no. 2023-2.1.2-KDP-2023-00011 of the NRDI Office and the New National Excellence Program grant no. ÚNKP-23-3-I-PPKE-114; both provided by the Ministry for Culture and Innovation from the National Research, Development and Innovation Fund.

References

[1] E. Ehlers, O. O. Talton, D. J. Schust, and L. C. Schulz, "Placental structural abnormalities in gestational diabetes and when they develop: A scoping review," *Placenta*, vol. 116, p. 58–66, Dec 2021.
[2] D. J. Hayes, J. Warland, M. M. Parast, R. W. Bendon, J. Hasegawa, J. Banks, L. Clapham, and A. E. Heazell, "Umbilical cord characteristics and their association with adverse pregnancy outcomes: A systematic review and meta-analysis," *PLOS ONE*, vol. 15, Sep 2020.
[3] P. K. Kalluru, H. R. Kalluru, T. R. Allagadda, M. Talur, M. C. Gonepogu, and S. Gupta, "Abnormal umbilical cord coiling and association with pregnancy factors," *Journal of the Turkish-German Gynecological Association*, vol. 25, p. 44–52, Mar 2024.
[4] P. A. Harris, R. Taylor, R. Thielke, J. Payne, N. Gonzalez, and J. G. Conde, "Research electronic data capture (redcap)—a metadata-driven methodology and workflow process for providing translational research informatics support," *Journal of Biomedical Informatics*, vol. 42, p. 377–381, Apr 2009.
[5] D. Wilke, J. Denier, T. Khong, and T. Mattner, "Estimating umbilical cord flow resistance from measurements of the whole cord," *Placenta*, vol. 103, p. 180–187, Jan 2021.

I. JÁNOKI, "Researching the physiological effects of the morphology of umbilical cord" in *PhD Proceedings – Annual Issues of the Doctoral School, Faculty of Information Technology and Bionics, Pázmány Péter Catholic University – 2024.* G. Prószéky, G. Szederkényi Eds. Budapest: Pázmány University ePress, 2024, pp. 53–53.

The experimental validation of a soft resistive sensor for arterial blood pressure waveform measurement

Rizal MAULANA
(Supervisor: György CSEREY)
Pázmány Péter Catholic University, Faculty of Information Technology and Bionics
50/a Práter street, 1083 Budapest, Hungary
rizal.maulana@itk.ppke.hu

***Abstract*—This study aims to develop a device that can precisely continuously measure the arterial blood pressure waveform on radial arteries in a non-invasive and comfortable way. The device utilized in this research uses resistive yarn as its main sensing component. In order to verify the accuracy of the measurement results obtained from the device that was designed, a comparison was made between these results and measurements obtained using the OptoForce 3D force sensor. The comparison of the results of the two measurements indicates a significant correlation.**

***Keywords*-arterial blood pressure waveform; continuous; non-invasive**

I. Summary

Continuous blood pressure monitoring is crucial since it is one of the vital signs of the human body. This continuous monitoring can be performed by examining the blood pressure waveform. Continuous monitoring of blood pressure waveform can be done using the arterial cannula. However, due to the invasive aspect of these measurements and their potential for causing vascular trauma, there is a need for a more convenient and non-invasive method to measure blood pressure waveform continuously. Several approaches exist for continuously monitoring blood pressure waveforms in a non-invasive method. These include Pulse Arrival Time (PAT), Pulse Wave Velocity (PWV), Pulse Decomposition Analysis (PDA), and Pulse Wave Analysis (PWA) [1].

Pulse Wave Analysis (PWA) is working by employing morphological analysis of the blood pressure waveform [2]. PWA can provide accurate measurements by utilizing a single sensor channel. This is the advantage of the PWA method over PAT and PWV, which require using two sensor channels in the measurement. The sensors commonly used in this technique include optical, force, and pressure sensors used to measure morphological signals in peripheral arteries. Foldi et al. [3] implemented the OptoForce 3D force sensor to measure the blood pressure waveform in the radial artery. Piezoelectric pressure sensors are also frequently used in blood pressure waveform measurement, as reported by Wang et al. [4]. This study highlights the design of an affordable wearable sensor utilizing a piezoelectric sensor made from ceramic materials.

This study presents the utilization of resistive yarn as the primary element for measuring continuous non-invasive blood pressure waveforms. Resistive yarn is a variety of yarn that has the ability to change its resistance value when pressure is applied to its surface. Along with the utilization of resistive yarn, other additional components are employed to improve the system's performance and provide optimal measurement results. In order to verify the accuracy of the sensor designed for monitoring blood pressure waveform, we will validate it by comparing its results with those obtained using the OptoForce 3D force sensor.

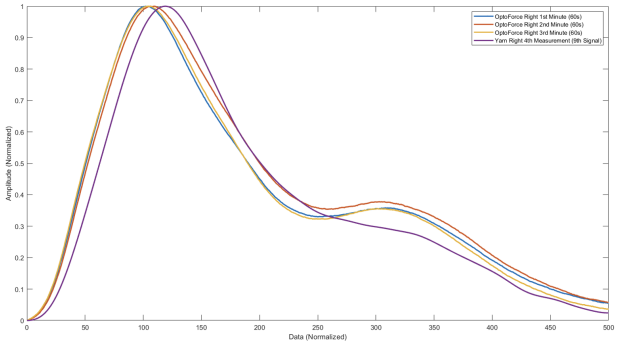

Fig. 1. Comparison of the resistive yarn and optoforce measurement results.

Fig. 1 shows the comparison between the one single-period signal from one of the five resistive yarn measurements and the average single-period signal from the OptoForce measurement, which are divided into sixty-second intervals, resulting in three average signals. The comparison of the two measurements demonstrates a substantial correlation. In general, the developed system is capable of effectively measuring the arterial blood pressure waveform. The systolic peak in the measurement is easily identifiable, and the signal's dominant frequency coincides with the heart rate frequency.

Acknowledgements

The author expresses gratitude to Prof. György Cserey and Dr. Sándor Földi for their valuable guidance in the development of this research.

References

[1] J. Solà, and R.D. Gonzalo, "The handbook of cuffless blood pressure monitoring: a practical guide for clinicians, researchers, and engineers," Springer, 2019.
[2] C. Vlachopoulos, M. O'Rourke, and W.W. Nichols, "McDonalds's blood flow in arteries: theroritical, experimental and clinical principles," CRC Press, 2011.
[3] S. Földi, T. Horváth, F. Zieger, P. Sótonyi, and G. Cserey, "A novel non-invasive blood pressure waveform measuring system compared to millar applanation tonometry," J Clin Monit Comput, 32(4), pp. 717-727, 2018.
[4] T.W. Wang and S.F. Lin, "Wearable piezoelectric-based system for continuous beat-to-beat blood pressure measurement," Sensors, vol. 20, 2020.

R. MAULANA, "The experimental validation of a soft resistive sensor for arterial blood pressure waveform measurement" in *PhD Proceedings – Annual Issues of the Doctoral School, Faculty of Information Technology and Bionics, Pázmány Péter Catholic University – 2024.* G. Prószéky, G. Szederkényi Eds. Budapest: Pázmány University ePress, 2024, pp. 54–54.

Kinematic model parameter identification of an fPAM actuated soft wrist exosuit

Katalin SCHÄFFER
(Supervisors: György CSEREY, Miklós KOLLER)
Pázmány Péter Catholic University, Faculty of Information Technology and Bionics
50/a Práter street, 1083 Budapest, Hungary
schaffer.katalin@itk.ppke.hu

***Abstract*—The aim of the presented research work is to identify the parameters of the kinematic model of our fabric pneumatic artificial muscle (fPAM) actuated wrist exosuit. We examine the behaviour of the exosuit composed of two antagonistic muscles which can move the wrist in flexion/extension. The methodology includes the simplification of the kinematic model and using this model to formulate the optimization problem for finding the endpoint position parameters of the fPAMs based on measured data. Our parameter optimization results indicate that the force modeling should be improved, however, the placement parameters can be identified by the introduced optimization method such that it results accurate joint angle estimation.**

***Keywords*-wearable devices; torque measurement; biological wrist torque**

I. Introduction

In the last decade, soft wearable exosuits gained interest in the research community, because, compared to their rigid counterparts, they have the potential to solve several design challenges, such as achieving a high strength-to-weight ratio, inherent safety, comfort, and low cost, as well as avoiding joint misalignment [1], [2]. Still, the accurate modeling and control of these devices remain challenging which hinder their commercial application. This also applies to our designed soft wrist exosuit [3] which is actuated by fabric pneumatic artificial muscles (fPAMs) (Fig. 1).

In our previous work [3], we derived and evaluated a torque model based on a two-dimensional geometric model of the exosuit. The results showed that the model can predict the exosuit torque, however, it is challenging to identify the model parameters, e.g., we need to use motion capture system to find the muscle placement parameters. For this reason, model-free, feedback control was implemented which provided limited accuracy for trajectory tracking tasks. Adding a model-based feed-forward term can help to resolve the shortcoming of the pure feedback control. To utilize the model for the exosuit control, the parameters for our model need to be identified.

II. Results

In this work, our goal is to find a solution to identify the parameters of the kinematic model using onboard sensors. First, we present the process of data collection through measuring the wrist angle and the muscle pressures at static wrist configurations. Then, we reduce the complexity of the model to make it adequate to be used in the parameter optimization process and chose the set of model parameters to be optimized.

For the kinematic model identification problem, the main challenge is to formulate an optimization problem using the measurement data and the exosuit torque model. This leads to a nonlinear program (NLP) to solve as the nonlinear function of the parameters appear in the constraint terms. It is possible to solve nonlinear programs but the solution is not guaranteed to converge. We introduce multiple approaches for formulating the optimization problem which are different from each other in how the fPAM force is handled.

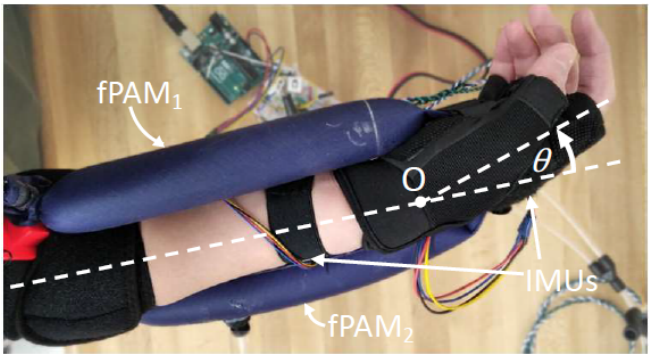

Fig. 1. The prototype and the geometric model of the fPAM actuated exosuit. The wrist exosuit with one pair of antagonistic muscle, the flexor (fPAM$_1$) and the extensor muscle (fPAM$_2$). The wrist angle (θ) can be measured by the two IMUs on the arm and hand.

Our work indicates that the fPAM placement parameters can be identified by solving the nonlinear optimization problem and using joint angle and muscle pressure data measured at static configurations. Comparing the results of the different variations of the optimization problem indicates that the modeling of the fPAM force that is acting on the hand should be improved.

Next steps of the research work will focus on improving the force modeling and also the optimization process and data collection. Then, the long-term goals for the further research include the application of the kinematic model to improve the current control by providing a model based feed-forward term and starting the dynamic modeling.

Acknowledgements

The research was conducted in the IRIS Lab of the University of Notre Dame. The authors acknowledge the support of the National Research, Development and Innovation Office – NKFIH – through grant no. TKP2021-NKTA-66.

References

[1] C. Thalman and P. Artemiadis, "A review of soft wearable robots that provide active assistance: Trends, common actuation methods, fabrication, and applications," *Wearable Technologies*, vol. 1, 2020.
[2] A. F. Pérez Vidal, J. Y. Rumbo Morales, G. Ortiz Torres, F. d. J. Sorcia Vázquez, A. Cruz Rojas, J. A. Brizuela Mendoza, and J. C. Rodríguez Cerda, "Soft exoskeletons: Development, requirements, and challenges of the last decade," *Actuators*, vol. 10, no. 7, p. 166, 2021.
[3] K. Schäffer, Y. Ozkan-Aydin, and M. M. Coad, "Soft wrist exosuit actuated by fabric pneumatic artificial muscles," *IEEE Transactions on Medical Robotics and Bionics*, vol. 6, no. 2, pp. 718–732, 2024.

K. SCHÄFFER, "Kinematic model parameter identification of an fPAM actuated soft wrist exosuit" in *PhD Proceedings – Annual Issues of the Doctoral School, Faculty of Information Technology and Bionics, Pázmány Péter Catholic University – 2024.* G. Prószéky, G. Szederkényi Eds. Budapest: Pázmány University ePress, 2024, pp. 55–55.

Time-symmetric generalization of multi-object tracking

Gergely SZABÓ
(Supervisor: András HORVÁTH)
Pázmány Péter Catholic University, Faculty of Information Technology and Bionics
50/a Práter street, 1083 Budapest, Hungary
szabo.gergely@itk.ppke.hu

***Abstract*—Multi-object tracking in videos is crucial across various fields, including videomicroscopy, autonomous driving, and traffic management. Despite numerous algorithmic and machine-learning-based solutions proposed over the past decades, none have achieved perfect real-world performance. Many existing algorithms exhibit systematic biases that, while beneficial for live-tracking due to reduced computational demands, compromise flexibility and overall performance. A common bias is forward-prediction-based tracking, which relies solely on past information. To address these limitations, we developed a novel multi-object instance segmentation and tracking pipeline specifically designed for scenarios where videos are processed post-recording, prioritizing performance over speed and computational efficiency. One of the primary motivations for this research was videomicroscopic cell recordings, which completely fall into this category. For the tracking of yeast cells, we have shown that our algorithm substantially outperforms other popular methods. Furthermore, we evaluated our method on several other diverse datasets to demonstrate its general applicability.**

I. Architecture overview

While the designed architecture was originally intended for tracking yeast cells in videomicroscopy recordings, with the re-training of the models, the pipeline can be applied to almost any multi-object segmentation and tracking task. The designed pipeline consists of the consecutive separate stages of instance segmentation and tracking. The instance segmentation module uses a Mask R-CNN-based [1] architecture via the Detectron2 environment with a ResNet-X feature pyramid network backbone, pretrained on the COCO instance segmentation dataset. The tracking pipeline employs a novel architecture that tracks objects based on their local temporal neighborhood in both directions, making the consecutive assignment step possible solely between predictions rather than between predictions and observations, as is the case for most tracking architectures. The temporally local tracking architecture employs a DeepLabV3+-based [2] semantic segmentation model, while the assignment step is performed using the Hungarian method [3]. Furthermore, this tracking architecture seamlessly enables the tracking of objects between non-consecutive frames, making interpolation of missed object instances possible. Thus, both the segmentator and the tracker modules support each other for the best possible outcomes. The current version of the architecture is available with tutorial examples at: https://github.com/SzaboGergely0419/Symmetry-Tracker.

II. Performance evaluation

We rigorously tested our architecture on a yeast cell segmentation and tracking dataset against Phylocell [4] and YeaZ [5], both of which are tools specifically designed for this task. Our pipeline substantially outperformed both tools in terms of segmentation and tracking quality. Using random elimination of segmented instances, we demonstrated the sample interpolation capabilities of our architecture, showcasing its ability for long-term continuous tracking even in difficult scenarios. We performed a hyperparameter analysis, revealing a connection between local tracking range and model robustness. Furthermore, to display the flexibility of the architecture, we designed several synthetic datasets with various object behaviors such as extremely high movement speeds, enabled and disabled object path crossings, clumping of objects, random noises, and artifacts, among others. Based on empirical results, the architecture performed well in all of these scenarios. The numerical evaluation of the results is currently in progress.

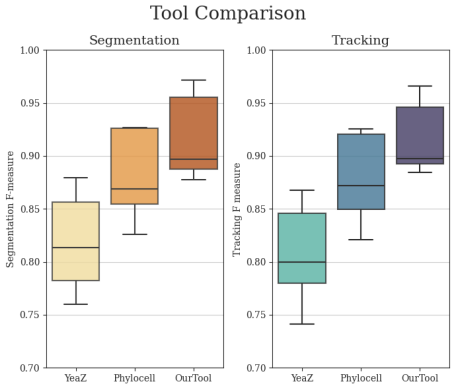

Fig. 1: Multi-object segmentation and tracking result comparison between Phylocell, YeaZ and our pipeline on a yeast cell tracking videomicroscopic dataset.

References

[1] He, Kaiming, et al. "Mask r-cnn." Proceedings of the IEEE international conference on computer vision. 2017.
[2] Chen, Liang-Chieh, et al. "Encoder-decoder with atrous separable convolution for semantic image segmentation." Proceedings of the European conference on computer vision (ECCV). 2018.
[3] Kuhn, Harold W. "The Hungarian method for the assignment problem." Naval research logistics quarterly 2.1-2 (1955): 83-97.
[4] Charvin, G. "PhyloCell." (2017).
[5] Padovani, Francesco, et al. "Segmentation, tracking and cell cycle analysis of live-cell imaging data with Cell-ACDC." BMC biology 20.1 (2022): 174.

G. SZABÓ, "Time-symmetric generalization of multi-object tracking" in *PhD Proceedings – Annual Issues of the Doctoral School, Faculty of Information Technology and Bionics, Pázmány Péter Catholic University – 2024.* G. Prószéky, G. Szederkényi Eds. Budapest: Pázmány University ePress, 2024, pp. 56–56.

PROGRAM 3
FEASIBILITY OF ELECTRONIC AND OPTICAL DEVICES, MOLECULAR AND NANOTECHNOLOGIES, NANO-ARCHITECTURES, NANOBIONIC DIAGNOSTIC AND THERAPEUTIC TOOLS

Head: Árpád CSURGAY

Design of a 2D, high performance Van Atta array

András ESZES
(Supervisor: Zsolt SZABÓ)
Pázmány Péter Catholic University, Faculty of Information Technology and Bionics
50/a Práter street, 1083 Budapest, Hungary
eszes.andras@itk.ppke.hu

***Abstract*—Retrodirective structures have the exceptional property of reflecting the excitation wave back to the source direction. Two designs are presented which operates under 1D and 2D excitation conditions. The 1D array operates at 9.75 GHz, with 100 MHz bandwidth, and acceptance angle of $\theta_i \in (-27^\circ, 27^\circ)$. Its geometry consists of eight linearly polarized microstrip patch antennas and four interconnection lines. The reflected wave of this design has the same polarization as the incident wave. The 2D array operates at 10 GHz with $\theta_i \in (-30^\circ; 30^\circ)$ and $\phi_i \in (-30^\circ; 30^\circ)$ acceptance angle. Its geometry consists of four dual-polarized microstrip patch antennas. To inrcease the isolation between the patch elements four optimized microstrip crossovers are utilized in the feeding network. For an easier detection this stucture is designed to produce reflected waves with orthogonal polarization. Closed-form equations are deduced to simplify the design procedure. The numerical simulations confirm the validity of these equations. The 1D retrodirective array has been fabricated and measured, its performences shows a good agreement with the simulations.**

***Keywords*-Van Atta array, Retrodirective array, microstrip crossover, wide-beamwidth antennas, dual-polarized antenna array**

I. Introduction and design

Retrodirective structures have the exceptional property, of reflecting the excitation wave back to the source direction. Retrodirective structures have huge potential in RFID and automotive fields as well as in telecommunication applications where the increased radar cross section (RCS) is important. Metamaterials [4] and metasurfaces [2] are often utilized to obtain retrodirective phenomena. They often suffer from severe efficiency, size, and feasibility issues. Our designs are based on Van Atta's work [1] where the retrodirectivity is realized by interconnecting linearly polarized antenna elements. Van Atta designs usually consist of at least 4 elements per dimension [5], [6], binary arrays are seldom used due to gain degradation of the array performance and the emerging pointing errors that occur at higher angles [8]. 1D and 2D linear arrays with single and dual-polarized antennas are utilized. The 2D geometry is presented in Figure 1.

II. Conclusion and future work

Design procedures have been presented for 1D and 2D retrodirective arrays. The deduced closed-form expressions are in good agreement with the numerical simulations and highly simplified the design procedure. The 1D retrodirective array has been fabricated, and measured in an anechoic chamber. The monostatic RCSs has been recorded at different frequencies. The measured results are in a good agreement with the simulations. The 2D array requires further improvements regarding the pointing error compensation. Therefore, wide-beamwidth antenna element with tilted main beam direction is required which is under development. Both designs are cost effective because vias have not been utilized. They can be widely applied in automotive applications, telecommunication and package sensing applications.

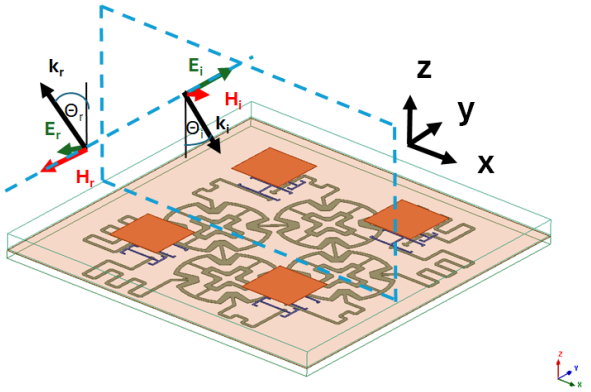

Fig. 1. The geometry of the 2D array, which also indicates the direction of the incident and the reflected wave.

Acknowledgment

This work was funded by the National Research, Development and Innovation Office of Hungary (NKFIH) under Grant K 132050. We thank Grante Co. for providing the measurement site and instrumentation.

References

[1] L. C. Van Atta, "Electromagnetic reflector," U.S. Patent 2 908 002, Oct. 6, 1963.
[2] M. Kalaagi and D. Seetharamdoo, "Retrodirective metasurface operating simultaneously at multiple incident angles," 12th European Conference on Antennas and Propagation (EuCAP 2018), London, 2018, pp. 1-5, doi: 10.1049/cp.2018.0545.
[3] Nanfang Yu et. al. "Light Propagation with Phase Discontinuities: Generalized Laws of Reflection and Refraction" Science 21 Oct 2011: Vol. 334, Issue 6054, pp. 333-337 DOI: 10.1126/science.1210713
[4] Ma, Y., Ong, C., Tyc, T. et al. An omnidirectional retroreflector based on the transmutation of dielectric singularities. Nature Mater 8, 639–642 (2009). https://doi.org/10.1038/nmat2489
[5] Wen-Jen Tseng, Shyh-Bong Chung and Kai Chang, "A planar Van Atta array reflector with retrodirectivity in both E-plane and H-plane," in IEEE Transactions on Antennas and Propagation, vol. 48, no. 2, pp. 173-175, Feb. 2000, doi: 10.1109/8.833066.
[6] Y. Wang, D. Piao and J. Zuo, "A Wide-Angle and Fully Polarimetric Retrodirective Array Based on Tri-Polarized Antennas With Pattern Complementation," in IEEE Transactions on Antennas and Propagation, vol. 70, no. 6, pp. 4518-4525, June 2022, doi: 10.1109/TAP.2022.3142370.
[7] M. Li, S. -L. Chen, Y. Liu and Y. J. Guo, "Wide-Angle Beam Scanning Phased Array Antennas: A Review," in IEEE Open Journal of Antennas and Propagation, vol. 4, pp. 695-712, 2023, doi: 10.1109/OJAP.2023.3296636.
[8] S. Yen, L. B. Boskovic and D. S. Filipovic, "Co-Circularly Polarized Van Atta Array Enabled by Quasi-Monostatic STAR Antennas," in IEEE Transactions on Antennas and Propagation, vol. 69, no. 11, pp. 7156-7165, Nov. 2021, doi: 10.1109/TAP.2021.3069586.

A. ESZES, "Design of a 2D, high performance Van Atta array" in *PhD Proceedings – Annual Issues of the Doctoral School, Faculty of Information Technology and Bionics, Pázmány Péter Catholic University – 2024.* G. Prószéky, G. Szederkényi Eds. Budapest: Pázmány University ePress, 2024, pp. 58–58.

Holographic image classification using spin-waves

Levente MAUCHA
(Supervisors: Ádám PAPP, György CSABA)
Pázmány Péter Catholic University, Faculty of Information Technology and Bionics
50/a Práter street, 1083 Budapest, Hungary
maucha.levente@itk.ppke.hu

***Abstract*—Here, I demonstrate a nanoscale system capable of functioning as a neural network, where all the neuromorphic functions, including the weights and interconnections of the network, are realized by the interference of spin-waves. The weights are realized by the distribution of the saturation magnetization, which can be achieved experimentally by Focused Ion Beam irradiation. Training the network involves finding the proper saturation magnetization map that scatters the spin-waves between the source and the output in such a way that the desired interference pattern appears in the magnetic film, resulting in constructive interference at the desired output and destructive interference at the non-desired outputs. To inverse-design the scatterer using machine learning, I used our micromagnetic solver SpinTorch, built on the machine learning framework PyTorch.**

***Keywords*-spin-wave, machine learning, holography**

I. Introduction

A significant challenge in the study of neuromorphic devices is that most computing models require highly interconnected systems, specifically artificial neurons with a large number of connections, often including all-to-all connections. Wave-based computing concepts offer a potential solution to this problem. If the computing device is realized in a wave-propagating substrate, interference patterns can create an all-to-all interconnection between points on the substrate [1].

II. Neuromorphic computing using spin-waves

Spin-wave-based devices have the potential to show substantial benefits over MOS-based systems in neuromorphic computing tasks. The aim is to design the distribution of the saturation magnetization (Ms) in such a way that the system directs the spin-waves excited by the input signal to the proper output. The Ms of the Yttrium Iron Garnet micromagnetic film can be modified experimentally by Focused Ion Beam irradiation [2]. Here we try a new way of applying the inputs, and imprint a 2D input pattern instead of the waveforms used in [1].

To achieve this, the SpinTorch micromagnetic solver was utilized to design the distribution of the saturation magnetization [3]. The SpinTorch is built upon the machine learning framework pytorch, solves the Landau-Lifshitz-Gilbert equation, and optimize the saturation magnetization distribution by machine learning using gradient-based method.

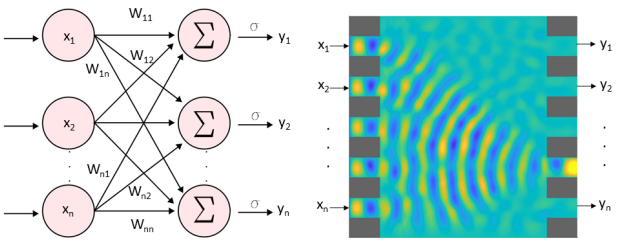

Fig. 1. Representation of the linear transformation of a perceptron layer as a spin-wave scatterer. The functioning of a single perceptron layer can be described as a linear transformation followed by a nonlinear activation function: $y = \sigma(Wx)$, where $x \in \mathbb{R}^{1\times n}$ represents the input, $W \in \mathbb{R}^{n\times m}$ contains the optimizable weights, $y \in \mathbb{R}^{1\times m}$ is the output vector, and σ is the nonlinear activation function [1]. In this way, one layer of perceptrons can implement m classifications. By utilizing sufficiently low amplitude excitation, the propagation of spin-waves can be described by a linear wave equation. Therefore, the linear transformation W can be achieved through a block of spin-wave scatterers. The input signal excites spin-waves through the antennas, which propagate in the film and form an interference pattern reflecting the magnonic index of refraction of the film. Consequently, different spin-wave intensities are observed at the outputs. However, since spin-wave propagation is linear in this scenario, the application of the nonlinear activation function σ must be performed after the readout.

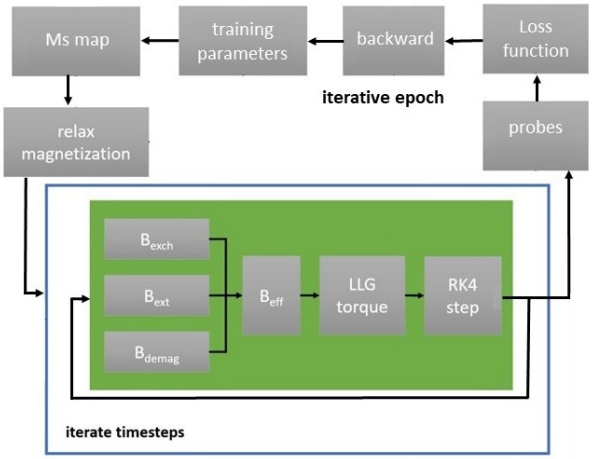

Fig. 2. The block diagram of the SpinTorch micromagnetic solver. The micromagnetic simulator core, shown in the green box in the middle, solves the Landau-Lifshitz-Gilbert equation by iterating through time using the 4th order Runge-Kutta method. The outcome is evaluated by the ratio of spin-wave intensity at the desired and non-desired outputs. The error is propagated back, and the training parameters are updated.

References

[1] Papp, Ádám, Wolfgang Porod, and Gyorgy Csaba. "Nanoscale neural network using non-linear spin-wave interference." Nature communications 12.1 (2021): 6422.
[2] Kiechle, Martina, et al. "Spin-Wave Optics in YIG Realized by Ion-Beam Irradiation." Small (2023): 2207293.
[3] https://github.com/a-papp/SpinTorch

L. MAUCHA, "Holographic image classification using spin-waves" in *PhD Proceedings – Annual Issues of the Doctoral School, Faculty of Information Technology and Bionics, Pázmány Péter Catholic University – 2024.* G. Prószéky, G. Szederkényi Eds. Budapest: Pázmány University ePress, 2024, pp. 59–59.

Pattern retrieval by oscillatory neural networks

Mitra MOAYED
(Supervisor: György CSABA)
Pázmány Péter Catholic University, Faculty of Information Technology and Bionics
50/a Práter street, 1083 Budapest, Hungary
Mitra.moayed@itk.ppke.hu

***Abstract*—The efficient retrieval of patterns from a high-dimensional space poses significant challenges in computational neuroscience and artificial intelligence. This study investigates the application of Kuramoto Oscillatory Neural Networks (KONNs) as a robust mechanism for pattern retrieval. Inspired by the synchronization phenomena observed in natural and biological systems, KONNs leverage the collective dynamics of coupled oscillators to store and recall information. Patterns are encoded as phase relations within the network, allowing KONNs to demonstrate the capacity to retrieve stored patterns through the process of spontaneous synchronization. The robustness of the network against noise and its ability to recover from partial information are critically assessed. Through a series of simulations, this paper demonstrates the conditions under which KONNs exhibit high fidelity in pattern retrieval and explores the scalability of the approach.**

***Keywords*-Pattern retrieval, ONN, oscillatory neural networks, oscillator-based computing,VO2.**

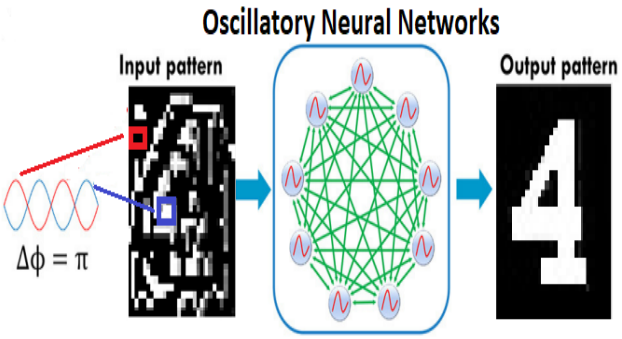

Fig. 1. illustrates a Kuramoto Oscillatory Neural Network (ONN) configured as a Hopfield Neural Network (HNN). In this setup, binary activations are expressed through phase differences between the oscillators and a reference oscillator, typically the first in the sequence.

I. DISCUSSION

Coupled oscillators have been studied for decades by scientists to describe natural phenomena (Winfree, 1967)[1] such as the synchronization of pacemaker cells responsible for the heart beating,the synchronous behavior of insect populations, or to model neuronal activity. Kuramoto Oscillatory Neural Networks (KONNs) stand out as an innovative paradigm.

This study explores the application of KONNs for robust pattern retrieval, focusing on their ability to spontaneously synchronize and thereby enable the precise recovery of stored patterns. The efficacy of KONNs is evaluated based on their resilience against noise and their capability to reconstruct incomplete patterns. Building on the foundational properties of KONNs, the next phase of this research integrates VO2 (Vanadium Dioxide) oscillators within the network architecture. VO2 oscillators are renowned for their unique phase transition properties near room temperature, which can significantly enhance the dynamic range and speed of neural networks. The addition of VO2 oscillators is poised to transform KONNs by improving their energy efficiency and computational power, offering new opportunities for real-time, adaptive pattern recognition systems. A small device capable of transitioning from a metallic to an insulating state (MIT) can be fabricated using vanadium dioxide (VO2) (Corti et al., 2018)[2]. Researchers have created oscillators using non-linear devices like spin-torque oscillators (Csaba, et al, 2020)[3] or materials that exhibit a hysteresis resistive state. These materials can generate electrical oscillations when they are appropriately biased (Sharma et al., 2015; Wang et al., 2017)[4].This innovative integration promises to elevate the capabilities of neural networks, making them more adept at handling the complexities of machine learning and cognitive computation in varied environmental conditions.

we observed that demonstrated the effectiveness of the Kuramoto Oscillatory Neural Network (ONN) with Hebbian learning in pattern recognition. The time taken for convergence depends on the clarity and complexity of the input pattern, with clearer patterns converging more quickly than noisy or ambiguous ones. In our **future work**, we plan to enhance our network by integrating VO2 oscillators, leveraging their phase transition properties to introduce dynamic adaptability. This adaptation could potentially allow for real-time tuning of oscillator interactions in response to environmental changes or new data inputs, enhancing the network's applicability to dynamic and real-time processing tasks.

REFERENCES

[1] Winfree, A. T. (1967). Biological rhythms and the behavior of populations of coupled oscillators. J. Theor. Biol. 16, 15–42. doi: 10.1016/0022-5193(67)90051-3
[2] Corti, E., Gotsmann, B., Moselund, K., Stolichnov, I., Ionescu, A., and Karg, S. (2018). "Resistive coupled vo2 oscillators for image recognition," in 2018 IEEE International Conference on Rebooting Computing (ICRC) (McLean, VA: IEEE), 1–7.
[3] G. Csaba, M. Pufall, W. Rippard and W. Porod, "Modeling of coupled spin torque oscillators for applications in associative memories," 2012 12th IEEE International Conference on Nanotechnology (IEEE-NANO), Birmingham, UK, 2012, pp. 1-4, doi: 10.1109/NANO.2012.6322201.
[4] Sharma, A. A., Bain, J. A., and Weldon, J. A. (2015). Phase coupling and control of oxide-based oscillators for neuromorphic computing. IEEE J. Exploratory Solid State Comput. Devices Circ. 1, 58–66. doi: 10.1109/JXCDC.2015.2448417

M. MOAYED, "Pattern retrieval by oscillatory neural networks" in *PhD Proceedings – Annual Issues of the Doctoral School, Faculty of Information Technology and Bionics, Pázmány Péter Catholic University – 2024.* G. Prószéky, G. Szederkényi Eds. Budapest: Pázmány University ePress, 2024, pp. 60–60.

PROGRAM 4
HUMAN LANGUAGE TECHNOLOGIES, ARTIFICIAL UNDERSTANDING, TELEPRESENCE, COMMUNICATION

Head: Gábor PRÓSZÉKY

Deploying wireless sensor networks: effect of spatial topology on routing performance

Bálint Áron ÜVEGES
(Supervisor: András OLÁH)
Pázmány Péter Catholic University, Faculty of Information Technology and Bionics
50/a Práter street, 1083 Budapest, Hungary
uveges.balint.aron@itk.ppke.hu

***Abstract*—Wireless sensor networks consist of battery-powered devices capable of computing, communicating, and sensing autonomously. The quantity of these devices can range within a single network from a few dozen to thousands. Due to their sensing and distributed properties, such networks are particularly suitable for monitoring natural and artificial spatial phenomena. Corresponding applications range from target tracking, through landslide detection, to structural health monitoring. Produced sensor information must be conveyed to a distinguished device, requiring the network to perform message routing. Spatial deployment of a sensor network is always constrained by environmental and application factors, resulting in topologies that can be sub-optimal in terms of coverage or communication. The impact of these factors can be amplified or mitigated by the utilised routing protocol, however, published works rarely evaluate and quantify the effect of spatial topology on routing.**

***Keywords*-Wireless Sensor Networks; Internet of Things; Spatial Topology; Routing**

I. Effect of spatial topology on routing performance

Evaluating a routing protocol with a spatial topology specific to an implemented wireless sensor network (WSN) provides the most accurate performance figures for the given application, however, it does not reveal the protocol's real capabilities. On the other hand, randomly generated topologies by simple means, such as uniform distribution may not bear the spatial attributes of real-life deployments. To generate spatial topologies that resemble properties of a genuine WSN, we utilise random node placement algorithms, for instance continuous diffusion [1], and randomised grid [2]. Metrics, such as network or node-level packet delivery ratio (PDR) or network-connected node ratio, used for WSN performance evaluation often fails to capture the network's real capabilities as they do not include spatial information. To appropriately characterise a network, we introduce two spatial-based metrics: Distance-corrected PDR (DC-PDR) uses a correction term to emphasise the PDR of distant nodes when calculating network-level average PDR. Minimum sensing radius (MSR) provides information about the WSN's effective coverage concerning the region of interest (RoI) via a single scalar value. For evaluation two state-of-the-art, environment-aware, multipath routing protocols were selected: Reliable Resilient Multipath Routing Protocol (R2MRP) [3] and Environment-Fusion Multipath Routing Protocol (EFMRP) [4]. Results summarised in Fig. 1 show, that R2MRP was able to outperform EFMRP, even if RoI size and node placement irregularity increased.

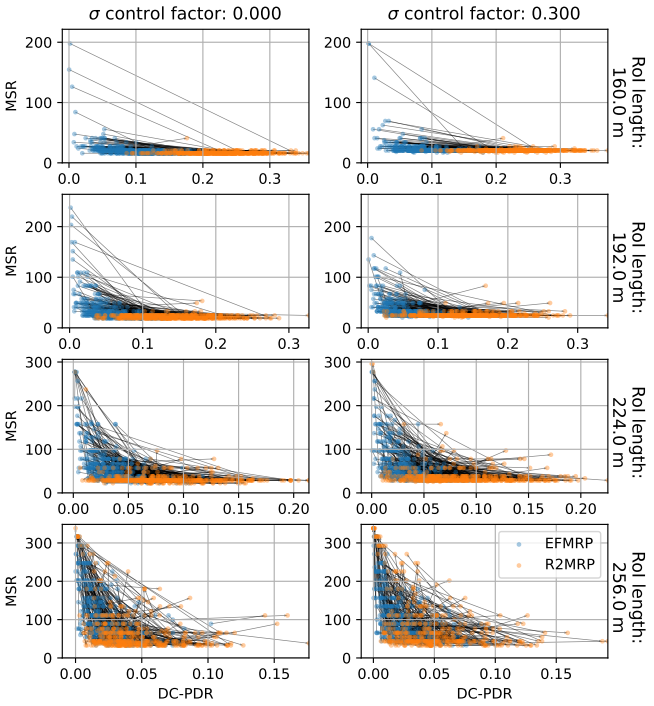

Fig. 1. MSR and DC-PDR results for R2MRP and EFMRP protocols with different topology irregularity (σ) and RoI settings. Grey lines connect the protocol results for the same spatial topology. Lower MSR and higher DC-PDR value indicates better performance, respectively.

Acknowledgements

This research was supported through project no. TKP2023-NVA-27. Project no. TKP2021-NVA-27 has been implemented with the support provided by the Ministry of Culture and Innovation of Hungary from the National Research, Development and Innovation Fund, financed under the TKP2021 funding scheme. This research was also supported by the Faculty of Information Technology and Bionics of Pázmány Péter Catholic University through the Dean's Doctoral Research Scholarship.

References

[1] E. Onur, C. Ersoy, H. Delic, and L. Akarun, "Surveillance wireless sensor networks: Deployment quality analysis," *IEEE Network*, vol. 21, no. 6, pp. 48–53, 2007.

[2] D. Pediaditakis, Y. Tselishchev, and A. Boulis, "Performance and scalability evaluation of the castalia wireless sensor network simulator," in *Proceedings of the 3rd International ICST Conference on Simulation Tools and Techniques*, SIMUTools '10, (Brussels, BEL), pp. 1–6, ICST (Institute for Computer Sciences, Social-Informatics and Telecommunications Engineering), 2010.

[3] B. A. Üveges and A. Oláh, "Enhanced reliability in hazardous event detection: A resilient multipath routing protocol for wireless sensor networks," *IET Wireless Sensor Systems*, vol. 14, no. 3-4, 2024.

[4] X. Fu, G. Fortino, P. Pace, G. Aloi, and W. Li, "Environment-fusion multipath routing protocol for wireless sensor networks," *Information Fusion*, vol. 53, pp. 4–19, 2020.

B. ÜVEGES, "Deploying wireless sensor networks: effect of spatial topology on routing performance" in *PhD Proceedings – Annual Issues of the Doctoral School, Faculty of Information Technology and Bionics, Pázmány Péter Catholic University – 2024.* G. Prószéky, G. Szederkényi Eds. Budapest: Pázmány University ePress, 2024, pp. 62–62.

PROGRAM 5
ON-BOARD ADVANCED DRIVER ASSISTANCE SYSTEMS

Head: Ákos ZARÁNDY

Solving NP-complete optimisation problems with a continuous time neural network

Dóra Eszter BABICZ
(Supervisors: András HORVÁTH, Csaba REKECZKY)
Pázmány Péter Catholic University, Faculty of Information Technology and Bionics
50/a Práter street, 1083 Budapest, Hungary
babicz.dora.eszter@itk.ppke.hu

NP-complete problems can be verified efficiently (in polynomial time), but finding a solution has an exponential worst-case complexity on Turing machines. [1]. Since every NP-complete problem can be converted into a Boolean satisfiability problem (k-SAT) in polynomial time, the importance of solving these problems is important [2]. Boolean satisfiability problems are a type of constraint satisfaction problem and are regarded as some of the most difficult ones. Transforming an NP-complete problem into a Boolean satisfiability (*k*-SAT) problem can be accomplished in polynomial time. A *k*-SAT problem is made up of logical variables which are in a conjunctive normal form in which every conjunction contains k number of variables. [3] demonstrated that *k*-SAT problems can be solved using analogue dynamics, which avoid local traps and operate in polynomial time, though with exponentially increasing power consumption. The definition of the *k*-SAT problem is the following: there are given *N* Boolean variables $x_i \in \{0, 1\}$ and a propositional formula $\mathcal{F}$ which is a conjugation form of *M* constraints C_i. Each constraint is a disjunctive form of k variables x_i or their negations $\bar{x}_i$. Solving this type of problem involves finding a variable assignment that satisfies all constraints. The dynamics used in these dynamics are very similar to those of regular cellular neural networks and are as follows:

$$\frac{\mathrm{d}x_i(t)}{\mathrm{d}t} = -x_i(t) + \sum_j w_{ij} f(x_j(t)) + u_i \tag{1}$$

where x_i is the state value of the cell, *f(x)* is the output function of the neuron, u_i is the input or bias of the neuron and w_{ij} are connection weights between cells i and j.
The Continuous-time recurrent neural network can be defined on a bipartite graph with two types of nodes/cells. One is called the "*s*-type" and represents the variables of *k*-SAT. Their state value will be denoted by s_i, *i*=1,...,*N* and the output function is defined as the following:

$$f(s_i) = \frac{1}{2}(\mid s_i + 1 \mid - \mid s_i - 1 \mid) \tag{2}$$

The output of $f(s_i)$ = 1 is assigned to x_i Boolean variable when it is $TRUE$ (x_i = 1) and if the variable is $FALSE$ (x_i = -1), then $f(s_i)$ = -1, but between these two extrema, any continuous value is allowed, meaning *f*(s_i) $\in$ [-1,1]. The self-coupling parameter will be a fixed value w_{ii} = *A* and the input is u_i = 0 $\forall i$.
The other type of the cells represent the constraints of *k*-SAT with value a_m, *m*=1, ..., *M* and with the output function of:

$$g(a_m) = \frac{1}{2}(1 + \mid a_m \mid - \mid a_m - 1 \mid) \tag{3}$$

The "*a*-type" cells determine the impact of a clause at a given moment on the dynamics of the state (*s*) variables. When the clause is true, then *g*(a_m) = 0 and *g*(a_m) = 1 if it is false. For these cells, the self-coupling w_{mm} = *B* and the input is u_m = *u* = 1 - *k* where k is the number of variables in the clause, in this case $k = 3$. The dynamics fulfil the following requirements:

- They have continuous-time dynamics
- All states, constraints and variables remain bounded
- The derivative of the dynamics is zero if and only if the formula is satisfied
- Starting from a chosen initial condition the system converges to a solution without getting trapped

The proof of the last two points along with a more detailed description can be found in [4]. An example problem in conjunctive form is the following:

$$F = (\neg s_1 \vee \neg s_2 \vee s_3) \wedge (\neg s_1 \vee \neg s_2 \vee \neg s_3) \wedge (s_2 \vee s_3 \vee \neg s_4) \wedge (\neg s_1 \vee s_3 \vee s_4) \tag{4}$$

Our research uses these dynamics to build a physical analogue system that can solve *k*-SAT problems. [5] It uses operational amplifiers to build an analogue computer. It is then implemented on a Printed Circuit Board.

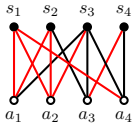

Fig. 1: Problem representation on a bipartite graph. The lines with black denote connections between constraint ("*a*") and state ("*s*") cells the red connections represent negative weights.

Acknowledgment

I gratefully acknowledge additional supervision of my research by Attila Tihanyi.

References

[1] Michael, R. Garey, and S. Johnson David. "Computers and intractability: a guide to the theory of NP-completeness." WH Freeman and Co., San Francisco (1979).
[2] Cook, Stephen A. "The complexity of theorem-proving procedures." Proceedings of the third annual ACM symposium on Theory of computing. ACM, 1971.
[3] Ercsey-Ravasz, Maria, and Zoltan Toroczkai. "Optimization hardness as transient chaos in an analog approach to constraint satisfaction." Nature Physics 7.12 (2011): 966-970.
[4] Molnar, Botond, Zoltan Toroczkai, and Maria Ercsey-Ravasz. "Continuous-time neural networks without local traps for solving Boolean satisfiability." Cellular Nanoscale Networks and Their Applications (CNNA), 2012 13th International Workshop on. IEEE, 2012.
[5] Dora Babicz, Attila Tihanyi, Miklos Koller, Andras Horvath, Csaba Rekeczky, "Simulation of an Analogue Circuit solving NP-Hard Optimization Problems", 2019 IEEE International Symposium on Circuits and Systems (ISCAS), 2019.

D. BABICZ, "Solving NP-complete optimisation problems with a continuous time neural network" in *PhD Proceedings – Annual Issues of the Doctoral School, Faculty of Information Technology and Bionics, Pázmány Péter Catholic University – 2024.* G. Prószéky, G. Szederkényi Eds. Budapest: Pázmány University ePress, 2024, pp. 64–64.

Targetless Lidar and camera calibration based on foreground segmentation

Marcell KÉGL
(Supervisor: Csaba BENEDEK)
Pázmány Péter Catholic University, Faculty of Information Technology and Bionics
50/a Práter street, 1083 Budapest, Hungary
kegl.marcell@itk.ppke.hu

I. Introduction

Automated systems, such as those in surveillance and self-driving applications, rely heavily on accurately perceiving environmental objects. Optical cameras offer high-resolution color information, yet are susceptible to lighting conditions and lack reliable distance measurements. Lidar sensors provide accurate spatial data but suffer from lower temporal resolution and lack color information. Combining these sensor modalities through fusion enhances environment perception, necessitating precise calibration to align their measurements accurately. However, calibrating multimodal sensors poses challenges due to differences in data representation, especially between 2D images and 3D point clouds.

Early calibration methods for cameras and Lidars primarily relied on target-based techniques such as using checkerboards or boxes, requiring manual effort and time-consuming marker preparation. Targetless methods, on the other hand, aim to automate calibration by extracting information directly from the scene or sensor movements, eliminating the need for artificial targets.

While several targetless calibration solutions exist for Lidars and cameras, they heavily depend on specific scene assumptions. These methods often necessitate a stationary sensor setup and long integration times, limiting their effectiveness in dynamic environments. Additionally, some approaches require strong features in the scene, which may not always be present in real-world scenarios like surveillance or self-driving applications. Alternative approaches, involve segmenting camera pixels and Lidar points to extract corresponding features for calibration [1]. These methods measure overlap between segmented areas after point projection, optimizing extrinsic parameters.

In this paper, a novel targetless and fully automatic extrinsic calibration method is proposed for Lidars and cameras. Unlike existing methods reliant on structural scene features, this approach leverages moving objects within the field of view of both sensors. By segmenting foreground motion jointly between the camera and Lidar, the method can operate in diverse dynamic environments without reliance on specific structural features. The proposed method involves two main steps: foreground segmentation for motion extraction and optimization-based calibration to estimate extrinsic parameters. With minimal sensor setup requirements, this method offers practical applicability in various surveillance and autonomous vehicle scenarios.

II. The proposed method

Our approach necessitates a fixed setup comprising a Lidar and an optical camera, aimed at a scene with moving objects during calibration. Initially, we conduct foreground segmentation independently on both Lidar [2] and camera [3] data, to isolate relevant areas. These segmented regions serve as the basis for identifying corresponding features in both Lidar and camera frames.

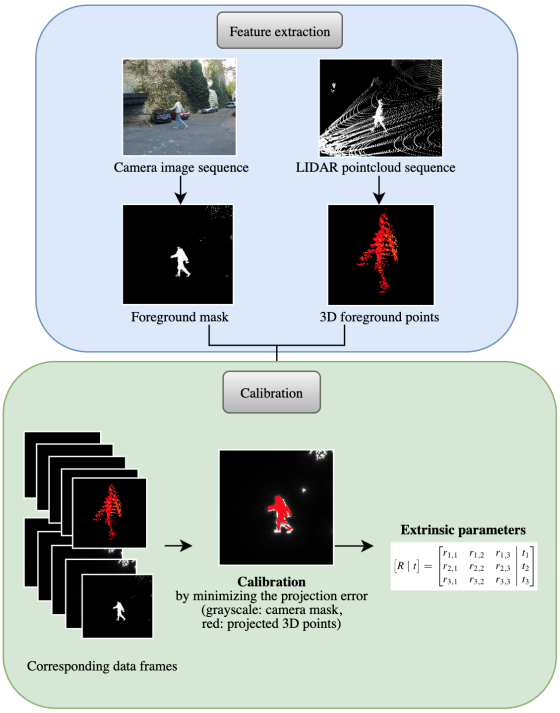

Fig. 1. Calibration method overview

Subsequently, extrinsic calibration parameters are determined by aligning the segmented foreground areas. To achieve this, we employ a two-step optimization process, minimizing transformation errors using a defined cost function. An overview of this process is depicted in Figure 1.

References

[1] C. Sun, Z. Wei, W. Huang, Q. Liu, and B. Wang, "Automatic targetless calibration for lidar and camera based on instance segmentation," *IEEE Robotics and Automation Letters*, vol. 8, no. 2, pp. 981–988, 2023.
[2] L. Kovács, M. Kégl, and C. Benedek, "Real-time foreground segmentation for surveillance applications in nrcs lidar sequences," *The International Archives of the Photogrammetry, Remote Sensing and Spatial Information Sciences*, vol. XLIII-B1-2022, pp. 45–51, 05 2022.
[3] Z. Zivkovic, "Improved adaptive gaussian mixture model for background subtraction," in *Proceedings of the 17th International Conference on Pattern Recognition*, 2004.

M. KÉGL, "Targetless Lidar and camera calibration based on foreground segmentation" in *PhD Proceedings – Annual Issues of the Doctoral School, Faculty of Information Technology and Bionics, Pázmány Péter Catholic University – 2024.* G. Prószéky, G. Szederkényi Eds. Budapest: Pázmány University ePress, 2024, pp. 65–65.

Outdoor vehicle-in-the-loop framework for UAVs

Viktor KÖRTVÉLYESI
(Supervisors: Antal HIBA, Ákos ZARÁNDY)
Pázmány Péter Catholic University, Faculty of Information Technology and Bionics
50/a Práter street, 1083 Budapest, Hungary
kortvelyesi.viktor@itk.ppke.hu

***Abstract*—Outdoor vehicle-in-the-loop testing has increasing importance in automotive applications, however, it has additional challenges when the target vehicle is a drone. The movement is real 3D with higher possible accelerations and the vehicle rarely has enough on-board resources to run the simulator environment on-board, which rises additional latency and bandwidth constraints.**

***Keywords*-UAV, optical navigation, vehicle-in-the-loop, hardware-in-the-loop**

I. Introduction

Prototype testing in aviation is expensive and possibly dangerous, thus several simulation-based techniques were developed for on-bard hardware and software validation. In the case of hardware-in-the-loop (HIL), the on-board flight computer generates control signals, which is directly used in a real-time flight dinamics simulator. Autonomous UAVs can utilize camera image data in real time for navigation, and the HIL testing of these systems requires a photorealistic simulator environment. The increasing autonomy of UAVs, and the advancement of photorealistic simulators makes it possible to perform vehicle-in-the-loop (VIL) testing, where the movements are also real, and only the mission sensors are replaced by simulated sensor data. Indoor VIL solution was presented in [1] and this work is aiming for the realization of the outdoor version.

II. Components and Methods

UAVs in most of the cases has not enough computational resources for running the simulator on-board, thus outdoor VIL have to address the issues of virtual sensor data latency and limited data bandwidth. The simulator runs on a performace laptop at the ground station, or in a cloud service. With proper estimation of the future position and orientation of the drone, the simulated twin can be placed ahead in time, to hide the communication latency. A component is required which estimates the current latency, and based on the known high-level controller and current state, the upcoming trajectory can be calculated at the simulator side.

References

[1] A. Hiba, V. Körtvélyesi, A. Kiskároly, O. Bhoite, P. David, and A. Majdik, "Indoor vehicle-in-the-loop simulation of unmanned micro aerial vehicle with artificial companion," in *2023 International Conference on Unmanned Aircraft Systems (ICUAS)*, pp. 137–143, 2023.

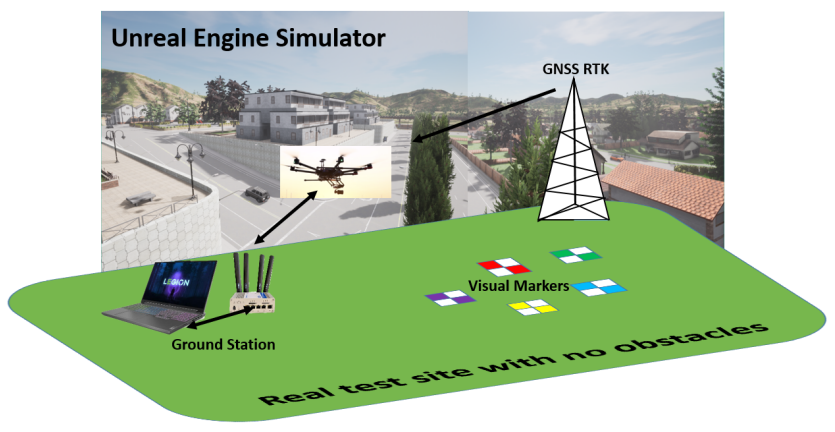

Fig. 1. Outdoor vehicle-in-the-loop test setup. A real drone flies above a designated test site, while a digital twin of it with simulated mission sensors can fly in various virtual environments. Mission sensor meaurements are emulated in a simulator in real-time.

V. KÖRTVÉLYESI, "Outdoor vehicle-in-the-loop framework for UAVs" in *PhD Proceedings – Annual Issues of the Doctoral School, Faculty of Information Technology and Bionics, Pázmány Péter Catholic University – 2024.* G. Prószéky, G. Szederkényi Eds. Budapest: Pázmány University ePress, 2024, pp. 66–66.

3D object completion methods in indoor environment

József KÖVENDI
(Supervisor: Csaba BENEDEK)
Pázmány Péter Catholic University, Faculty of Information Technology and Bionics
50/a Práter street, 1083 Budapest, Hungary
kovendi.jozsef@itk.ppke.hu

***Abstract*—Time-of-flight (ToF) depth sensors are compact and cost-efficient, and thus widely used on mobile devices such as the Microsoft HoloLens2 for depth measurement and obstacle detection. However, due to the low-quality and noisy depth measurements, light-weight ToF sensors are rarely considered for precise 3D mapping. In this work we present two approaches to retrieve lost information from indoor scans. Specifically, we propose a multi-modal and multi-view scene representation that enables the detection and completion of objects contained in the scene by utilizing an RGB camera alongside the ToF sensor. A General Adversial Network (GAN) and a multi-step algorithm complemented with a Convolutional Neutral Network (CNN) is proposed for object completion. We demonstrate the effectiveness of our approaches on real-world data, where the proposed methods improve the interpretability of the 3D environment. Furthermore, we examine the possibility of conditional object generation to replace the inaccurate objects.**

***Keywords*-Sensor fusion, object detection, segmentation, deep learning, image inpainting**

I. Introduction

Accurate indoor 3D mapping has extensive applications in augmented reality and indoor robotics. It usually relies on high-precision and high-resolution depth sensors, such as Lidars or structured light sensors. While less precise, light-weight ToF sensors are compact and cost-effective. Recently, as a result of these properties such sensors were integrated into numerous smart devices. With the wide-spread of Tof senors in ordinary devices, it would be beneficial to fully utilize these sensors for accurate and dense 3D environment mapping, thus we propose two approaches to multi-class object-level scene reconstruction utilizing the RGB and the low-quality depth images collected by the Microsoft HoloLens 2 smart device.

II. Methods

We propose a depth image inpainting network that follows an adversarial model [1] and the input data representation and structure proposed by [2]. Our method consists of 2 subsequent steps: (a) multi-view image-based representation of the incomplete scene captured by depth camera, (b) Shape and color completion in the 2D domain at the desired pixel areas. We also introduce object replacement as an environment completion technique, but in contrast to inpainting, where deep-learning is the main component, this approach utilizes direct mathematical methods, neural-networks just compliment the main algorithm.

III. Results

Both algorithms were able to improve the overall quality of a scene based on the depth and rgb camera image. Image inpainting achieved an *accuracy* of $0.311\ m$ and a *completion* of $0.083\ m$. Object replacement's successfulness

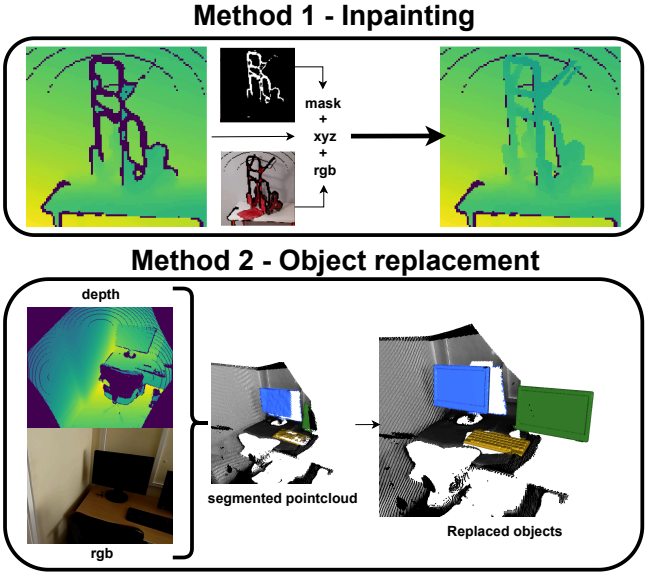

Fig. 1: The proposed methods: Inpainting in 2D (top) and object replacement in 3D (bottom)

is measured with *Intersection over Union* and the prosed algorithm achieved a value of 0.511 IoU.

IV. Conclusion

The proposed techniques improve the quality of the input data which was proven by comparing the results against state-of-the-art methods.

Acknowledgements

The research presented in this paper was supported by the Artificial Intelligence National Laboratory (RRF-2.3.1-21-2022-00004) program and by project grant OTKA K 143274 of the Hungarian NRDI Office.

References

[1] Goodfellow, I., Pouget-Abadie, J., Mirza, M., Xu, B., Warde-Farley, D., Ozair, S., Courville, A., Bengio, Y.: Generative adversarial nets. In: Advances in neural information processing systems. pp. 2672–2680 (2014)

[2] Ibrahim, Y., Nagy, B., Benedek, C. (2022, August). Multi-view based 3D point cloud completion algorithm for vehicles. In 2022 26th International Conference on Pattern Recognition (ICPR) (pp. 2121-2127). IEEE.

J. KÖVENDI, "3D object completion methods in indoor environment" in *PhD Proceedings – Annual Issues of the Doctoral School, Faculty of Information Technology and Bionics, Pázmány Péter Catholic University – 2024.* G. Prószéky, G. Szederkényi Eds. Budapest: Pázmány University ePress, 2024, pp. 67–67.

Mesh-based 3D ultrasound segmentation

Bálint MAGYAR
(Supervisor: András HORVÁTH)
Pázmány Péter Catholic University, Faculty of Information Technology and Bionics
50/a Práter street, 1083 Budapest, Hungary
magyar.balint@itk.ppke.hu

***Abstract*—Segmenting medical images presents significant challenges, especially when handling low-resolution, noisy data such as 3D cardiac ultrasound. In comparison to voxel-based segmentation, the application of geometric models tends to offers a more robust solution for this type of data.**

In this work, we present an artificial neural network-based solution for predicting the contours of the right ventricle as a triangular mesh. Unlike previous techniques, this algorithm directly predicts the vertices of this anatomically defined mesh.

***Keywords*-echocardiography, image segmentation, deep learning, geometric models**

I. Summary

Echocardiograms are extensively utilized for evaluating cardiac function. By analyzing the 3D shape of the heart and its chambers, such as the right ventricle (RV), critical metrics like the ejection fraction and longitudinal strains can be computed. These measures are pivotal for estimating the patient's condition, assessing the risk of heart failure, and determining the appropriate treatment course [1].

Several methods have been proposed for 3D echocardiography segmentation. One approach involves performing pixel-wise segmentation on 2D slices and then constructing a 3D model by combining these masks [2]. Another method begins with an average anatomical atlas mesh model and trains a model to predict transformations from this base model [3]. A third approach, utilized in the MeshDeformNet method, employs a combined segmentation and mesh regression algorithm. In this approach, a 3D segmentation network extracts relevant features from the raw image data, which are then passed to a graph convolutional network that predicts the final mesh [4].

Our proposed method directly predicts the vertices of a triangular mesh that accurately represents the anatomical shape of the RV, shown at the bottom of Figure 1. It is a plug-and-play module that can be integrated with any 3D image segmentation neural network. This module takes the output of the segmentation model and computes the 3D coordinates of the mesh vertices. The model was trained using anatomical RV meshes, with each vertex representing an anatomical landmark, such as the apex of the ventricle or the center of a valve.

For model training and evaluation, we collected a substantial dataset comprising over 45,000 3D echocardiographic recordings, each with manual RV mesh annotations.

Our approach achieved results comparable to state-of-the-art segmentation methods and demonstrated exceptional performance, particularly on noisy and incomplete data.

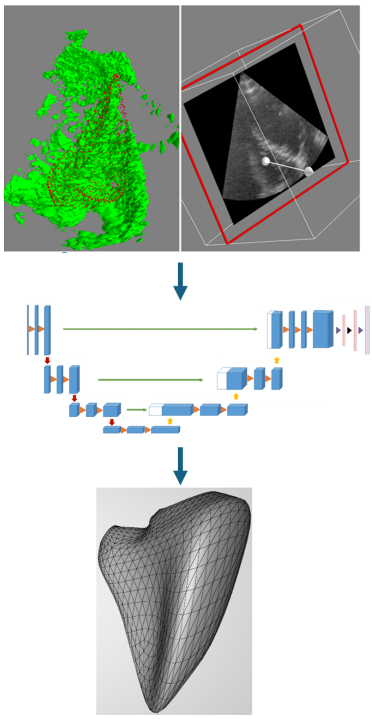

Fig. 1. Model Overview: The process begins with the input of a 3D image volume and its corresponding ground truth mesh (top). This is followed by the mesh predictor model (middle), resulting in the predicted anatomical mesh (bottom).

Acknowledgements

The research presented in this paper was supported by the ÚNKP-23-3-II-PPKE-29 New National Excellence Program of the Ministry of Culture and Innovation with support from the National Research Development and Innovation Fund.

References

[1] A. Kovacs, B. Lakatos, M. Tokodi, and B. Merkely, "Right ventricular mechanical pattern in health and disease: Beyond longitudinal shortening," *Heart failure reviews*, vol. 24, no. 4, pp. 511–520, 2019.

[2] S. Dong, G. Luo, K. Wang, S. Cao, Q. Li, and H. Zhang, "A combined fully convolutional networks and deformable model for automatic left ventricle segmentation based on 3d echocardiography," *BioMed research international*, vol. 2018, 2018.

[3] S. Dong, G. Luo, C. Tam, *et al.*, "Deep atlas network for efficient 3d left ventricle segmentation on echocardiography," *Medical image analysis*, vol. 61, p. 101 638, 2020.

[4] F. Kong, N. Wilson, and S. Shadden, "A deep-learning approach for direct whole-heart mesh reconstruction," *Medical image analysis*, vol. 74, p. 102 222, 2021.

B. MAGYAR, "Mesh-based 3D ultrasound segmentation" in *PhD Proceedings – Annual Issues of the Doctoral School, Faculty of Information Technology and Bionics, Pázmány Péter Catholic University – 2024.* G. Prószéky, G. Szederkényi Eds. Budapest: Pázmány University ePress, 2024, pp. 68–68.

Environment interpretation from Lidar point clouds

Balázs PÁLFFY
(Supervisor: Csaba BENEDEK)
Pázmány Péter Catholic University, Faculty of Information Technology and Bionics
50/a Práter street, 1083 Budapest, Hungary
palffy.balazs.1@itk.ppke.hu

***Abstract*—This paper introduces a novel method for completing sparse lidar depth data using range images. The method, designed for low-end lidar devices, employs a Convolutional Neural Network (CNN) trained with a discriminator model, following a Generative Adversarial Network (GAN) approach. The final output is a complete depth image generated through pixel-wise regression. The training process incorporates feature- and 3D point cloud-based losses. Experiments on synthetic data show the method outperforms state-of-the-art techniques. Additionally, utilizing completed depth data by the proposed method improved the Intersection over Union (IoU) score of a common downstream task, namely semantic segmentation.**

***Keywords*-Depth image completion, Semantic segmentation, Sythetic data, Deep learning in automation**

I. Introduction

Lidars (light detection and ranging) are highly accurate sensors used in fields like robotics, autonomous driving and 3D mapping. They vary in cost from thousands to hundreds of thousands of dollars. Despite their accuracy, Lidars produce sparse depth maps compared to RGB cameras which affects the efficiency of subsequent algorithms in environmental interpretation. To address this, various depth completion methods exist. Some rely solely on raw LIDAR data, losing precision in the conversion process, while others use sensor fusion with additional sensors like RGB cameras. Real-life dataset preparation is challenging due to sensor limitations. This paper proposes a sensor-independent, LIDAR-based range image completion method using a Convolutional Neural Network (CNN). The method works with both single and multi-frame inputs, transforming 3D point clouds into high-resolution depth images.

II. Proposed method

This paper presents a method to produce high density, accurate and precise depth image from sparse lidar data. The process starts with fetching a Lidar point cloud and converting it into image space through a pre-processing phase, which includes calculating the focal length for accurate projection. Later on, our specifically designed neural network, trained on our synthethic dataset with designed losses performs operations on the incoming sparse data, resulting in a high resolution depth image as output presented in Fig. 1. Our network in trained in a Generative Adverserial Network manner, and adopts the common U-net architecture with encoder, middle, and decoder sections.

III. Conclusion

With the proposed lidar based, single-frame, depth image completion method, we are able to complete incoming lidar data, achieving accurate and dense depth images as output. The model is able to outperform the baseline method, and can improve the prediction accuracy of downstream tasks.

Input as depth image, and the completed output

Fig. 1.

TABLE I
Comparison of the best performing network with the baselines using Avia Lidar sensor data

Method	RMSE ↓	MAE ↓	MSE ↓
ST-DepthNet [1]	27.5399	17.1280	769.8456
Ours	**5.8375**	**1.1064**	**39.4729**

TABLE II
Semantic segmentation performance, measured by Intersection over Union (IoU), evaluated using both raw depth images and depth images completed with the proposed method as input.

Sensor	Raw depth image ↑	Completed depth image ↑
Avia	0.7214	**0.7970**

IV. Acknowledgements

The author is grateful to HUN-REN SZTAKI, particularly to Csaba Benedek for the opportunity to work on this project.

References

[1] Ö. Zováthi, B. Pálffy, Z. Jankó, and C. Benedek, "ST-DepthNet: A spatio-temporal deep network for depth completion using a single non-repetitive circular scanning Lidar," *IEEE Robotics and Automation Letters*, vol. 8, no. 6, pp. 3270–3277, 2023.

B. PÁLFFY, "Environment interpretation from Lidar point clouds" in *PhD Proceedings – Annual Issues of the Doctoral School, Faculty of Information Technology and Bionics, Pázmány Péter Catholic University – 2024.* G. Prószéky, G. Szederkényi Eds. Budapest: Pázmány University ePress, 2024, pp. 69–69.

APPENDIX

PROGRAM 1: Bionics, Bio-inspired Wave Computers, Neuromorphic Models	
Name	**Supervisor**
András ADOLF	István ULBERT MD DSc
Zsófia BALOGH-LANTOS	Zoltán FEKETE PhD
Gréta Lilla BÁNYAI	Tamás GARAY PhD
Ramóna BIRÓ-KOVÁCS	Balázs LIGETI PhD, Zsolt ZSÓFI PhD
Eszter BIRTALAN	Miklós KOLLER PhD
Martin János BLAZSEK	Judit MAKARA PhD, Balázs Benedek UJFALUSSY PhD
Camilla CANCRINI	Andrea CILIBERTO PhD
Fanni FARKAS	Zoltán GÁSPÁRI PhD
Gábor FARKAS	Szabolcs KÁLI PhD
Amelita FODOR	József LACZKÓ PhD
Bence Tamás GAIZER	Attila CSIKÁSZ-NAGY DSc, János JUHÁSZ PhD
Valentina GUARINO	Andrea CILIBERTO PhD
Júlia Ágnes HORVÁTH	György CSEREY PhD, Katalin CSIGÓ PhD
Dorottya KOCSIS	Franciska ERDŐ PhD
Valentina MADÁR	Attila CSIKÁSZ-NAGY DSc
Vilmos MADARAS	Csaba BENEDEK PhD
Zsófia MOLNÁR	András HORVÁTH PhD
Kristóf MÜLLER	Miklós KOLLER PhD
Gábor NAGY	György CSEREY PhD, László GRAND PhD
Eszter NAGY-KANTA	Zoltán GÁSPÁRI PhD
Afrodité NÉMETH	Tamás GARAY PhD
Bence NÉMETH	András HORVÁTH PhD
Ábel PETIK	István ULBERT MD DSc, Dániel HILLIER PhD
Bíborka PILLÉR	Attila CSIKÁSZ-NAGY DSc
Balázs RADELECZKI	József LACZKÓ PhD
Anna SÁNTA	Zoltán GÁSPÁRI PhD
András László SZABÓ	Zoltán GÁSPÁRI PhD
Péter József SZABÓ	Gergő ORBÁN PhD, András HORVÁTH PhD
Péter SZABÓ	György CSEREY PhD, Katalin CSIGÓ PhD
János SZALMA	Attila CSIKÁSZ-NAGY DSc, Erzsébet FICHÓ PhD
Giorgio TALLARICO	Andrea CILIBERTO PhD
Brigitta UNGVÁRI	György CSEREY PhD, Katalin CSIGÓ PhD
Mihály András VÁGHY	Mihály KOVÁCS DSc, Gábor SZEDERKÉNYI DSc
Soma VARGA	Bálint PÉTERFIA PhD
Áron WEBER	Attila CSIKÁSZ-NAGY DSc, Erzsébet FICHÓ PhD

PROGRAM 2: Computer Technology Based on Many-core Processor Chips, Virtual Cellular Computers, Sensory and Motoric Analog Computers	
Name	**Supervisor**
Boldizsár Zsolt BALOG	György CSEREY PhD, Gábor NYÍRI PhD
Balázs CSUTAK	Gábor SZEDERKÉNYI DSc
Lóránt Szabolcs DAUBNER	Kálmán TORNAI PhD, Tamás ZSEDROVITS PhD
Mary GUINDY	Péter SZOLGAY DSc, Vamsi Kiran ADHIKARLA PhD
Gergely HORVÁTH	Gábor SZEDERKÉNYI DSc
Imre Gergely JÁNOKI	Péter FÖLDESY DSc
Rizal MAULANA	György CSEREY PhD
Katalin SCHÄFFER	Miklós KOLLER PhD
Gergely SZABÓ	András HORVÁTH PhD

PROGRAM 3: Feasibility of Electronic and Optical Devices, Molecular and Nanotechnologies, Nano-architectures, Nanobionic Diagnostic and Therapeutic Tools	
Name	**Supervisor**
András ESZES	Zsolt SZABÓ DSc
Levente MAUCHA	György CSABA PhD, Ádám PAPP PhD
Mitra MOAYED	György CSABA PhD

PROGRAM 4: Human Language Technologies, Artificial Understanding, Telepresence, Communication	
Name	**Supervisor**
Bálint Áron ÜVEGES	András OLÁH PhD

PROGRAM 5: On-board Advanced Driver Assistance Systems	
Name	**Supervisor**
Dóra Eszter BABICZ	Csaba REKECZKY PhD, András HORVÁTH PhD
Marcell KÉGL	Csaba BENEDEK PhD
Viktor KÖRTVÉLYESI	Ákos ZARÁNDY DSc, Antal HIBA PhD
József KÖVENDI	Csaba BENEDEK PhD
Bálint MAGYAR	András HORVÁTH PhD
Balázs PÁLFFY	Csaba BENEDEK PhD